AD_____

AWARD NUMBER: W81XWH-06-1-0213

TITLE: Analysis of p21-Activated Kinase Function in Neurofibromatosis Type 2

PRINCIPAL INVESTIGATOR: Jonathan Chernoff, M.D., Ph.D.

CONTRACTING ORGANIZATION: Institute for Cancer Research
Philadelphia, PA 19111

REPORT DATE: January 2010

TYPE OF REPORT: Final

PREPARED FOR: U.S. Army Medical Research and Materiel Command
Fort Detrick, Maryland 21702-5012

REPORT DOCUMENTATION PAGE

Form Approved
OMB No. 0704-0188

1. REPORT DATE	2. REPORT TYPE	3. DATES COVERED
1 January 2010	Final	1 Jan 2006 – 31 Dec 2009

4. TITLE AND SUBTITLE

Analysis of p21-Activated Kinase Function in Neurofibromatosis Type 2

5a. CONTRACT NUMBER

5b. GRANT NUMBER
W81XWH-06-1-0213

5c. PROGRAM ELEMENT NUMBER

6. AUTHOR(S)

Jonathan Chernoff, M.D., Ph.D.

E-Mail: Jonathan.Chernoff@fccc.edu

5d. PROJECT NUMBER

5e. TASK NUMBER

5f. WORK UNIT NUMBER

7. PERFORMING ORGANIZATION NAME(S) AND ADDRESS(ES)
Institute for Cancer Research
Philadelphia, PA 19111

8. PERFORMING ORGANIZATION REPORT NUMBER

9. SPONSORING / MONITORING AGENCY NAME(S) AND ADDRESS(ES)
U.S. Army Medical Research and Materiel Command
Fort Detrick, Maryland 21702-5012

10. SPONSOR/MONITOR'S ACRONYM(S)

11. SPONSOR/MONITOR'S REPORT NUMBER(S)

12. DISTRIBUTION / AVAILABILITY STATEMENT
Approved for Public Release; Distribution Unlimited

13. SUPPLEMENTARY NOTES

14. ABSTRACT

In this project, we sought to determine if p21-activated kinases (Paks) are required for Schwann cell growth and invasiveness in cells lacking the tumor suppressor Merlin (the protein product of the neurofibromatosis-2 gene). We found that Paks are highly expressed in Schwann cells and that inhibitor of Pak – either by a peptide or by a small molecule developed by us during the course of this project – blocked proliferation and invasiveness of two different Merlin-deficient cell lines. Importantly, inhibition of Pak also blocked tumor formation in mice xenografted with Merlin-deficient cells. We also found that the beneficial effects of Pak blockade in Merlin-deficient cells were not mediated by the ERK signaling pathway. These results are important because they 1) establish Paks as potential therapeutic targets in NF2, and 2) they show that these events occur through an unexpected molecular mechanism, a problem we will continue to examine in future work.

15. SUBJECT TERMS
NF2, Merlin, p21-activated kinase, Schwann cells, Signal Transduction

16. SECURITY CLASSIFICATION OF:			17. LIMITATION OF ABSTRACT	18. NUMBER OF PAGES	19a. NAME OF RESPONSIBLE PERSON
a. REPORT	b. ABSTRACT	c. THIS PAGE			USAMRMC
U	U	U	UU	57	19b. TELEPHONE NUMBER *(include area code)*

Standard Form 298 (Rev. 8-98)
Prescribed by ANSI Std. Z39.18

Table of Contents

INTRODUCTION:

The goal of this project was to determine if group A p21-activated kinases (Paks) are important elements in signaling in neurofibromatosis type II (NF2). Our hypothesis was that inactivation of the *NF2* gene disrupts a signaling pathway emanating from the small GTPase Rac and its effector, p21-activated kinase (Pak). We proposed that stimulation of the Rac/Pak signaling axis in cells lacking Merlin leads to changes in transcriptional activity and cytoskeletal dynamics, ultimately resulting in enhanced cell proliferation and motility, which are hallmarks of tumorigenesis. If this hypothesis is correct, then inhibition of Pak signaling should disable the growth advantages of cells lacking Merlin. We planned to test this theory using Pak loss-of-function cells and animals.

BODY: We set ourselves two specific tasks. These were:

Task 1. To determine if Pak function is required for mitogenic or morphogenic signaling in fibroblasts and Schwann cells lacking Merlin (Months 1-24):

a. Analyze the expression level and activity of group A Paks in fibroblasts and Schwann cells (Months 1-6).
b. Analyze effects of loss of Pak function on mitogenic and morphogenic signaling in mouse embryo fibroblasts lacking Merlin (Months 6-18).
c. Analyze effects of loss of Pak function on mitogenic and morphogenic signaling in mouse Schwann cells lacking Merlin (Months 18-24).

Task 2. To investigate the influence of Pak on the formation of tumors in transgenic mice expressing a dominant negative form of Merlin (SchΔ(39-121), by determining if crossing such mice with a) transgenic mice expressing a Pak inhibitor (PID), or b) *Pak1*$^{-/-}$ mice affects their predisposition to the tumors typically seen in NF2 (Months 6-48):

a. Generate PID transgenic cells (Months 6-12).
b. Generate and analyze PID transgenic mice (Months 12-24)
c. Mate P0-SchΔ(39-121) mice with the PID transgenics and *Pak1*$^{-/-}$ mice and analyze crosses (Months 24-48).

Progress

We have met almost all our goals for the project, and in some cases, exceeded them, as detailed below.

Task 1

a) Analyze the expression level and activity of group A Paks in fibroblasts and Schwann cells. This was accomplished in the first year when we showed that Pak1 is the predominant group A Pak expressed in both fibroblasts and Schwann cells but that Pak2 is also expressed at reasonably high levels. These results

confirmed our strategy to focus on these two isoforms of Pak in our genetic and biochemical experiments.

b) Analyze effects of loss of Pak function on mitogenic and morphogenic signaling in mouse embryo fibroblasts lacking Merlin. As described in previous progress reports, we created both retroviral and adenoviral expression vectors encoding the Pak1 inhibitor domain (PID). These were altered to avoid binding of the PID region to the Fragile X (FGX) protein. We found that the newly constructed PID vectors do not bind FGX or interfere with normal cell cycle progression, while retaining the ability to inhibit group A Paks. Thus, these reconfigured reagents are suitable for evaluating the role of Pak in NF2. Rather than use NF2 $^{-/-}$ MEFs, we instead carried out our analysis in mouse fibroblasts transformed with the NF2 BBA mutant (1). The results of these studies are summarized in Task 2b, below.

In addition, as described previously, we developed a small molecule inhibitor of Pak, termed IPA3. This compound inhibits Pak1 at a K_i of 2.4 μM in fibroblasts and is also a potent inhibitor of the other two group A Paks, Pak2 and Pak3. IPA3 does not inhibit the three group B Paks at 10 μM concentrations. Remarkably, when tested against a panel of ~240 protein kinases, we found that the specificity of IPA3 is comparable to that of some of the best protein kinase inhibitors known, such as the Abl inhibitor Imatinib (Gleevac) and the Rho kinase inhibitor Y-27632 (2). IPA3 thus represents an additional reagent for testing the role of group A Pak function in NF2-deficient cells. In cell-based experiments, we found that IPA3 blocks Pak activation and subsequent downstream activation of ERK, as well as preventing ruffling of the plasma membrane.

c) As noted in our last progress report, in 2009 we focused on Pak function in Schwann cells. We used HEI-193 cells, which are derived from a human patient with NF2 (3). We determined that the growth and motility of these cells was markedly decreased by Pak inhibition, using either the Pak PID or the small molecule inhibitor IPA3.

Task 2

a) As described in previous progress reports, we encountered a problem in our attempts to analyze schwannoma formation in our NF2 mouse model. We had crossed transgenic mice expressing dominant negative NF2 in Schwann cells (P0-SchΔ(39-121)) (4) with *Pak1*$^{-/-}$ mice, creating two cohorts with the genotypes P0-SchΔ(39-121) *Pak1*$^{+/+}$ and P0-SchΔ(39-121) *Pak1*$^{-/-}$. Over a two-year period, we watched these cohorts for the development of Schwannoma and other malignancies. We found that 6/30 P0-SchΔ(39-121) *Pak1*$^{+/+}$ mice developed NF2-related pathologies (schwannomatosis, nerve sheath tumors, sarcomas), whereas 2/34 P0-SchΔ(39-121) *Pak1*$^{-/-}$ mice developed NF2-related pathologies. These data suggest that our main hypothesis is correct: Pak1 is required for the efficient development of NF2-related pathologies, and also support the corollary idea that Pak inhibitors might be useful in the treatment of NF2. However, since

the incidence of disease was so low, we did not obtain statistically significant data from this experiment. As explained in previous progress reports, we then learned that the mixed C57 Bl6/C129 background is not ideal for studying the effects of the NF2 transgene (P0-SchΔ(39-121). The creator of the P0-Sch Δ(39-121) transgenic mice, Marco Giovannini, recently found that the C3H background is much more favorable for analysis (M.G., personal communication), as schwannomatosis develops in all the transgenic mice by three months of age. We have therefore crossed P0-Sch Δ(39-121) mice and *Pak1*$^{-/-}$ mice into the C3H background and are repeating the studies listed above.

b) As reported previously, we added a new task to those originally specified in the grant proposal. We used two cell lines: mouse fibroblasts transduced with a dominant negative form of NF2 (the NF2 BBA mutant (1)), and HEI-193 cells, a human NF2 schwannoma cell line (3), and characterized these for invasiveness and for growth properties. To assess invasiveness, cells were plated in a chamber above a layer of Matrigel and assessed for their ability to penetrate through this layer. As shown in Fig. 1A, the invasiveness of ΔBB cells was almost twice that of control NIH-3T3 cells. Expression of PID, but not inactive PID LF, significantly inhibited the invasive capacity of Merlin ΔBB cells. As in ΔBB cells, PID expression also decreased the invasiveness of HEI-193 cells, whereas PID LF expression did not (Fig. 1B). Thus, in both cell lines, a Pak inhibitor substantially reduced invasiveness in the absence of Merlin function.

As regards proliferation, in the mouse fibroblasts, we found, as expected, that ΔBB cells showed an increased growth rate compare to vector control cells (Fig. 2A). Co-expression of PID in these cells inhibited proliferation. Conversely, cells expressing PID LF resulted in slight stimulation on cell proliferation. Even more pronounced effects were found in HEI-193 Schwanomma cells expressing PID, which showed substantially slowing of proliferation relative to controls (Fig. 2B). Expression of PID LF had no effect in these cells.

Pak inhibition suppresses cell growth via a G2/M blockade. To better understand the effects of Pak blockade on cell proliferation, we analyzed the effect of PID expression on the cell cycle (Fig. 2C). In ΔBB cells, PID expression led to a significant accumulation of cells in G2/M, an effect not seen in ΔBB/PID LF cells. Similar effects were noted in HEI-193 cells, in which PID expression substantially increased the percentage of cells in G2/M (Fig. 2D).

Effects of PID on Erk cascade. To determine the molecular basis of the effects of PID expression on Merlin signaling, we examined a number of signal transduction pathways. In many cell types, group A Pak function is required for activation of Erk, most likely by phosphorylation of c-Raf at S338 and Mek1 at S298 (5). In ΔBB cells, basal levels of Pak, Mek, and Erk activity were elevated but could be further stimulated by PDGF (Fig. 3). PID expression suppressed Pak activation, as assessed by two distinct anti-phospho Pak antibodies. Surprisingly, despite the suppressive effects of PID on Merlin ΔBB invasion, and proliferation,

expression of this inhibitor did not have a significant effect on the activity of Mek and Erk, even though it did reduce Pak activity significantly.

We also assessed the effects of Pak inhibition in HEI-193 Schwannoma cells. As in ΔBB cells, PID expression substantially reduced Pak activity in Schwannoma cells, with little effect on Mek or Erk activities (Fig. 3). However, unlike the results in ΔBB cells, PID expression extinguished phosphorylation of Mek at S298, the putative site of Pak phosphorylation. Thus, in these cells, despite effective suppression of Pak, with consequent reduction of phosphorylation of one of its major targets in the Erk pathway, Mek activity (as assessed by phospho Ser 217/221 antibodies) and downstream Erk activity were unaffected.

Inhibition of tumor formation by Pak inhibition. HEI-193 cells do not grow as xenografts (6); therefore, to assess the effects of Pak inhibition on NF2-related tumorigenicity, we injected nude mice only with ΔBB, ΔBB/PID, or ΔBB/PID LF cells. In agreement with previous studies, ΔBB cells developed substantial tumors by 6 weeks post-injection (average volume >200 mm^3) (1, 7). Tumors derived from ΔBB/PID cells were much smaller in size, with an average volume of 38 mm^3 (Fig. 4). Interestingly, mice injected with ΔBB/PID LF cells developed tumors even larger (average volume ~450 mm^3) than those injected with ΔBB cells.

Lastly, we examined signaling activity in tumor lysates from these xenografts. Pak activity was inhibited in ΔBB/PID cells, indicating that this suppressor remained effective *in vivo*. Surprisingly, while Akt and Erk were not active in tumors derived from animals injected with ΔBB or ΔBB/PID LF cells, both Akt and Erk were activated in lysates from the small tumors that developed in mice injected with ΔBB/PID (Fig. 5). It is also of interest that, in the tumors from ΔBB/PID mice, Merlin expression (presumably exogenous Merlin ΔBB) was substantially elevated. These data show that PID expression strongly inhibited tumor formation in the NF2 xenograft model, suggesting that Group I Paks are required for transformation in cells that have lost Merlin function. Despite this requirement, loss of Pak function did not reduce Akt or Erk activity; on the contrary, it activated them.

KEY RESEARCH ACCOMPLISHMENTS: Bulleted list of key research accomplishments emanating from this research.

- Published a small molecule inhibitor of group A Paks and showed that this inhibitor affects morphology of NF2-null Schwann cells.
- Completed crosses of NF2 and *Pak1*$^{-/-}$ mice into C3H genetic background and initiated study of Pak1 effects in this genetic background.
- Carried out cell-based and xenograft models to evaluate the role of group A Paks in NF2, showing that Pak activity is required for tumorigenesis in setting

of loss of NF2, and that these effects are not mediated by the Mek/ERK pathway.

REPORTABLE OUTCOMES:

1. A manuscript on the development of IPA3, a small molecule inhibitor of group A Paks, was published Chemical Biology (Deacon et al., An isoform-selective, small-molecule inhibitor targets the autoregulatory mechanism of p21-activated kinase, Chem Biol. 15:322, 2008). This manuscript describes the first specific inhibitor of group A Paks, and has already been cited more than a dozen times.
2. A second paper, describing Pak function in human schwannomas, was published in collaboration with the Hanemann lab in Experimental Neurology (Flaiz et al. PAK kinase regulates Rac GTPase and is a potential target in human schwannomas. PAK kinase, *Exp. Neurology* 218:137-144, 2009.
3. We have recently submitted a third paper, "Chow, H.-Y. and Chernoff, J. p21-activated kinases are required for transformation in neurofibromatosis type 2", to Oncogene.
4. Finally, based on the results of this study, my postdoctoral fellow, Betty Chow, recently received a postdoctoral fellowship grant from the DOD to continue and expand upon these experiments.

CONCLUSION:

With the exception of one experiment (the comparison between P0-Sch Δ(39-121) mice with P0-Sch Δ(39-121); Pak1$^{-/-}$ mice), we completed the objectives of our plan, as well as two additional objectives. There are two new approaches that we have added: i) the use of a small molecule Pak inhibitor to supplement our cell- based studies and ii) xenograft studies as a quick readout of Pak's role in NF2-related tumorigenesis. We have made significant progress on both these fronts.

REFERENCES:

1. Johnson, K.C., Kissil, J.L., Fry, J.L., and Jacks, T., Cellular transformation by a FERM domain mutant of the Nf2 tumor suppressor gene. *Oncogene*, 21:5990-7, 2002.
2. Deacon, S.W., Beeser, A., Fukui, J.A., Rennefahrt, U.E., Myers, C., Chernoff, J., and Peterson, J.R., An isoform-selective, small-molecule inhibitor targets the autoregulatory mechanism of p21-activated kinase. *Chem Biol*, 15:322-31, 2008.
3. Fraenzer, J.T., Pan, H., Minimo, L., Jr., Smith, G.M., Knauer, D., and Hung, G., Overexpression of the NF2 gene inhibits schwannoma cell proliferation through promoting PDGFR degradation. *Int J Oncol*, 23:1493-500, 2003.
4. Giovannini, M., Robanus-Maandag, E., Niwa-Kawakita, M., van der Valk, M., Woodruff, J.M., Goutebroze, L., Merel, P., Berns, A., and Thomas, G., Schwann cell hyperplasia and tumors in transgenic mice expressing a naturally occurring mutant NF2 protein. *Genes Dev.*, 13:978-986, 1999.

5. Hofmann, C., Shepelev, M., and C hernoff, J., The genetics of Pak . *J Cell Sci*, 117:4343-54, 2004.
6. Mukherjee, J., Ka mnasaran, D., Balasubr amaniam, A., Radovanovic, I., Zadeh, G., Kiehl, T.-R., and Guha, G., Human Schwannomas Express Activated Platelet-Derived Growth Factor Receptors and c-kit and Are Growth Inhibited by Gleevec (Imatinib Mesylate). *Cancer Res*, 69:5099-, 2009.
7. Yi, C., W ilker, E.W ., Yaffe, M.B., Stem mer-Rachamimov, A., and Kissil, J.L., Validation of the p21-activated kina ses as targets for inhibition in neurofibromatosis type 2. *Cancer Res*, 68:7932-7, 2008.

BIBLIOGRAPHY OF PUBLICATIONS:

Deacon, S.W., Beeser, A., Fukui, J.A., Rennefahrt, U.E.E., Myers, C., Marchaud, G., Chernoff, J., Peterson, J.R. An isoform-selective, small-molecule inhibitor targets the autoregulatory mechanism of p21-activated kinase. *Chem Biol*. **15**:322, 2008.

Flaiz, C., Chernoff, J. Ammoun, S., Peterson, J.R., and Hanemann, C.R. PAK kinase regulates Rac GTPase and is a potential target in human schwannomas. *Exp. Neurology* 218:137-144, 2009.

Chow, H.-Y. and Chernoff, J. p21-activated kinases are required for transformation in neurofibromatosis type 2. (submitted).

LIST OF PERSONNEL:

Jonathan Chernoff, M.D., Ph.D. – Principal Investigator
Zahara Jaffer, Ph.D. – Research Associate
Sophie Cotteret, Ph.D. – Postdoctoral Associate
Clemens Hofmann, Ph.D. – Research Associate
Dina Stepanova – Scientific Technician I
Luis Arias Romero, Ph.D. – Postdoctoral Associate
Olga Villamar-Cruz – Scientific Technician II
Marc Leshner – Summer Assistant II
Barbra Dickerman – Summer Assistant II
Hoi Yee Chow, Ph.D. – Postdoctoral Associate
Maria Radu, Ph.D. – Postdoctoral Associate
Sayanti Saha, Ph.D. – Postdoctoral Associate
Christine Lightcap, Ph.D. – Postdoctoral Associate

APPENDICES:

1) Figures 1-5

2) Manuscripts:
Deacon, S.W., Beeser, A., Fukui, J.A., Rennefahrt, U.E.E., Myers, C., Marchaud, G., Chernoff, J., Peterson, J.R. An isoform-selective, small-molecule inhibitor targets the

autoregulatory mechanism of p21-activated kinase. *Chem Biol*. **15**:322, 2008. PMID: 18420139.
Flaiz, C., Chernoff, J. Ammoun, S., Peterson, J.R., and Hanemann, C.R. PAK kinase regulates Rac GTPase and is a potential target in human schwannomas. *Exp. Neurology* 218:137-144, 2009. PMID: 19409384.
Chow, H.-Y. and Chernoff, J. p21-activated kinases are required for transformation in neurofibromatosis type 2. (submitted).

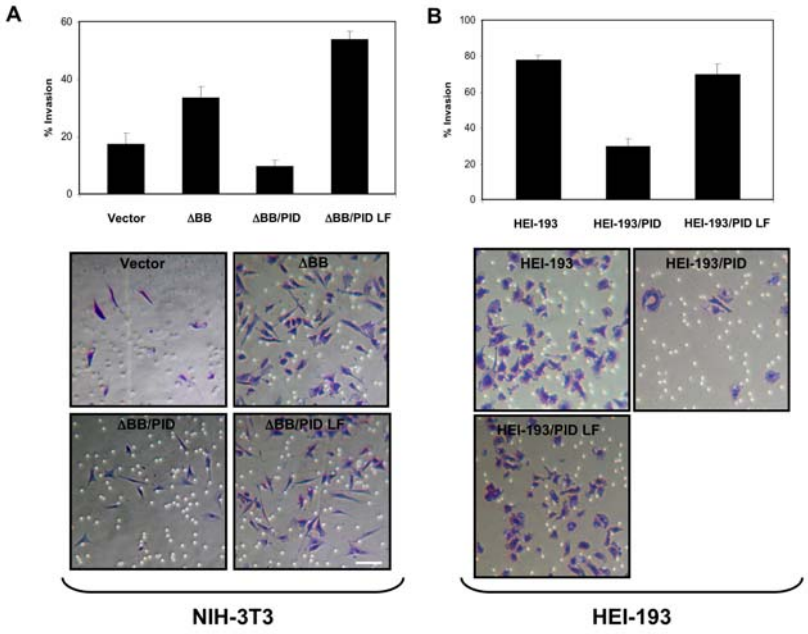

Fig. 1. Effects of PID on invasion. (**A**) The invasiveness of control cells or cells expressing Merlin ΔBB, Merlin ΔBB/PID, or Merlin ΔBB/PID LF was determined by Matrigel invasion chamber assay as compared against uninfected control cells. The experiments were performed three times with similar results. The data are presented as the means ± S.D. of duplicate well measurements from one representative experiment. (**B**) Staining pattern of cells that have migrated and adhered to the bottom surfaces of filters in cell invasion assay. The small circles are cross-sections of 8 μm pores. Scale bar = 50 μm.

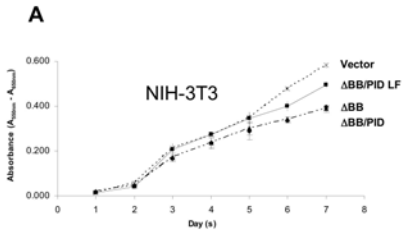

C

	% G0/G1	% S	%G2/M
Vector	57	26	14
ΔBB	55	30	12
ΔBB/PID	43	26	28
ΔBB/PID LF	53	27	16

D

	% G0/G1	% S	%G2/M
HEI-193	31	39	20
HEI-193 /PID	37	31	31
HEI-193 /PID LF	32	36	23

Figure 2. Inhibition of cell proliferation and induction of G2/M arrest by expression of PID. (**A**) Equal numbers of the indicated cells were seeded in 96-well plate and monitored by MTT assay for 7 days. The experiments were conducted three times with similar results. (**B**) Cells were stained with propidium iodide and subjected to cell cycle analysis by FACS. Results are representative of three independent experiments.

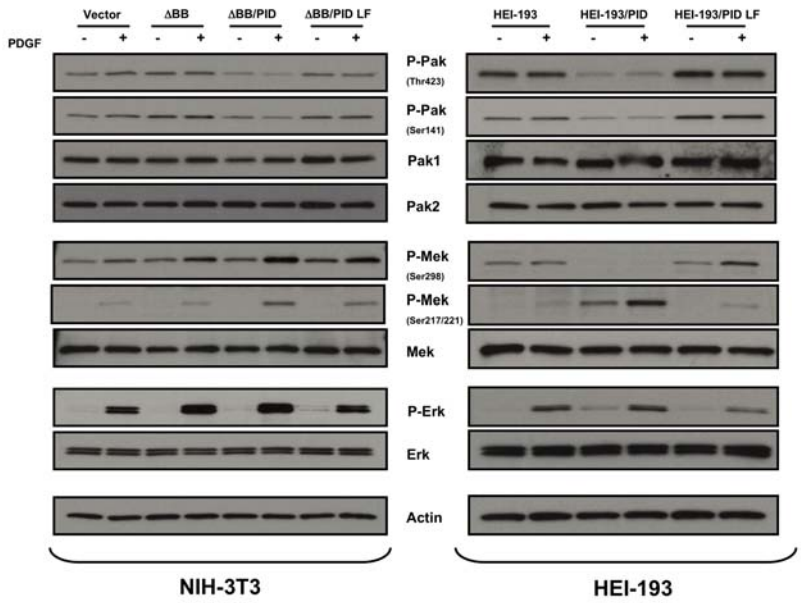

Figure 3. Lack of effect of Pak inhibition on Erk pathway. Cells were cultured in serum-free medium for 24 hr and then stimulated with 5 ng/ml of PDGF for 5 m in, as described in Material and Methods. Lysed cells were separated by S DS-PAGE and incubated with the indicated antibodies. Data shown represent the means ± SD of data fro m three experiments.

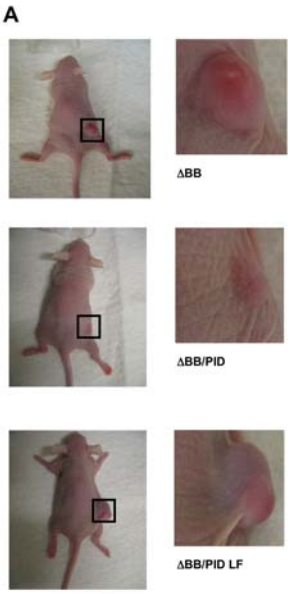

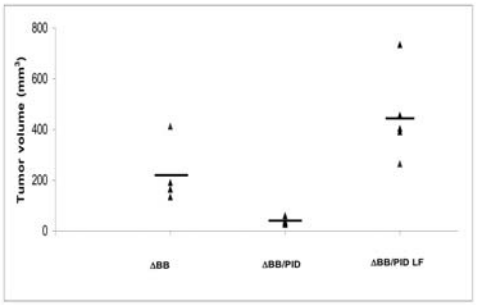

C

Injected cell types	ΔBB	ΔBB/PID	ΔBB/PID LF
Average tumor volume (mm^3)	213.56	38.37	450.61

Figure 4. Effects of PID on tumor formation. Tumor formation was assessed by subcutaneously inoculating 1 X 10^6 NIH-3T3 cells infected with empty vector (Vector) into left flanks and equal number of Merlin-expressing cells (ΔBB, ΔBB/PID and ΔBB/PID LF, respectively) into right flank of the same mice. Five mice were used for each cell line. Tumor diameters were measured every 3 days using caliper for 6 weeks following injection. (**A**) Representative photographs of nude mice with solid tumors (left panel). Enlarged images of boxed area in the left panel (right panel). (**B, C**) Tumor volume was calculated by the formula described in Material and Methods. Horizontal lines represent the average tumor diameter.

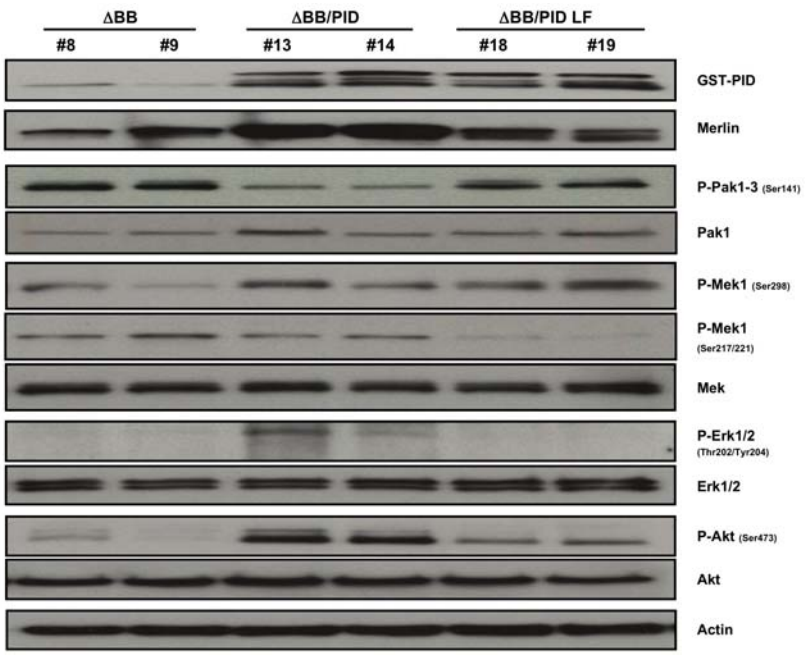

Figure 5. Activity of signaling pathways in tumor samples from xenografts. Tumors were resected and immediately lysed in a buffer containing 10 mM PBS pH 7.2, 1% Triton X-100, 0.1% SDS, 20% glycerol, plus complete protease and phosphatase inhibitor tablets (Roche). Lysates were separated by SDS-PAGE and incubated with the indicated antibodies.

Chemistry & Biology
Article

An Isoform-Selective, Small-Molecule Inhibitor Targets the Autoregulatory Mechanism of p21-Activated Kinase

Sean W. Deacon,[1,2] Alexander Beeser,[1,2,3] Jami A. Fukui,[1] Ulrike E.E. Rennefahrt,[1] Cynthia Myers,[1] Jonathan Chernoff,[1] and Jeffrey R. Peterson[1,*]
[1]Basic Sciences Division, Fox Chase Cancer Center, Philadelphia, PA 19111, USA
[2]These authors contributed equally to this work.
[3]Present address: Division of Biology, Kansas State University, Manhattan, KS 66506, USA.
*Correspondence: jeffrey.peterson@fccc.edu
DOI 10.1016/j.chembiol.2008.03.005

SUMMARY

Autoregulatory domains found within kinases may provide more unique targets for chemical inhibitors than the conserved ATP-binding pocket targeted by most inhibitors. The kinase Pak1 contains an autoinhibitory domain that suppresses the catalytic activity of its kinase domain. Pak1 activators relieve this autoinhibition and initiate conformational rearrangements and autophosphorylation events leading to kinase activation. We developed a screen for allosteric *i*nhibitors targeting *P*ak1 *a*ctivation and identified the inhibitor IPA-3. Remarkably, preactivated Pak1 is resistant to IPA-3. IPA-3 also inhibits activation of related Pak isoforms regulated by autoinhibition, but not more distantly related Paks, nor >200 other kinases tested. Pak1 inhibition by IPA-3 in live cells supports a critical role for Pak in PDGF-stimulated Erk activation. These studies illustrate an alternative strategy for kinase inhibition and introduce a highly selective, cell-permeable chemical inhibitor of Pak.

INTRODUCTION

Protein kinases are important therapeutic targets and are considered highly druggable owing to their conserved ATP-binding pocket that can accommodate small molecules. However, because of the evolutionary conservation of this pocket across kinases, ATP-competitive inhibitors can inhibit large numbers of other kinases in addition to their intended targets (Bain et al., 2007; Karaman et al., 2008). Recently, it was demonstrated that ATP-competitive inhibitors such as imatinib (Gleevec) can achieve unusually high kinase selectivity by binding a less conserved region adjacent to the ATP-binding pocket (Nagar et al., 2002; Schindler et al., 2000), thus underscoring the idea that inhibitor interactions with less conserved regions of a kinase can provide opportunities for greater kinase selectivity. Indeed, many kinases contain nonconserved sequence elements outside the kinase domain that mediate important facets of their function such as localization, substrate recruitment, or the regulation of catalytic activity. Several kinases contain autoinhibitory domains that bind and inhibit the activity of the catalytic domain (Cheetham, 2004). We, and others, have proposed that proteins regulated by autoinhibition may be susceptible to inhibition by small molecules that perturb the conformational changes that accompany relief of autoinhibition (Cheetham, 2004; Liu and Gray, 2006; Peterson et al., 2004; Peterson and Golemis, 2004). The additional domains and conformational changes that mediate kinase autoregulation may, therefore, provide novel opportunities for more specific small-molecule inhibition than ATP-competitive compounds.

Members of the *p*21-*a*ctivated *k*inases (Paks) are one such family that is subject to autoregulation. Group I Paks (Paks 1–3) are regulated by autoinhibition that is relieved by binding to the 21 kDa GTP-binding proteins Rac and Cdc42. This distinct regulatory mechanism is not observed, however, in the more distantly related group II Paks (Paks 4–6). However, Pak5 may undergo autoinhibition mediated by an unrelated domain (Ching et al., 2003). Autoinhibition of Pak1 is mediated by the formation of an inactive homodimer in which the autoregulatory region of one monomer binds and inhibits the catalytic domain of its partner and vice versa (Lei et al., 2000; Parrini et al., 2002). One critical element of the autoregulatory region is the kinase-inhibitory segment, which binds in the active site cleft and sequesters the kinase activation loop in an inactive conformation (Lei et al., 2000). Pak1 activation involves the local unfolding of the autoinhibitory domain caused by binding of Rac/Cdc42 to a partially overlapping region, resulting in Pak1 monomer dissociation and displacement of the inhibitory segment. Subsequent autophosphorylation events at multiple sites along Pak1 stabilize the catalytically competent, monomeric conformation (Chong et al., 2001; Lei et al., 2000; Parrini et al., 2002). This multistep activation cascade may offer additional opportunities for small-molecule binding that could selectively inhibit group I Paks.

Increasing data implicate Pak1 in tumorigenesis and metastasis (reviewed in Kumar et al., 2006). Thus, inhibitors of Pak1 have been suggested as a novel oncologic therapy (Kumar et al., 2006; Nheu et al., 2002). Although no highly selective inhibitors of Pak1 have been reported, several compounds originally identified for their ability to target other kinases also inhibit Pak family members (Eswaran et al., 2007; Nheu et al., 2002; Porchia et al., 2007). Here we report the identification and characterization of a highly selective, non-ATP-competitive inhibitor that targets the

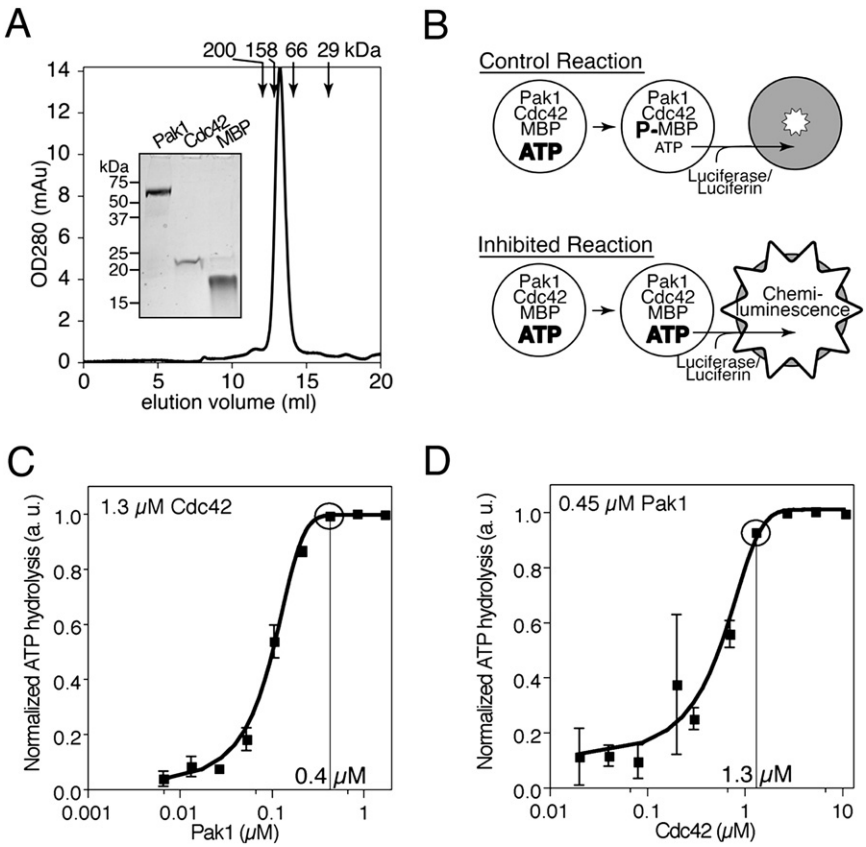

Figure 1. An ATP Depletion Assay Reports Cdc42-Dependent Pak1 Activation

(A) Recombinant Pak1 is a homodimer. The gel-filtration elution profile of Pak1 is shown. Elution volumes of standards are indicated. Inset: Coomassie-stained SDS-PAGE analysis of Pak1 and other proteins used in the screen.

(B) Pak1 assay scheme. Pak1 is incubated with its activator, GTPγS-charged Cdc42, and a substrate, myelin basic protein (MBP), in the presence of 10 μM ATP. Control kinase reactions (top) hydrolyze a substantial fraction of the starting ATP resulting in low final ATP concentrations, whereas inhibited reactions (bottom) do not. Residual ATP is enzymatically converted to chemiluminescence proportional to residual ATP.

(C) ATP hydrolysis is strictly Pak1-dependent. Cdc42 was incubated with MBP, ATP, and the indicated concentrations of Pak1. Residual ATP levels were measured as in (B). Results are expressed as ATP hydrolyzed in arbitrary units (normalized to the maximum ATP hydrolyzed) as a function of Pak1 concentration. Data points and error bars show mean and SEM of triplicate wells. Circled point indicates Pak1 concentration used in the screen.

(D) ATP hydrolysis by Pak1 is Cdc42-dependent. ATP depletion was monitored in reactions as in (C) except that the indicated concentrations of Cdc42 were used. Circled point indicates Cdc42 concentration used in the screen.

autoregulatory mechanism of group I Paks. This work illustrates how conformational rearrangements accompanying kinase activation can be exploited by compounds to achieve greater target specificity, and introduces a selective reagent for Pak inhibition.

RESULTS

A Chemical Screen Identifies IPA-3 as an Inhibitor of Pak1

To identify inhibitors of Pak1 activation, we developed a high-throughput assay measuring ATP hydrolysis as an indicator of Pak1 catalytic activity. Recombinant, full-length Pak1 exhibited an apparent molecular weight of ~130 kDa by gel-filtration chromatography (Figure 1A). SDS-PAGE analysis demonstrated the appropriate monomer molecular weight of ~60 kDa (Figure 1A, inset), as expected for the inactive Pak1 homodimer (Lei et al., 2000). Pak1 was incubated with individual compounds followed by addition of recombinant Cdc42-GTPγS (hereafter simply Cdc42) and myelin basic protein (MBP) as substrate (Figure 1A, inset) in the presence of 10 μM ATP (Figure 1B). Following incubation, nonhydrolyzed ATP was quantified using Kinase-Glo (Koresawa and Okabe, 2004). Titrations of both Pak1 (Figure 1C) and Cdc42 (Figure 1D) demonstrated that ATP hydrolysis was strictly dependent on both Pak1 and Cdc42. These results demonstrate that ATP hydrolysis measured in this assay is due to Pak1 kinase activity and confirm that the recombinant Pak1 utilized in the screen is autoinhibited yet activatable by Cdc42 as expected.

This assay was used to screen 33,000 structurally diverse small molecules in duplicate. Compounds inhibiting ATP hydrolysis by greater than three standard deviations below the mean of control reactions in both replicates were considered for further analysis. Approximately 1% of the compounds tested met this criterion. A secondary screen was then conducted on active compounds to identify those that were potentially non-ATP competitive. Individual compounds (10 μM) were incubated with Pak1, Cdc42, and MBP in the presence of [γ-^{32}P]ATP and were assayed for their ability to inhibit incorporation of [^{32}P]phosphate into MBP. To reduce the detection of undesired ATP-competitive inhibitors, reactions were conducted in the presence of 1 mM unlabeled ATP. Of the 342 compounds identified in the primary screen, 32 compounds continued to exhibit robust inhibition at 1 mM ATP. These compounds were ranked according to their relative potency and reproducibility of inhibition in subsequent assays, as well as their commercial availability. The cumulative results of these secondary assays led us to focus on one particular compound, 2,2′-dihydroxy-1,1′-dinaphthyldisulfide (Figure 2A; hereafter called IPA-3), that at 10 μM inhibited Pak1 activity by 95% ± 3%.

IPA-3 Is a Direct, Noncompetitive Inhibitor of Pak1

To determine the protein target of IPA-3, we performed Pak1 kinase assays in which MBP was omitted. Pak1 kinase activity was measured by monitoring Pak1 autophosphorylation using phospho-specific antibodies against threonine 423 within the activation loop (Thr423; Zenke et al., 1999). IPA-3 (10 μM) prevented Cdc42-stimulated Pak1 autophosphorylation on

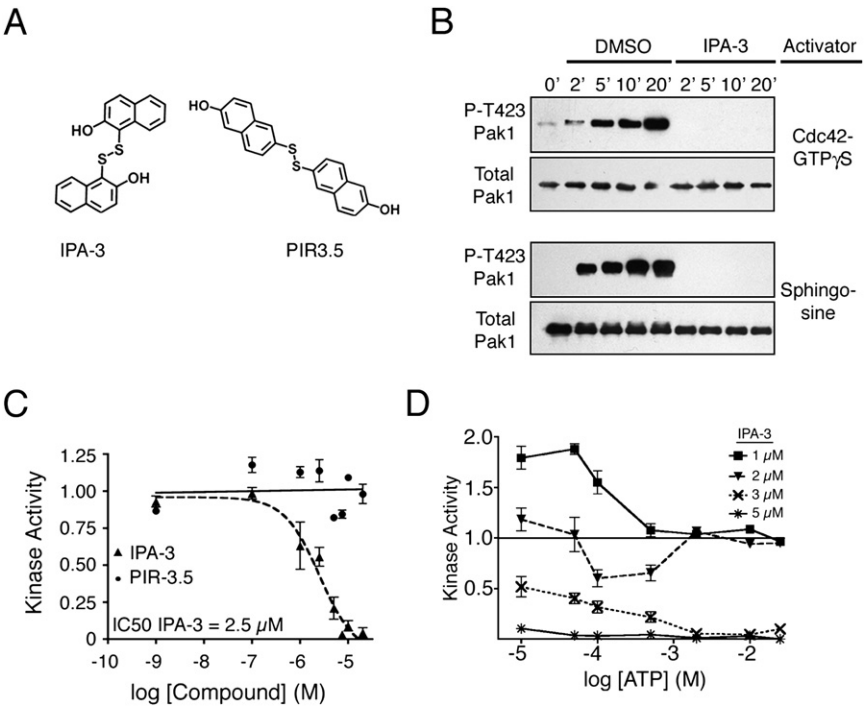

Figure 2. IPA-3 Is a Direct, Non-ATP-Competitive Inhibitor of Pak1

(A) Structure of IPA-3 and an inactive relative, PIR-3.5.

(B) IPA-3 directly inhibits Pak1 autophosphorylation. Pak1 was incubated with ATP and either Cdc42 (top panels) or sphingosine (bottom panels) in the presence of DMSO or 10 μM IPA-3. Samples were probed using phospho-specific antibodies against Pak1 Thr423. Data are representative of three experiments.

(C) IPA-3 inhibits Pak1 kinase activity with low micromolar potency. Pak1 was preincubated with the indicated concentrations of IPA-3 or PIR-3.5. Kinase reactions were started by addition of Cdc42, MBP, and a mixture of 1 mM ATP and [γ-^{32}P]ATP. Kinase activity is reported as phosphate incorporation onto MBP expressed as a ratio to MBP phosphorylated in reactions in the presence of solvent alone (1% DMSO). Data are represented as the mean ± SEM. n ≥ 3.

(D) IPA-3 is noncompetitive with ATP. Kinase assays were performed as in (C) at the indicated concentrations of ATP and IPA-3. n = 3.

Thr423 (Figure 2B, top), demonstrating that IPA-3 must target either Cdc42 or Pak1. We next substituted Cdc42 with a distinct Pak1 activator, the sphingolipid sphingosine (Bokoch et al., 1998). IPA-3 also prevented sphingosine-dependent Pak1 autophosphorylation (Figure 2B, bottom panel). Together, these assays demonstrate that Pak1 is the protein target of IPA-3. Furthermore, the inhibition of Thr423 phosphorylation, which is required for full activation of Pak1 (Zenke et al., 1999), indicates that IPA-3 may inhibit a step in the Pak1 activation process.

To confirm the chemical identity of the active compound, we developed a novel chemical synthesis of IPA-3 (see Figure S1 in the Supplemental Data available with this article online). The inhibitory activity of resynthesized IPA-3 was confirmed using in vitro kinase assays (data not shown), demonstrating that 2,2′-dihydroxy-1,1′-dinaphthyldisulfide was indeed the agent responsible for inhibition of Pak1 activity.

To determine the potency of IPA-3, kinase assays were performed at a range of compound concentrations, yielding an IC_{50} for IPA-3 of 2.5 μM (Figure 2C). A number of structurally related compounds were also tested (Figure S2), yet none inhibited Pak1 kinase activity as potently as IPA-3. A structural isomer of IPA-3, 2-naphthalenol-6,6′-dithiobis (Figure 2A, right), termed PIR-3.5 (*P*ak1 *i*nhibitor-*r*elated 3.5), displayed no inhibitory activity toward Pak1 (Figure 2C), and was therefore chosen as a negative-control compound for subsequent analyses.

The ability of IPA-3 to inhibit Pak1 activity at 1 mM ATP (Figure 2C) suggested that this compound might be noncompetitive with ATP. Indeed, when tested at a range of ATP concentrations, the inhibitory activity of IPA-3 was not decreased by increasing concentrations of ATP (Figure 2D). These results clearly demonstrate that Pak1 inhibition by IPA-3 is not competitive with ATP.

IPA-3 Does Not Target Exposed Cysteine Residues on Pak1

Cysteine-modifying agents that form mixed disulfides with protein targets have been shown to perturb the biological activity of proteins (Rice et al., 1995). Therefore, initial experiments to determine the mechanism of Pak1 inhibition by IPA-3 focused on the role of the disulfide bond in IPA-3 (Figure 2A). We found that IPA-3 inhibitory activity was dramatically reduced in the presence of >1 mM of the reducing agent dithiothreitol (DTT) (Figure 3A). We also found that addition of DTT could relieve inhibition of Pak1 when added after IPA-3 (Figure 3B). Thus, IPA-3 inhibition of Pak1 could be both prevented and reversed by 1 mM DTT.

The sensitivity of IPA-3 inhibition to DTT could be a result of reduction of IPA-3 itself or the reduction of an IPA-3-Pak1 adduct. We first considered the possibility that IPA-3 formed mixed disulfides with Pak1. Pak1 contains five cysteine residues, all of which are found in the kinase domain. Computational analysis of crystal structures of Pak1 kinase domain in both active (Lei et al., 2005) and autoinhibited conformations (Lei et al., 2000) using UCSF Chimera demonstrated that only two of those residues, Cys360 and Cys411, are surface exposed. To determine whether inhibition by IPA-3 could be a result of the formation of mixed disulfides with these cysteines, we mutated both residues to serine. Like wild-type Pak1, the mutated Pak1 (Pak1-CS) exhibited a basal level of kinase activity that was stimulated by addition of Cdc42 (Figure 3C). Importantly, Pak1-CS was similarly inhibited by 10 μM IPA-3 compared to wild-type Pak1 (Figure 3C), demonstrating that the mechanism of IPA-3 inhibition is not through the formation of mixed disulfides with Cys360 or Cys411. In addition, Pak1 migration in nonreducing SDS-PAGE and size-exclusion chromatography was not affected by IPA-3, ruling out IPA-3-mediated formation of Pak1 multimers or aggregates (not shown).

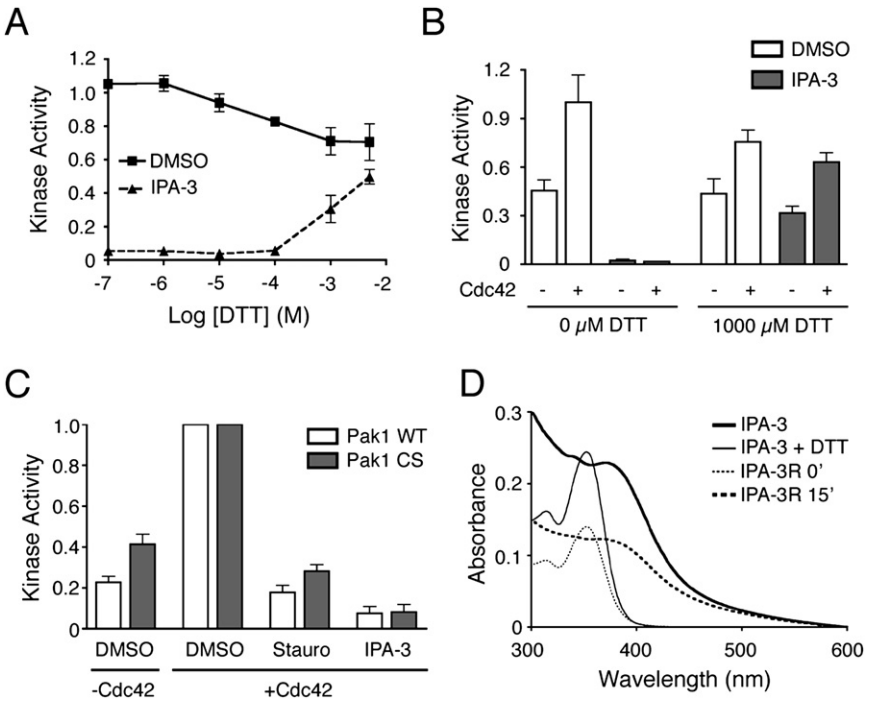

Figure 3. The Role of Disulfides in IPA-3-Mediated Pak1 Inhibition

(A) IPA-3 activity is diminished in the presence of the reducing agent DTT. IPA-3 (10 μM) was incubated with the indicated concentrations of DTT, followed by the addition of Pak1. Kinase activity was determined as in Figure 2. n = 6.

(B) DTT relieves IPA-3-dependent inhibition of Pak1 and restores Cdc42-mediated activation. Pak1 was incubated with IPA-3 and divided into vessels containing 0 or 1000 μM DTT, followed by addition of Cdc42 where indicated. Samples were subjected to kinase assays as in Figure 2. Data are represented as the mean ± SEM. n = 3.

(C) Mutation of solvent-accessible cysteine residues in Pak1 to serine does not prevent inhibition by IPA-3. Pak1-CS (Cys360 mutated to serine, Cys411 mutated to serine) and wild-type Pak1 were preincubated with either DMSO or the indicated compound. Kinase activity was determined as in Figure 2, and was normalized to the maximum activity in the presence of solvent alone (1% DMSO) and Cdc42. n = 5.

(D) Absorption spectroscopy suggests that the disulfide bond in IPA-3 is sensitive to reduction by DTT. Absorption spectra were recorded for 20 μM IPA-3 in the presence of 0 (thick trace) or 1000 μM (thin trace) DTT. A freshly prepared solution (20 μM) of the reduced form of IPA-3, IPA-3R (1-mercapto-2-hydroxynaphthalene), was also analyzed either immediately (thin dotted trace) or following a 15 min incubation on the benchtop (thick dotted trace). Data are representative of multiple experiments.

To test whether IPA-3 itself was sensitive to DTT, we analyzed a solution of IPA-3 by absorption spectroscopy in the presence of a range of DTT concentrations. We observed a dramatic change in the absorption spectrum of IPA-3 at ≥1 mM DTT (Figure 3D). Interestingly, chemically synthesized 1-mercapto-2-hydroxynaphthalene (IPA-3R), the expected product of the reduction of the disulfide in IPA-3, exhibited an absorption spectrum indistinguishable from that of IPA-3 in the presence of 1 mM DTT (Figure 3D). Furthermore, IPA-3R rapidly reoxidized into IPA-3 under our buffer conditions (Figure 3D). Thus, the sensitivity of IPA-3 inhibition to DTT is likely due to direct reduction of the IPA-3 disulfide, although we cannot formally rule out the possibility that IPA-3 forms a DTT-sensitive adduct with residues other than surface-exposed cysteines.

IPA-3 Targets the Pak1 Activation Mechanism

Pak1 activation is a multistep process involving the relief of autoinhibitory interactions and autophosphorylation at key residues (Buchwald et al., 2001; Chong et al., 2001; Zenke et al., 1999). IPA-3 inhibition of Thr423 autophosphorylation suggests that IPA-3 may inhibit steps in the Pak1 activation mechanism. To determine the point in Pak1 activation at which IPA-3 may be acting, a series of kinase assays were performed in which the order of addition of reaction components was systematically varied. Consistent with the results of the initial screen, when IPA-3 was added prior to Cdc42 and ATP, it significantly inhibited Pak1 kinase activity (Figure 4A, condition A). When added to Pak1 *after* incubation with Cdc42, but prior to the addition of ATP, IPA-3 similarly inhibited Pak1 (Figure 4A, condition B). Finally, we tested the ability of IPA-3 to inhibit Pak1 when added after both Cdc42 and ATP, when Pak1 is preactivated (Figure 2B, 20′). Strikingly, IPA-3 was much less effective at inhibiting this preactivated Pak1 (Figure 4A, IPA-3, condition C). In contrast, the ATP-competitive inhibitor staurosporine inhibited Pak1 kinase activity equally regardless of when it was added (Figure 4A, Stauro). The requirement that IPA-3 be present prior to Pak1 activation to be effective was also observed for Pak1 activated by sphingosine (data not shown). These results demonstrate that IPA-3 is ineffective at inhibiting preactivated Pak1. Moreover, the ability of IPA-3 to dramatically inhibit Pak1 only when added prior to Pak1 autophosphorylation suggests that IPA-3 inhibits a step in the Pak1 activation process.

The Conformation of Inhibitor-Bound Pak1

We hypothesized that IPA-3 might inhibit Pak1 activation by stabilizing the autoinhibited Pak1 conformation. Indeed, conformational stabilization of the autoinhibitory domain of N-WASP, which is structurally related to the autoinhibitory domain of Pak1 (Kim et al., 2000; Lei et al., 2000), has been reported for a small-molecule N-WASP inhibitor (Peterson et al., 2004). In addition, the symmetrical dimeric structure of IPA-3 suggests that this compound might contact both Pak1 monomers within the autoinhibited dimer. One important feature of the Pak1 autoinhibited conformation is the folding of the activation loop (residues 408–428) into the catalytic site of the kinase (Lei et al., 2000), thereby masking the activation loop and rendering Thr423

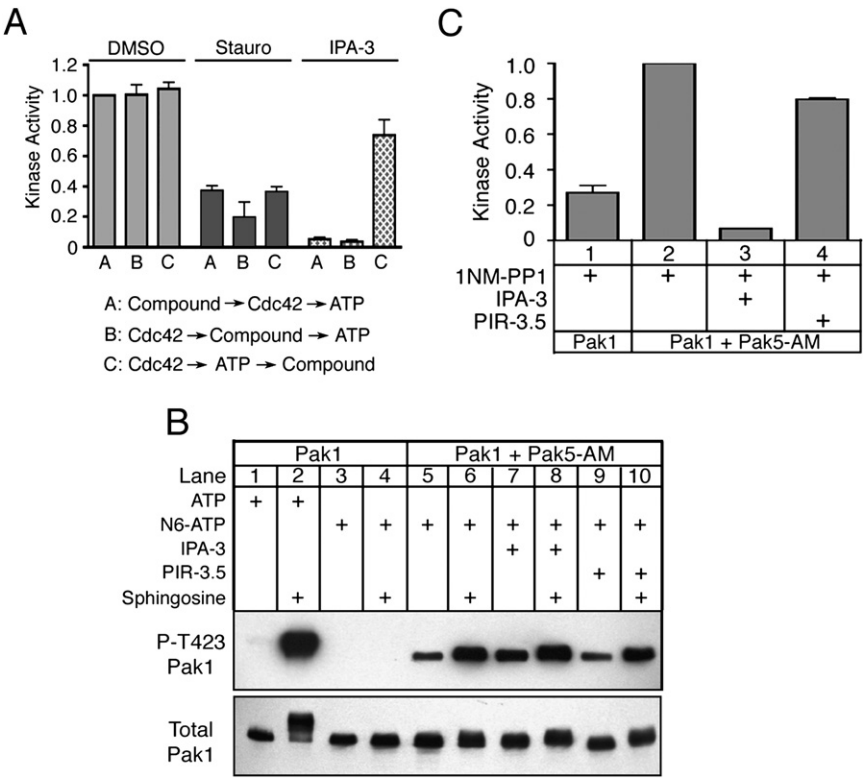

Figure 4. IPA-3 Targets the Pak1 Autoregulatory Mechanism

(A) IPA-3 inhibits Pak1 activation but does not inhibit preactivated Pak1. Pak1 was incubated with components in the following order: condition A: 10 μM compound, Cdc42 and ATP; condition B: Cdc42, compound, ATP; condition C: Cdc42 and ATP, compound. After all incubations, kinase reactions were initiated by addition of MBP and [γ-^{32}P]ATP. Kinase activity is reported as in Figure 2 and was normalized to reactions in the presence of 1% DMSO and Cdc42 under condition A. n ≥ 4.

(B) IPA-3 promotes the accessibility of Thr423 to phosphorylation by exogenous kinases. Pak1 was incubated with the indicated compound followed by addition of the ATP-binding pocket mutant Pak5 (Pak5-AM), sphingosine, and ATP or N^6-benzyl-ATP (N6-ATP). Reactions were analyzed using phospho-specific antibodies against Pak1 Thr423 or total Pak1. Data are representative of three experiments.

(C) Exogenous phosphorylation of Thr423 does not restore the kinase activity of IPA-3-inhibited Pak1. Pak1 was incubated as in (B) in the presence of 125 μM sphingosine and N6-ATP. Postincubation, 2 μM 1NM-PP1 was added to inhibit Pak5-AM, and kinase assays were conducted. Kinase activity is reported as in Figure 2 and normalized to the reaction in lane 2. Data are represented as the mean ± SEM. n = 4.

inaccessible to phosphorylation. On relief of autoinhibition, a large conformational change in the activation loop exposes Thr423 to phosphorylation by other Pak1 monomers as well as other kinases (King et al., 2000; Parrini et al., 2002; Zenke et al., 1999). Thus, accessibility of Thr423 to phosphorylation can be used to reveal whether the activation loop is in the "open" (active) or "closed" (inactive) conformation. We therefore tested the ability of exogenous kinases to phosphorylate Thr423 in the presence of IPA-3. We have found that Pak5 can phosphorylate Thr423 of Pak1 in vitro but is itself insensitive to IPA-3 (see below). For this reason, Pak5 was chosen as the exogenous kinase for this assay.

To ensure that at all Thr423 phosphorylation was mediated by Pak5, we mutated the gatekeeper residue of Pak5 (methionine 523) to glycine according to the strategy pioneered by Shokat and colleagues (Liu et al., 1998). This Pak5 *A*TP-binding pocket *m*utant (Pak5-AM) can utilize the bulky ATP derivative N^6-benzyl-ATP (N6-ATP), whereas wild-type Pak1 cannot (Figure 4B, compare lanes 3 and 5). In vitro kinase assays using N6-ATP revealed that Pak5-AM phosphorylates Pak1 on Thr423, and that these phosphorylation events were enhanced in the presence of sphingosine (Figure 4B, lanes 5 and 6). Importantly, IPA-3 did not prevent Pak1 phosphorylation by Pak5-AM and, indeed, promoted Thr423 phosphorylation in the absence of sphingosine (Figure 4B, compare lanes 5 and 7). Thus, IPA-3 does not stabilize the native autoinhibited conformation of Pak1 but instead promotes a conformation of Pak1 in which Thr423 is exposed. Similar results were obtained using 3-phosphoinositide-dependent kinase 1 (PDK1), another Thr423-directed kinase (King et al., 2000 Figure S3A).

That Thr423 can be phosphorylated by exogenous kinases but not by Pak1 itself in the presence of IPA-3 suggested that phosphorylation of this residue by exogenous kinases might overcome Pak1 inhibition by IPA-3. To test this, we took advantage of the observation that the gatekeeper residue mutation in Pak5-AM renders Pak5-AM sensitive to inhibition by the ATP-competitive inhibitor 1NM-PP1, whereas wild-type Pak1 kinase activity was unaffected (Figure S3B). We first incubated Pak1 with Pak5-AM and N6-ATP in the presence of sphingosine and either DMSO or IPA-3. Next we added 1NM-PP1, MBP, and a mixture of ATP and [γ-^{32}P]ATP to specifically measure Pak1 catalytic activity. Prephosphorylation of Pak1 with Pak5-AM and N6-ATP led to a significant increase in Pak1 catalytic activity (Figure 4C, lane 1 versus 2). However, Pak5-AM phosphorylation of Pak1 did not overcome inhibition by IPA-3 (Figure 4C, lane 3). Inhibition of MBP phosphorylation by IPA-3 is due to direct inhibition of Pak1, as the Pak5-AM phosphorylation of Pak1 was not affected by IPA-3 (Figure 4B, lanes 6 and 8). Together, these results demonstrate that in the presence of IPA-3, Pak1 adopts a conformation in which Thr423 is exposed and therefore must be distinct from the autoinhibited conformation. Nevertheless, this conformation is catalytically inactive and cannot be reactivated by phosphorylation by exogenous kinases. In addition, these results demonstrate that a group II Pak (Pak5) can phosphorylate the activation loop of a group I Pak (Pak1) in vitro, suggesting the possibility of regulatory crosstalk between the two Pak groups.

IPA-3 Targets Group I Paks

The Pak1 autoregulatory strategy is conserved in all group I Paks (Paks 1–3). By contrast, the group II Paks (Paks 4–6) do not contain the inhibitory domain found in group I Paks, and are not thought to undergo autoinhibition by the same mechanism. We

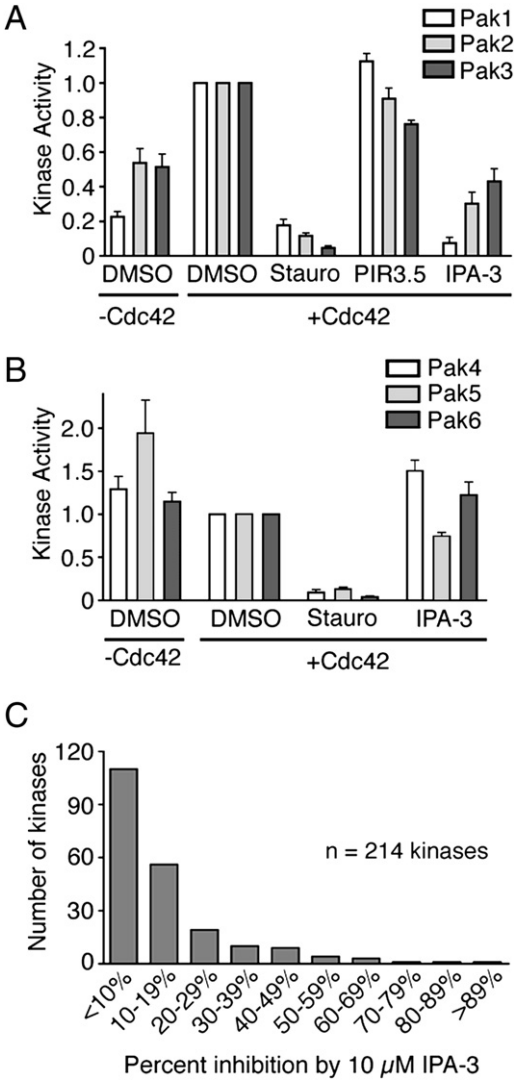

Figure 5. IPA-3 Kinase Selectivity

(A) IPA-3 inhibits all group I Paks. Paks were incubated with 10 μM indicated compound followed by addition of buffer or Cdc42, MBP, and a mixture of 1 mM ATP and [γ-^{32}P]ATP. Kinase activity is reported as in Figure 2. n ≥ 3.

(B) IPA-3 is not an effective inhibitor of group II Paks. Purified Pak4 kinase domain or full-length Pak5 and Pak6 were tested in kinase reactions as described in (A). n ≥ 4.

(C) Distribution of IPA-3 inhibitory activity against recombinant kinases. Full-length human kinases (214) were treated with 10 μM IPA-3 and subjected to kinase assays. The histogram represents the number of kinases that displayed the indicated mean percent inhibition compared to control reactions without inhibitor in two independent experiments. Data are represented as the mean ± SEM.

therefore tested IPA-3 on all members of the Pak family. As expected, full-length Paks 1–3 displayed basal levels of kinase activity that were stimulated by the addition of Cdc42 (Figure 5A). Dramatic inhibition of kinase activity in the presence 10 μM IPA-3 but not PIR-3.5 was observed for all three group I Paks, with the strongest inhibition observed for Pak1 (Figure 5A).

We next tested the ability of IPA-3 to inhibit full-length Pak5 and Pak6 and a catalytic fragment of Pak4. Consistent with reports demonstrating that these kinases do not undergo autoinhibition or Rac/Cdc42-mediated activation (Abo et al., 1998; Cau et al., 2001; Lee et al., 2002), the basal kinase activity of the group II Paks was not stimulated by Cdc42 (Figure 5B). Importantly, the kinase activity of Paks 4–6 was not dramatically inhibited by 10 μM IPA-3 (Figure 5B, IPA-3). Taken together, these results demonstrate that IPA-3 exhibits selectivity for the group I versus group II Paks.

Kinase Specificity of IPA-3

To determine the specificity of IPA-3 across a larger fraction of the kinome, we tested the ability of this compound to inhibit 214 full-length human kinases using an assay that monitors phosphorylation of a peptide substrate (Invitrogen Z′-Lyte). IPA-3 (10 μM) significantly inhibited (≥50% inhibition) only 9 of the kinases tested (4% of total) (Figure 5C; Table S1). By comparison, the broad-spectrum kinase inhibitor staurosporine, the highly selective Bcr-Abl inhibitor imatinib, and the receptor tyrosine kinase inhibitor gefitinib inhibited (by ≥50%) 93%, 12%, and 21% of the kinases tested, respectively (data not shown). Although Pak2 and Pak3 were represented in the collection of kinases tested, they were not significantly inhibited by IPA-3. This can be explained by the fact that the recombinant Paks used in the Z′-Lyte assay are preactivated and no longer responsive to Cdc42 (Figure S4). It should be also be noted that 34 of 214 kinases were tested in the presence of 1 mM DTT (see Table S1), conditions sufficient to reduce the IPA-3 disulfide. Nevertheless, these data demonstrate the remarkable kinase specificity of IPA-3, and further support the notion that this inhibitor acts on the unique regulatory cycle of group I Paks.

IPA-3 Inhibits Pak1-Mediated Signaling In Vivo

Platelet-derived growth factor (PDGF) promotes Pak activation in fibroblasts (Beeser et al., 2005). We therefore tested the ability of IPA-3 to inhibit PDGF-stimulated Pak activation in mouse embryonic fibroblasts. Both basal and PDGF-stimulated Pak activities were impeded by 30 μM IPA-3 as assessed by in-gel kinase assay (Figure 6, upper panel, arrows). In contrast, the activity of an unidentified ~40 kDa kinase was unaffected (upper panel, arrowhead). Western blotting of the same lysates with group I-specific Pak antibodies showed that the increase in Pak apparent molecular weight in control PDGF-stimulated cells, likely due to Pak autophosphorylation, was also inhibited by IPA-3 (Figure 6, Total Pak). The inhibition of Pak's apparent molecular weight increase by IPA-3 in cells was also observed in vitro (Figure 2B, bottom panel), supporting a common inhibitory mechanism. These data show that IPA-3 can inhibit activation of group I Paks in cells. The need for higher concentrations of IPA-3 for Pak inhibition in cells compared to in vitro is likely due to reduction of the IPA-3 disulfide bond in the reducing cytoplasmic environment. This would be expected to be counteracted by the large, exchangeable reservoir of IPA-3 present in the nonreducing cell-culture medium, thus maintaining a sufficient intracellular concentration of active compound.

To assess the effect of IPA-3 on signaling components upstream of Pak, the same cell lysates were analyzed using phospho-specific antibodies against activated forms of the PDGF receptor and Akt. IPA-3 had little effect on these signaling events upstream of Pak. By contrast, Erk activation by PDGF, which

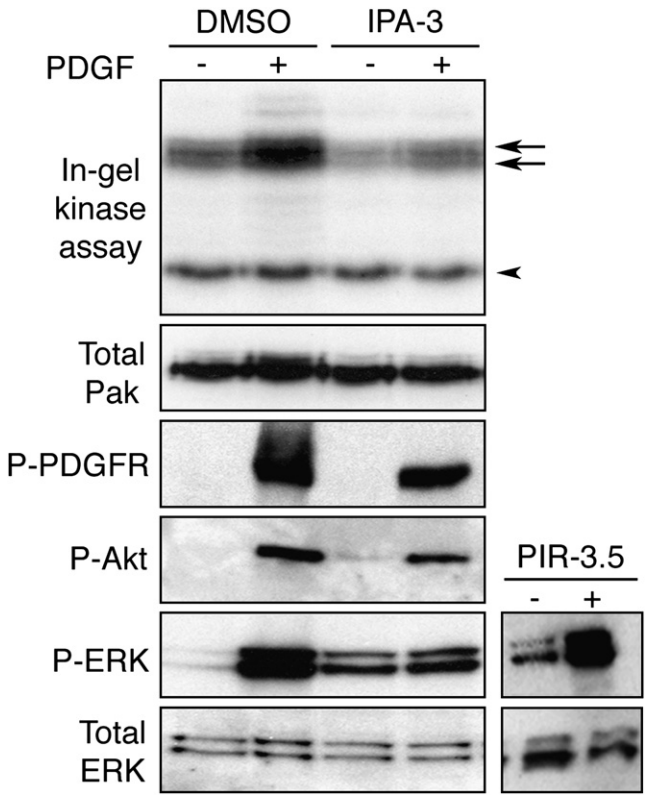

Figure 6. IPA-3 Selectively Inhibits Pak1 Activation in Mammalian Cells

Mouse embryonic fibroblasts were serum starved for 18 hr, followed by treatment with 30 μM IPA-3, PIR-3.5 (right panels), or DMSO for 10 min. Cells were stimulated with 10 μg/ml PDGF-BB for 5 min and lysed. Cell lysates were normalized by protein concentration and probed with antibodies as described in Experimental Procedures. Endogenous Pak kinase activity was observed by in-gel kinase assay.

we and others have shown is dependent on Pak (Beeser et al., 2005; Tang et al., 1997), was strongly inhibited by IPA-3 (Figure 6). Interestingly, IPA-3 caused a slight elevation in basal Erk activity even in the absence of PDGF, although this effect was cell-type-dependent (data not shown). As expected, the control compound PIR-3.5 did not inhibit Erk activation (Figure 6, right panels). Thus, IPA-3 specifically and selectively inhibits signaling events mediated by group I Paks.

DISCUSSION

The work presented here describes the identification of a highly selective inhibitor of group I Pak kinases that achieves this selectivity by targeting the distinct autoregulatory mechanism conserved in group I Paks. That IPA-3 targets this regulatory mechanism and not the kinase active site directly is supported by the following findings. First, the inhibition of Pak1 is noncompetitive with respect to ATP. Second, IPA-3 targets the group I but not group II Pak kinases, which share a highly conserved C-terminal kinase domain but differ in their N-terminal regulatory sequence elements. Third, IPA-3 inhibits activation of Pak1 by diverse activators, but does not inhibit preactivated Pak1. Finally, IPA-3 does not prevent rearrangements of the activation loop that result in phosphorylation by exogenous kinases. One interpretation of these findings is that IPA-3 prevents Pak1 activation by stabilizing an activation intermediate that is semi-open yet catalytically inactive. A precise understanding of the molecular basis of Pak1 inhibition by IPA-3, however, awaits detailed structural studies.

A number of endogenous protein regulators of Pak1 kinase activity have been reported that appear to target the Pak1 autoregulatory strategy. hPIP1 (Xia et al., 2001), CRIPak (Talukder et al., 2006), and the tumor suppressor merlin (Kissil et al., 2003) have all been shown independently to bind the Pak1 autoregulatory region and inhibit kinase activity. CIB1 also binds this region but, like Rac and Cdc42, promotes Pak1 activity rather than inhibiting it (Leisner et al., 2005). These observations suggest that modulation of the Pak1 autoregulatory domain may be a physiologically relevant strategy for regulating catalytic activity. Therefore, it is conceivable that IPA-3 may bind and/or inhibit Pak1 in a manner that mimics endogenous protein inhibitors.

As expected for an allosteric kinase inhibitor, kinase profiling experiments revealed a high degree of kinase selectivity to IPA-3 inhibition (Table S1). The lack of kinase domain sequence similarity or functional overlap in IPA-3 kinase targets is not unexpected for a compound targeting a nonconserved regulatory mechanism. Indeed, specificity profiling of clinical kinase inhibitors has shown that many selective compounds also target seemingly unrelated kinases (Karaman et al., 2008). These observations emphasize the importance of broad kinase profiling experiments in the characterization of kinase inhibitor selectivity. To our knowledge, the profiling studies of IPA-3 reported here (Table S1) describe the first chemical inhibitor of Pak1 that achieves documented specificity comparable to that of the clinically relevant kinase inhibitors imatinib and gefitinib.

Although IPA-3 represents a novel experimental reagent to inhibit Pak kinase activity, other groups have reported the use of small molecules derived from known ATP-competitive kinase inhibitors to target Pak1 (Nheu et al., 2002; Porchia et al., 2007). However, these inhibitors target a number of other kinases, and their broader kinase selectivity has not been reported. An alternative approach to inhibiting Pak kinase activity has been the expression of recombinant fragments such as the Pak inhibitory domain or catalytically inactive mutants of Pak1 that inhibit the activity of endogenous Pak protein, although these may cause unintended Pak-independent side effects (Thullberg et al., 2007). By contrast, we show here that IPA-3 is Pak isoform selective, cell permeable, and rapidly acting. As such, this compound can serve as a distinct tool to elucidate Pak function in cells and may facilitate the validation of Pak inhibitors as a therapeutic strategy.

The screening strategy used to identify IPA-3 relied on the use of full-length Pak1 prepared under conditions that preserve the native autoregulatory mechanism. This is in contrast to the dominant paradigm in kinase-targeted screens of utilizing constitutively active kinase or isolated kinase domains (Sebolt-Leopold and English, 2006). These screens are biased toward inhibitors targeting the active site and are restricted in their ability to exploit sequence differences outside the catalytic domain. The results presented here support the possibility that screens using full-length kinase may provide unexpected opportunities for allosteric inhibition. This strategy need not be restricted to kinases,

however, and could be utilized for other enzymes or noncatalytic proteins that undergo conformational regulation (Peterson and Golemis, 2004). Indeed, for scaffolding proteins, conformational inhibitors of this type may provide the only route to achieving inhibition by small molecules.

SIGNIFICANCE

Lack of target specificity is a major limitation of many widely used kinase inhibitors. This results in part from the high degree of evolutionary conservation in the ATP-binding pocket targeted by these compounds across the human kinome. Nonconserved regulatory elements found in some kinases may offer unique targets for more selective kinase inhibition. Here we test this hypothesis using the p21-activated kinase 1 and report the screening for and identification of a highly selective, cell-permeable inhibitor that targets the Pak1 autoregulatory mechanism. Biochemical studies suggest that IPA-3 may trap a transient intermediate step in Pak activation, because preactivated Pak1 is insensitive to IPA-3. In addition, IPA-3-bound Pak1 exhibits some but not all structural features of the active conformation, and is catalytically inactive. Critically, kinase specificity profiling studies reveal an exceptional degree of kinase selectivity by IPA-3, consistent with its targeting the unique Pak1 regulatory domain. Furthermore, cell-based experiments using IPA-3 provide evidence that Pak promotes mitogen-activated protein kinase activation and illustrate selective inhibition of Pak in live cells. Thus, kinase autoregulatory mechanisms provide an alternative target for kinase inhibition by small molecules. The widespread use of constitutively active, recombinant kinase forms in kinase inhibitor screening programs likely limits the identification of compounds acting by such novel allosteric mechanisms. Our results suggest that screening assays that recapitulate biologically important regulatory mechanisms may reveal additional opportunities for selective kinase inhibition.

EXPERIMENTAL PROCEDURES

Protein Purification and Characterization

The following proteins were purified as described: Cdc42-GTPγS (Peterson et al., 2001), Pak2 (Rennefahrt et al., 2007), Pak4 and Pak5 catalytic domains (Eswaran et al., 2007), and full-length Pak1 (Rennefahrt et al., 2007). Full-length Pak3 (Bagrodia et al., 1995) and Pak5 (Cotteret et al., 2003) were expressed in HEK293 cells and immunopurified (see below). Full-length Pak6 (PV3502) was purchased from Invitrogen. MBP was purchased (Sigma) or purified from bovine brain acetone powder (Sigma) as described (Prowse et al., 2000).

Recombinant Pak1 was characterized by analytical gel-filtration chromatography on a calibrated Superdex 200 10/300 GL column. For the identification of surface-exposed cysteine residues within Pak1, computational analysis of crystal structures of Pak1 kinase domain in both active (Lei et al., 2005) and autoinhibited conformations (Lei et al., 2000) was performed using the MS/MS solvent accessibility module of UCSF Chimera (Pettersen et al., 2004).

Immunopurification of Pak3 and Pak5

HEK293 cells were transfected with 0.5 μg Pak3 or myc-Pak5 DNA using liposome-mediated transfection (Lipofectamine 2000, Invitrogen). Forty-eight hours posttransfection, cells were washed in ice-cold phosphate-buffered saline (PBS) and lysed into lysis buffer (20 mM Tris [pH 7.5], 150 mM NaCl, 1 mM EDTA, 1 mM EGTA, 1% Triton X-100, 1 mM phenylmethylsulfonyl fluoride (PMSF), and 10 μg/ml each of chymostatin, leupeptin, and pepstatin). Insoluble material was removed by centrifugation at 12,000 × g for 10 min at 4°C. Lysates were incubated with protein A agarose (Pierce) and either anti-Pak3 (Cell Signaling Technology) or anti-myc (Santa Cruz Biotechnology) for at least 2 hr at 4°C. Precipitates were washed twice in lysis buffer and once in assay buffer (50 mM HEPES [pH 7.5], 25 mM NaCl, 1.25 mM $MgCl_2$, 1.25 mM $MnCl_2$).

Chemical Compounds

The compound library consisted of 30,000 diverse compounds, largely conforming to Lipinski's rules, obtained from ChemDiv and the Challenge Set, Mechanistic Diversity Set, Natural Products Set, and Structural Diversity Set provided by the Developmental Therapeutic Program (DTP) of the National Cancer Institute. Compounds were stored as 5 mM DMSO stock solutions (except for the Mechanistic Diversity Set compounds, which were stored at 0.5 mM) at −80°C and were thawed immediately prior to use in a dessicator. IPA-3 was resynthesized and characterized as described in the Supplemental Experimental Procedures. PIR (*P*ak *i*nhibitor-*r*elated) compounds were provided as dry powder by the DTP.

High-Throughput Luminescence Assay for Inhibitors of Pak1 Activation

Recombinant Pak1 (8 μl of a 50 μg/ml solution) in assay buffer was aliquotted using a BioTek MicroFill into wells of columns 2–23 of a 384-well plate (Corning). Individual compounds were then added using disposable 384-pin polypropylene pin replicators (Genetix) to transfer ~20 nl from compound stock plates. Reactions were started by the addition of a solution (7 μl per well) containing MBP (0.32 mg/ml), GTPγS-charged Cdc42 (2.9 mg/ml), and ATP (21 μM) in assay buffer. Final reaction composition: 450 nM Pak1, 1.3 μM Cdc42, 0.15 mg/ml MBP, 10 μM ATP, 0.1% DMSO, and library compounds at ~7 μM. Plates were incubated for 2 hr at 30°C. Reactions were stopped by the addition of an equal volume of Kinase-Glo reagent (Promega) and incubated for 10 min at room temperature. Chemiluminescence was measured at 555 nm (20 nm emission slit) using a Cary Eclipse fluorescence spectrophotometer (Varian) equipped with a microplate carrier.

Compound stock plates were organized with library compounds in columns 3–22 (20 μl of a 5 mM solution in DMSO). Column 2 contained three wells of 2 mM staurosporine as positive controls and the remaining wells of column 2 contained DMSO as negative controls. Column 23 was empty and these wells served as a "no-addition" control. All compound plates were screened in duplicate.

Data analysis was conducted on a plate-by-plate basis in Microsoft Excel. Mean and standard deviation of the luminescence intensity of all wells were calculated. Wells containing compounds that resulted in luminescence intensities greater than three standard deviations above the mean of control samples in both replicate plates were considered hits.

In Vitro Kinase Assays

Pak1 (571 nM final) in assay buffer was mixed with DMSO or compound for 5 min at room temperature, followed by addition of 4 μM Cdc42 and 8.3 μM MBP for an additional 5 min. Kinase reactions were started by addition of unlabeled ATP and 1–10 μCi [γ-^{32}P]ATP per reaction for 10 min at 30°C. Final DMSO concentration was 1%. Kinase reactions were stopped on dry ice. Under these conditions, MBP phosphorylation was linear with time.

Kinase assays for Figure 4 were carried out as follows. Condition A: Pak1 was incubated for 5 min at room temperature with compound followed by addition of 4 μM Cdc42 and ATP for 20 min at 30°C. Condition B: Pak1 was incubated with Cdc42 for 20 min at 30°C, followed by addition of compound for 5 min. Condition C: Pak1 was incubated with Cdc42 and ATP for 20 min at 30°C, followed by addition of compound for 5 min. These incubations were followed by addition of 8.3 μM MBP and a mixture of ATP and [γ-^{32}P]ATP for 10 min at 30°C. Final conditions for all reactions were 1% DMSO, 1 mM ATP, and 1–10 μCi [γ-^{32}P]ATP. Reaction products were analyzed by scintillation counting (Rennefahrt et al., 2007) or by phosphorimager analysis (Fujifilm). Background counts from no kinase controls were subtracted from all values (scintillation counting assays) and kinase activity was reported as phosphate incorporation onto MBP expressed as a ratio to MBP phosphorylated in the presence of solvent alone. Phosphorimager background values were defined as the signal density of an area surrounding each individual phospho-MBP band and were subtracted from the corresponding phospho-MBP band.

Pak1 Autophosphorylation Assays

Recombinant Pak1 (571 nM final) in assay buffer was incubated with either DMSO or the indicated compound in DMSO (1% DMSO final). This mixture was incubated for 5 min at room temperature followed by the addition of either 4 μM Cdc42-GTPγS or 50 μM sphingosine (Avanti Polar Lipids) for 5 min. Kinase reactions were started by the addition of 1 mM ATP. Reactions were stopped by addition of SDS sample buffer (62.5 mM Tris [pH 6.8], 70 mM SDS, 100 mM DTT, 10% glycerol) and boiled at 95°C for 5 min. Samples were subjected to SDS-PAGE and western blotting analysis using phospho-specific antibodies against the activation loop autophosphorylation site threonine 423 (Cell Signaling Technology). Total Pak1 was detected with anti-Pak antibodies (C19, Santa Cruz).

Spectral Analysis of IPA-3

IPA-3 was diluted to 20 μM in 50 mM Tris (pH 8.0) containing the indicated concentration of DTT. Samples were vortexed and analyzed in a Cary 50 Bio spectrophotometer (Varian). IPA-3 spectral traces were background subtracted from traces of buffer containing DMSO alone (0.1%). Individual traces were normalized to 0 absorbance units at 600 nm.

The absorption spectrum of IPA-3R was obtained by preparing a fresh 20 mM DMSO stock from powder that was immediately diluted into degassed 50 mM Tris (pH 7.5) to 20 μM (0.1% DMSO). This sample was vortexed and the spectrum was obtained as described above either immediately or after incubation for 15 min on the benchtop.

Thr423 Accessibility Assay

Pak1 (571 nM) in assay buffer was incubated with compound and Pak5-AM (692.5 nM final), ATP or N^6-benzyl-ATP (25 μM; Axxora), and 125 μM sphingosine or DMSO at 30°C for 20 min. Samples were analyzed by immunoblot analysis using antibodies against Pak1 phospho-Thr423.

For determination of Pak1 kinase activity, samples prepared as above received DMSO or 2 μM 1NM-PP1 (Calbiochem) (3% final DMSO), 8.3 μM MBP, and a mixture of ATP and [γ-^{32}P]ATP (25 μM). Samples were incubated for 10 min at 30°C. Pak1 kinase activity was determined via phosphorimager analysis.

Dephosphorylation of Recombinant Pak2

To obtain inactive, dephosphorylated Pak2, 100 nM recombinant full-length Pak2 was treated with 100 U λ protein phosphatase (New England Biolabs) for 30 min at 30°C in assay buffer supplemented with 3.25 μM $MnCl_2$. Dephosphorylation of Pak2 was confirmed by western blot using phospho-specific antibodies against Pak T423. Phosphatase activity was inhibited by addition of 50 μM $NaVO_4$ and 1 mM β-glycerophosphate.

Z-Lyte Assay

The Z-Lyte assay was performed by Invitrogen. Percent inhibition was expressed as a ratio of phosphorylated product formed in the presence of 10 μM IPA-3 compared to phosphorylated product formed in reactions containing 1% DMSO. Inhibition data reflect mean kinase inhibition from two independent trials.

Cell Treatment with IPA-3

Mouse embryonic fibroblasts immortalized with SV40 large T antigen were grown in DMEM + 10% serum. Cells at 60%–80% confluency were starved for 18 hr in serum-free DMEM. Cells were pretreated with DMSO or 30 μM compound for 10 min, followed by addition of PDGF-BB (10 ng/ml; Sigma) for 5 min. Cells were washed in ice-cold PBS and lysed into Roberts buffer (50 mM Tris [pH 8], 10% glycerol, 1 mM EDTA, 137 mM NaCl, 1% NP-40 plus aprotinin, 1 mM PMSF, 1 mM $NaVO_4$). Insoluble material was removed by centrifugation, and protein concentration was determined by BCA assay (Pierce). Equal protein amounts were subjected to SDS-PAGE and western blotting using anti-Pak1 (C19, Santa Cruz), anti-phospho-PDGFR (3161), anti-phospho-Akt (9271), anti-phospho-ERK (9102) (Cell Signaling Technologies), and anti-ERK (V1141, Promega). In-gel kinase assays were performed as described (Beeser et al., 2005) with MBP as substrate.

Additional methods can be found in the Supplemental Experimental Procedures.

SUPPLEMENTAL DATA

Supplemental Data include four figures, one table, Supplemental Experimental Procedures, and Supplemental References and can be found with this article online at http://www.chembiol.com/cgi/content/full/15/4/322/DC1/.

ACKNOWLEDGMENTS

We thank B. Turk and H. Roeder for comments on the manuscript, and G. Michaud for his contribution to IPA-3 specificity profiling. This work was supported by the Department of Defense NF Research Program (W81XWH-05-1-0200), by an AACR-FCCC Career Development Award, and by a grant from the Pennsylvania Department of Health to J.R.P., and by the NIH (RO1-CA117884) and the Department of Defense NF Research Program (W81XWH-06-1-0213) to J.C. The Pennsylvania Department of Health disclaims responsibility for any analyses, interpretations, or conclusions. S.W.D. was supported by NCI funding (CA009035). Further support was provided by the NIH (CA006927) and an appropriation from the Commonwealth of Pennsylvania to Fox Chase Cancer Center. The authors declare no conflicts of interest.

Received: November 15, 2007
Revised: February 25, 2008
Accepted: March 3, 2008
Published: April 18, 2008

REFERENCES

Abo, A., Qu, J., Cammarano, M.S., Dan, C., Fritsch, A., Baud, V., Belisle, B., and Minden, A. (1998). PAK4, a novel effector for Cdc42Hs, is implicated in the reorganization of the actin cytoskeleton and in the formation of filopodia. EMBO J. *17*, 6527–6540.

Bagrodia, S., Taylor, S.J., Creasy, C.L., Chernoff, J., and Cerione, R.A. (1995). Identification of a mouse p21Cdc42/Rac activated kinase. J. Biol. Chem. *270*, 22731–22737.

Bain, J., Plater, L., Elliott, M., Shpiro, N., Hastie, C.J., McLauchlan, H., Klevernic, I., Arthur, J.S., Alessi, D.R., and Cohen, P. (2007). The selectivity of protein kinase inhibitors: a further update. Biochem. J. *408*, 297–315.

Beeser, A., Jaffer, Z.M., Hofmann, C., and Chernoff, J. (2005). Role of group A p21-activated kinases in activation of extracellular-regulated kinase by growth factors. J. Biol. Chem. *280*, 36609–36615.

Bokoch, G.M., Reilly, A.M., Daniels, R.H., King, C.C., Olivera, A., Spiegel, S., and Knaus, U.G. (1998). A GTPase-independent mechanism of p21-activated kinase activation. Regulation by sphingosine and other biologically active lipids. J. Biol. Chem. *273*, 8137–8144.

Buchwald, G., Hostinova, E., Rudolph, M.G., Kraemer, A., Sickmann, A., Meyer, H.E., Scheffzek, K., and Wittinghofer, A. (2001). Conformational switch and role of phosphorylation in PAK activation. Mol. Cell. Biol. *21*, 5179–5189.

Cau, J., Faure, S., Comps, M., Delsert, C., and Morin, N. (2001). A novel p21-activated kinase binds the actin and microtubule networks and induces microtubule stabilization. J. Cell Biol. *155*, 1029–1042.

Cheetham, G.M. (2004). Novel protein kinases and molecular mechanisms of autoinhibition. Curr. Opin. Struct. Biol. *14*, 700–705.

Ching, Y.P., Leong, V.Y., Wong, C.M., and Kung, H.F. (2003). Identification of an autoinhibitory domain of p21-activated protein kinase 5. J. Biol. Chem. *278*, 33621–33624.

Chong, C., Tan, L., Lim, L., and Manser, E. (2001). The mechanism of PAK activation. Autophosphorylation events in both regulatory and kinase domains control activity. J. Biol. Chem. *276*, 17347–17353.

Cotteret, S., Jaffer, Z.M., Beeser, A., and Chernoff, J. (2003). p21-activated kinase 5 (Pak5) localizes to mitochondria and inhibits apoptosis by phosphorylating BAD. Mol. Cell. Biol. *23*, 5526–5539.

Eswaran, J., Lee, W.H., Debreczeni, J.E., Filippakopoulos, P., Turnbull, A., Fedorov, O., Deacon, S.W., Peterson, J.R., and Knapp, S. (2007). Crystal structures of the p21-activated kinases PAK4, PAK5, and PAK6 reveal catalytic domain plasticity of active group II PAKs. Structure *15*, 201–213.

Karaman, M.W., Herrgard, S., Treiber, D.K., Gallant, P., Atteridge, C.E., Campbell, B.T., Chan, K.W., Ciceri, P., Davis, M.I., Edeen, P.T., et al. (2008). A quantitative analysis of kinase inhibitor selectivity. Nat. Biotechnol. *26*, 127–132.

Kim, A.S., Kakalis, L.T., Abdul-Manan, N., Liu, G.A., and Rosen, M.K. (2000). Autoinhibition and activation mechanisms of the Wiskott-Aldrich syndrome protein. Nature *404*, 151–158.

King, C.C., Gardiner, E.M., Zenke, F.T., Bohl, B.P., Newton, A.C., Hemmings, B.A., and Bokoch, G.M. (2000). p21-activated kinase (PAK1) is phosphorylated and activated by 3-phosphoinositide-dependent kinase-1 (PDK1). J. Biol. Chem. *275*, 41201–41209.

Kissil, J.L., Wilker, E.W., Johnson, K.C., Eckman, M.S., Yaffe, M.B., and Jacks, T. (2003). Merlin, the product of the Nf2 tumor suppressor gene, is an inhibitor of the p21-activated kinase, Pak1. Mol. Cell *12*, 841–849.

Koresawa, M., and Okabe, T. (2004). High-throughput screening with quantitation of ATP consumption: a universal non-radioisotope, homogeneous assay for protein kinase. Assay Drug Dev. Technol. *2*, 153–160.

Kumar, R., Gururaj, A.E., and Barnes, C.J. (2006). p21-activated kinases in cancer. Nat. Rev. Cancer *6*, 459–471.

Lee, S.R., Ramos, S.M., Ko, A., Masiello, D., Swanson, K.D., Lu, M.L., and Balk, S.P. (2002). AR and ER interaction with a p21-activated kinase (PAK6). Mol. Endocrinol. *16*, 85–99.

Lei, M., Lu, W., Meng, W., Parrini, M.C., Eck, M.J., Mayer, B.J., and Harrison, S.C. (2000). Structure of PAK1 in an autoinhibited conformation reveals a multistage activation switch. Cell *102*, 387–397.

Lei, M., Robinson, M.A., and Harrison, S.C. (2005). The active conformation of the PAK1 kinase domain. Structure *13*, 769–778.

Leisner, T.M., Liu, M., Jaffer, Z.M., Chernoff, J., and Parise, L.V. (2005). Essential role of CIB1 in regulating PAK1 activation and cell migration. J. Cell Biol. *170*, 465–476.

Liu, Y., and Gray, N.S. (2006). Rational design of inhibitors that bind to inactive kinase conformations. Nat. Chem. Biol. *2*, 358–364.

Liu, Y., Shah, K., Yang, F., Witucki, L., and Shokat, K.M. (1998). Engineering Src family protein kinases with unnatural nucleotide specificity. Chem. Biol. *5*, 91–101.

Nagar, B., Bornmann, W.G., Pellicena, P., Schindler, T., Veach, D.R., Miller, W.T., Clarkson, B., and Kuriyan, J. (2002). Crystal structures of the kinase domain of c-Abl in complex with the small molecule inhibitors PD173955 and imatinib (STI-571). Cancer Res. *62*, 4236–4243.

Nheu, T.V., He, H., Hirokawa, Y., Tamaki, K., Florin, L., Schmitz, M.L., Suzuki-Takahashi, I., Jorissen, R.N., Burgess, A.W., Nishimura, S., et al. (2002). The K252a derivatives, inhibitors for the PAK/MLK kinase family selectively block the growth of RAS transformants. Cancer J. *8*, 328–336.

Parrini, M.C., Lei, M., Harrison, S.C., and Mayer, B.J. (2002). Pak1 kinase homodimers are autoinhibited *in trans* and dissociated upon activation by Cdc42 and Rac1. Mol. Cell *9*, 73–83.

Peterson, J.R., and Golemis, E.A. (2004). Autoinhibited proteins as promising drug targets. J. Cell. Biochem. *93*, 68–73.

Peterson, J.R., Lokey, R.S., Mitchison, T.J., and Kirschner, M.W. (2001). A chemical inhibitor of N-WASP reveals a new mechanism for targeting protein interactions. Proc. Natl. Acad. Sci. USA *98*, 10624–10629.

Peterson, J.R., Bickford, L.C., Morgan, D., Kim, A.S., Ouerfelli, O., Kirschner, M.W., and Rosen, M.K. (2004). Chemical inhibition of N-WASP by stabilization of a native autoinhibited conformation. Nat. Struct. Mol. Biol. *11*, 747–755.

Pettersen, E.F., Goddard, T.D., Huang, C.C., Couch, G.S., Greenblatt, D.M., Meng, E.C., and Ferrin, T.E. (2004). UCSF Chimera—a visualization system for exploratory research and analysis. J. Comput. Chem. *25*, 1605–1612.

Porchia, L.M., Guerra, M., Wang, Y.C., Zhang, Y., Espinosa, A.V., Shinohara, M., Kulp, S.K., Kirschner, L.S., Saji, M., Chen, C.S., and Ringel, M.D. (2007). 2-amino-N-{4-[5-(2-phenanthrenyl)-3-(trifluoromethyl)-1H-pyrazol-1-yl]-phenyl} acetamide (OSU-03012), a celecoxib derivative, directly targets p21-activated kinase. Mol. Pharmacol. *72*, 1124–1131.

Prowse, C.N., Hagopian, J.C., Cobb, M.H., Ahn, N.G., and Lew, J. (2000). Catalytic reaction pathway for the mitogen-activated protein kinase ERK2. Biochemistry *39*, 6258–6266, Erratum: Biochemistry *39*(45), 2000.

Rennefahrt, U.E., Deacon, S.W., Parker, S.A., Devarajan, K., Beeser, A., Chernoff, J., Knapp, S., Turk, B.E., and Peterson, J.R. (2007). Specificity profiling of Pak kinases allows identification of novel phosphorylation sites. J. Biol. Chem. *282*, 15667–15678.

Rice, W.G., Supko, J.G., Malspeis, L., Buckheit, R.W., Jr., Clanton, D., Bu, M., Graham, L., Schaeffer, C.A., Turpin, J.A., Domagala, J., et al. (1995). Inhibitors of HIV nucleocapsid protein zinc fingers as candidates for the treatment of AIDS. Science *270*, 1194–1197.

Schindler, T., Bornmann, W., Pellicena, P., Miller, W.T., Clarkson, B., and Kuriyan, J. (2000). Structural mechanism for STI-571 inhibition of Abelson tyrosine kinase. Science *289*, 1938–1942.

Sebolt-Leopold, J.S., and English, J.M. (2006). Mechanisms of drug inhibition of signalling molecules. Nature *441*, 457–462.

Talukder, A.H., Meng, Q., and Kumar, R. (2006). CRIPak, a novel endogenous Pak1 inhibitor. Oncogene *25*, 1311–1319.

Tang, Y., Chen, Z., Ambrose, D., Liu, J., Gibbs, J.B., Chernoff, J., and Field, J. (1997). Kinase-deficient Pak1 mutants inhibit Ras transformation of Rat-1 fibroblasts. Mol. Cell. Biol. *17*, 4454–4464.

Thullberg, M., Gad, A., Beeser, A., Chernoff, J., and Stromblad, S. (2007). The kinase-inhibitory domain of p21-activated kinase 1 (PAK1) inhibits cell cycle progression independent of PAK1 kinase activity. Oncogene *26*, 1820–1828.

Xia, C., Ma, W., Stafford, L.J., Marcus, S., Xiong, W.C., and Liu, M. (2001). Regulation of the p21-activated kinase (PAK) by a human Gβ-like WD-repeat protein, hPIP1. Proc. Natl. Acad. Sci. USA *98*, 6174–6179.

Zenke, F.T., King, C.C., Bohl, B.P., and Bokoch, G.M. (1999). Identification of a central phosphorylation site in p21-activated kinase regulating autoinhibition and kinase activity. J. Biol. Chem. *274*, 32565–32573.

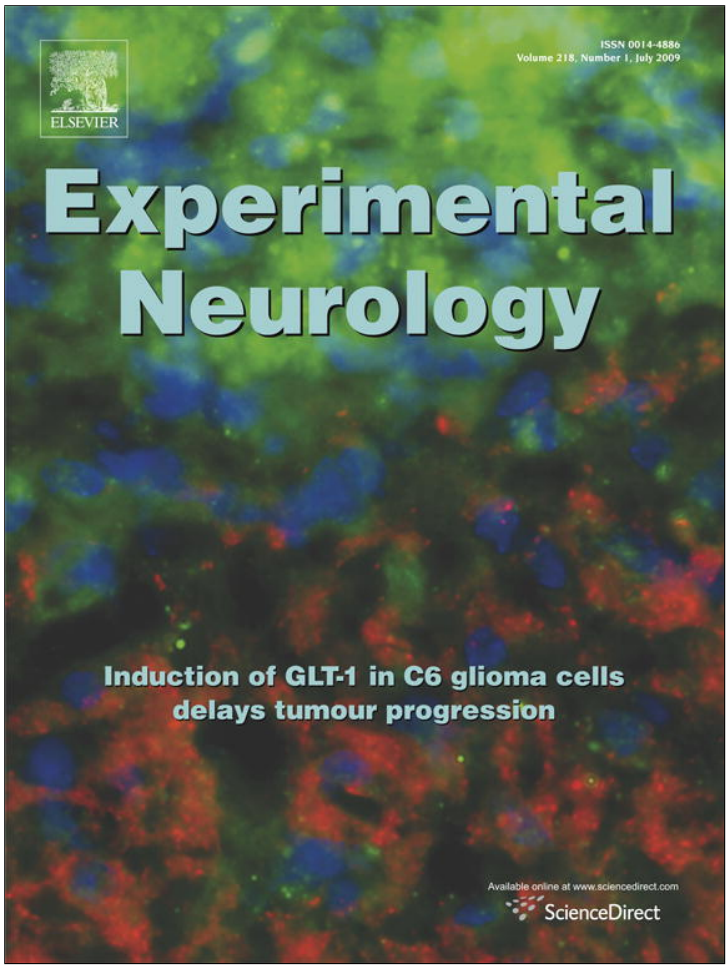

Experimental Neurology 218 (2009) 137–144

Contents lists available at ScienceDirect

Experimental Neurology

journal homepage: www.elsevier.com/locate/yexnr

PAK kinase regulates Rac GTPase and is a potential target in human schwannomas

Christine Flaiz [a], Jonathan Chernoff [b], Sylwia Ammoun [a], Jeffrey R. Peterson [b], Clemens O. Hanemann [a,*]

[a] Clinical Neurobiology, Peninsula College for Medicine and Dentistry, The John Bull Building, Tamar Science Park, Research Way, Plymouth PL6 8BU, UK
[b] Fox Chase Cancer Center, 333 Cottman Avenue, Philadelphia, PA 19111, USA

ARTICLE INFO

Article history:
Received 25 February 2009
Revised 20 April 2009
Accepted 22 April 2009
Available online 3 May 2009

Keywords:
Schwannoma
PAK
Merlin
Small GTPases

ABSTRACT

Merlin loss causes benign tumours of the nervous system, mainly schwannomas and meningiomas. Schwannomas show enhanced Rac1 and Cdc42 activity, the p21-activated kinase 2 (PAK2) activation and increased ruffling and cell adhesion. PAK regulates activation of merlin. PAK has been proposed as a potential therapeutic target in schwannomas. However where PAK stands in the Rac pathway is insufficiently characterised. We used a novel small-molecule PAK inhibitor, IPA-3, to investigate the role of PAK activation on Rac1/Cdc42 activity, cell spreading and adhesion in human primary schwannoma and Schwann cells. We show that IPA-3 blocks activation of PAK2 at Ser192/197 that antagonises PAK's interaction with Pix. Accordingly, Pix-mediated Rac1 activation is decreased in IPA-3 treated schwannoma cells, indicating that PAK acts upstream of Rac. We show that this Rac activation at the level of focal adhesions in schwannoma cells is essential for cell spreading and adhesion in Schwann and schwannoma cells.

Introduction

Merlin is a tumour suppressor whose loss leads to the formation of benign tumours of the nervous system, mainly schwannomas and meningiomas that are also hallmarks of the inherited disease neurofibromatosis type 2 (NF2). P21-activated kinase (PAK) phosphorylates merlin and is inhibited by merlin in a negative feedback-loop. PAK is thus being regarded as potential therapeutic target in NF2 (Xiao et al., 2002; Kissil et al., 2003; Hirokawa et al., 2004). PAK can crosstalk to the MEK/ERK pathway (Beeser et al., 2005) which could affect Schwann cell proliferation, but foremost PAK is known to act as an effector of the RhoGTPases Rac1 and Cdc42 and is thereby supposed to regulate cellular processes like cell spreading, formation of ruffles and adhesion to the extracellular matrix (Bokoch 2003; Zhao and Manser 2005). Merlin-deficient human primary schwannoma cells do show elevated levels of activated Rac1 that colocalises with phospho-PAK2 at the membrane (Kaempchen et al., 2003; Flaiz et al., 2007). Ongoing ruffling through Rac1 activation leads to decreased intercellular adhesion in schwannoma cells (Flaiz et al., 2008) and subsequent loss of contact inhibition of growth in fibroblasts and keratinocytes (Lallemand et al., 2003). In addition, merlin-deficient human schwannoma cells show elevated levels of Cdc42, overexpression of integrin beta1 and numerous stable paxillin-containing focal adhesions and increased adhesion to ECM (Utermark et al., 2003; Flaiz et al., 2009). Activation of Rac in merlin-deficient cells (Shaw et al., 2001; Kaempchen et al., 2003) has also been linked to an inability to ensheath axons (Nakai et al., 2006). GTPase activation at the membrane is seen as one of the major properties linked to merlin deficiency and accounts for many of the pathological processes in merlin-deficient tumours. Despite considering PAK as a target, PAK's position in the Rac pathway and PAK's role in cell spreading, ruffling and adhesion in merlin-deficient tumours is yet insufficiently characterised. Recently we found evidence for Rac activation through the Rac/Cdc42 exchange factor Pix at the levels of focal adhesions, thereby providing a link between the pathological adhesion and increased Rac1 activation in schwannoma (Flaiz et al., 2009). PAK interacting exchange factor (Pix) (Rosenberger and Kutsche 2006) localises to paxillin via G-protein coupled receptor kinase-interacting protein (GIT) in a complex with PAK (Manser et al., 1998). Using different cell lines ten Klooster et al. (2006) provided an interesting model in which PAK dissociates from Pix in focal adhesions after phosphorylation through Cdc42 that itself has been activated through integrin engagement after adhesion to the extracellular matrix (ten Klooster et al., 2006). After phosphorylated PAK has dissociated from Pix, Rac can be activated and translocates to the membrane. According to this model, PAK is not only a Rac effector, but also acts upstream of Rac, a phenomenon that was suggested before in cell lines after PAK overexpression (Obermeier et al., 1998). Thus we hypothesise that in merlin-deficient schwannoma cells activated PAK is leading to Rac activation and altered adhesion.

Using the novel isoform-selective, small-molecule PAK inhibitor IPA-3 ("inhibitor targeting PAK1 activation") targeting the autoregulatory mechanism of PAK 1, 2 and 3 (Deacon et al., 2008), we show that PAK acts downstream of Cdc42 but upstream of Rac1 in merlin-deficient human primary schwannoma cells. PAK and the Pix-PAK-mediated Rac activation are involved in cell spreading and adhesion of human primary schwannoma cells. We show that PAK activity is

* Corresponding author. Fax: +44 1752 517 846.
E-mail address: oliver.hanemann@pms.ac.uk (C.O. Hanemann).

0014-4886/$ – see front matter © 2009 Elsevier Inc. All rights reserved.
doi:10.1016/j.expneurol.2009.04.019

also needed for normal Schwann cell spreading as suggested by Thaxton et al., 2007 as well as for adhesion to the extracellular matrix and development of polarity. Taken together our findings contribute to the understanding of the mechanism of GTPase activation in schwannoma and the role of PAK in cell spreading and adhesion in Schwann and schwannoma cells. They demonstrate that IPA-3 can be used to elucidate PAK functions in human primary cells, that PAK acts upstream of Rac and is a relevant target in schwannomas.

Materials and methods

Preparation of human primary Schwann and schwannoma cells

Schwann cells were obtained from peripheral nerves from tissue donors not carrying any predisposition to a peripheral neuropathy. Schwannomas were kindly provided by NF2 patients after informed consent. Diagnosis of NF2 was based on clinical criteria defined by the NIH Consensus Conference on Neurofibromatosis.

Isolation and culturing were carried out as previously described (Rosenbaum et al., 1998). Briefly, cells were cultured in proliferation medium and grown on poly-L-lysine/laminin coated 6-well plates (Greiner bio-one, Stonehouse, UK), 8-well permanox chamber slides (Nunc, Wiesbaden, Germany) or glass-bottom-dishes (Mattek, Ashland, MA, USA). At least three different schwannoma from different patients or Schwann cells from three different donors were used in each experiment. Every experiment was carried out between the second and the fourth passage, when proliferation rates are best and the number of fibroblasts is negligible (less than 2%, routinely checked by S-100 staining).

Cell viability assay

The effect of IPA-3 and PIR-3.5 on schwannoma cell's viability was assessed with a cell titer 96© aqueous non-radioactive cell proliferation assay (MTS test from Promega).

Human primary schwannoma cells were grown on 96 well plates for 2 days. Cells were left untreated or treated with 5 μM IPA-3, 20 μM IPA-3 or 20 μM PIR-3.5 for 24 h. The MTS-solution was left on the cells for 3 h, before the absorbance at 490 nm was measured. The experiments were conducted three times and mean and standard error of the mean was calculated with Excel.

Western blot analysis

Schwannoma cells were grown until subconfluent and serum starved overnight. Cells were left untreated or pre-incubated with 2 μM, 5 μM or 20 μM IPA-3 ("inhibitor targeting PAK1 activation" 2,2′-dihydroxy-1.1′-dinaphthylsulfide) or 20 μM of the control substance PIR-3.5 ("PAK1 inhibitor relative 3.5" 2-naphthalenol-6,6′-dithiobis) for 10 min, before stimulation with 10% FCS (PAA, Pasching, Austria), 0.5 μM forskolin (Sigma-Aldrich, St. Louis, USA), 10 nM β1-heregulin$_{144-244}$, (Mark Sliwkowski, Genentech, San Francisco, USA), 0.5 mM 3-isobutyl-1-methylxanthin and 2.5 μg/ml insulin (both from Sigma-Aldrich) for 5 min. Cells were lysed as previously described (Utermark et al., 2005a). Equal amounts of total cell lysates were separated by SDS-PAGE on a 12% polyacrylamide gel. Blocking was done in TBS-T containing 5% milk, 2% BSA. Membranes were then incubated with anti-phospho-PAK1/2 (PAK1 serines, 198/203; PAK2 serines, 192/197, 1:500, Cell Signaling Technology, Davis MA, USA) followed by incubation with appropriate HRP-conjugated secondary antibodies (Biorad Laboratories, Hercules, USA). As actin and tubulin are differentially regulated in our system (cDNA array, data not shown), we use RhoGDI (anti-RhoGDI, 1:500, Santa Cruz, CA, USA) that is not regulated in our system (Hanemann et al., 2006) as a loading control. ECL (Amersham, Buckinghamshire, UK) was used for detection. Optical density measurements were performed, after correction of background levels, with a Biorad FluorS Multi Imager, using the Quantity One software (Bio-Rad Laboratories). Experiments were carried out at least three times, using different patient material. Protein levels of IPA-3 or PIR-3.5 treated cells were normalised to levels of untreated schwannoma cells to allow comparison of blots. Mean and standard error of the mean were calculated with Excel. Two-tailed student's *t*-test was performed to find out whether the detected difference is significant.

Rac G-protein linked immunosorbent assay (GLISA)

To measure the effect of IPA-3 or PIR-3.5 on Rac activation, human primary schwannoma and for comparison untreated Schwann cells were cultured in Poly-L-lysin/laminin coated 6 well plates until 70% confluent. Cells were serum starved over night. Schwannoma cells were either left untreated or pre-incubated with 20 μM PIR-3.5 or 2 μM, 5 μM or 20 μM IPA-3 for 10 min. Cells were then stimulated with 10% FCS (PAA), 0.5 μM forskolin (Sigma-Aldrich), 10 nM β1-heregulin$_{144-244}$ (Genentech), 0.5 mM 3-isobutyl-1-methylxanthin (IBMX, Sigma-Aldrich) and 2.5 μg/ml insulin (Sigma-Aldrich) for 5 min. Rac1-GTP was detected using the GLISA Rac1 activation assay biochem Kit™ (absorbance based) from cytoskeleton (cytoskeleton, Denver, USA) using the aforementioned procedure. Briefly, cells were lysed according to the manufacturer's protocol and lysates incubated on 96-well plates that contain a Rac-GTP-binding protein. Bound Rac-GTP is detected with a Rac specific primary antibody and a HRP-conjugated secondary antibody. Appropriate controls were carried out (positive control: Rac control protein, negative control: lysis buffer alone). Levels of Rac1-GTP in IPA-3 or PIR-3.5 treated human primary schwannoma cells from 3 different patients were normalised to the corresponding untreated cells. Mean and standard error of the mean was calculated with Excel and the two-tailed student's *t*-test was performed to find out whether the detected differences were significant.

Cdc42 activation assay

Serum starved schwannoma cells were left untreated or pre-treated with 20 μM IPA-3 for 30 min, before stimulating as described above. Cdc42 assay was performed as described (Flaiz et al., 2007). Briefly Cells were lysed and probes were placed on Swell Gel Immobilized Glutathione Disc and 20 μg of GST-PAK1-PBD were added. As controls cell lysates, obtained from a mesothelioma cell line, were incubated with 0.1 mM GTPγS (positive control) or 1 mM GDP (negative control). A small portion of Schwann and schwannoma cell lysate was removed prior to the pull-down procedure to analyse total Cdc42 levels. Samples, controls and untreated cell lysates were then separated by 12% SDS-PAGE, blotted and blocked with TBS-T containing 2% BSA, 5% milk, incubated with anti-Cdc42 as described (Flaiz et al., 2007). Optical density measurements were performed, as described above. All experiments were carried out at least three times, using different patient material. Protein levels of IPA-3 treated cells were normalised to the levels of untreated schwannoma cells to allow comparison of blots. Mean and standard error of the mean were calculated with Excel and the two-tailed student's *t*-test was performed to find out whether the detected differences are significant.

Ruffling/cell spreading assay, immunocytochemistry

Schwann and schwannoma cells were serum starved overnight prior to trypsination. Trypsination was stopped in 10 ml DMEM (Gibco), containing 2.5 mg soy bean trypsine inhibitor (Sigma-Aldrich) and 1% BSA (PAA). Cells were centrifuged, the pellet resuspended in DMEM and left untreated or treated with IPA-3 or

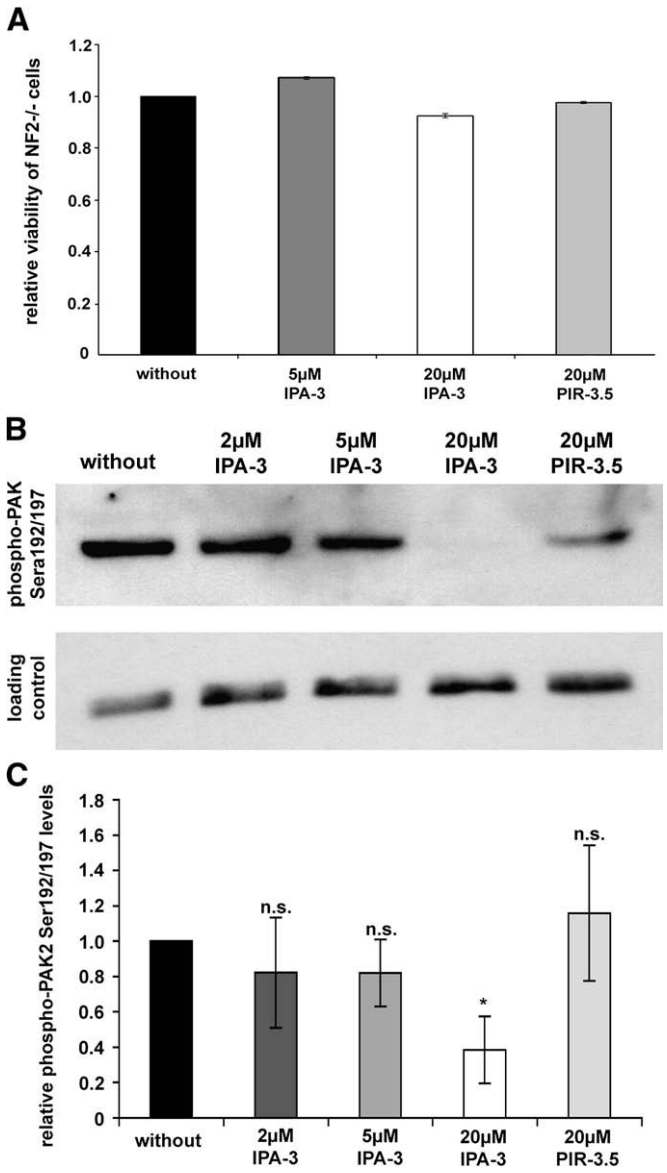

Fig. 1. Effect of IPA-3 and PIR-3.5 on cell viability and on PAK phosphorylation at Ser199/204/Ser192197 in human primary schwannoma cells. (A) Human primary schwannoma cells were left untreated (without) or treated with 5 μM IPA-3, 20 μM or 20 μM PIR-3.5 for 24 h. MTS-assays revealed that 5 μM IPA-3 and 20 μM PIR-3.5 had no effect on schwannoma cell's viability. Even a treatment with 20 μM IPA-3 for 24 h, reduced schwannoma cell's viability by only 7.6%. Viable schwannoma cells were measured using a non-radioactive cell proliferation assay (MTS-assay). Bars represent mean of the percentage of viable cells normalised to cells without treatment ($n=3$). Scale bars represent standard error of the mean. (B) Western Blot analysis revealed that 20 μM IPA-3 clearly reduces PAK2 phosphorylation at Ser192/197 in human primary schwannoma cells. The ineffective control substance PIR-3.5 only mildly affects PAK phosphorylation. RhoGDI, that is not regulated in schwannoma cells, served to control equal loading on each filter. (C) Optical density measurements, normalised to phospho-PAK2 Ser192/194 levels in untreated cells, are depicted as bars. Scale bars represent standard error of the mean (SEM). 20 μM IPA-3 reduced PAK2 phosphorylation at Ser192/194 to 40% of phospho-PAK2 levels of untreated schwannoma cells (*: significant; $p<0.05$ in student's t-test), whereas 2 μM and 5 μM IPA-3, as well as 20 μM PIR-3.5 did not significantly alter phospho-PAK2 Ser192/194 levels. Phospho-PAK2 localises to the membrane of untreated human primary schwannoma cells (NF2−/−).

PIR-3.5 as above. After stimulation with 10% FCS (PAA) 0.5 μM forskolin (Sigma-Aldrich), 10 nM β1-heregulin$_{144-244}$ (Genentech), 0.5 mM 3-isobutyl-1-methylxanthin and 2.5 μg/ml insulin (both from Sigma-Aldrich), equal cell numbers were seeded into poly-L-lysine/laminin coated, flexiperm containing lumox dishes (Greiner). Cells were allowed to spread for 30 min. For washout experiments, inhibitor-containing medium was changed to inhibitor-free one and cells were allowed to spread for another 30 min. Cells were fixed in 4% paraformaldehyde, permeabilised with 1% Triton X-100 and blocked with 10% normal goat serum and incubated anti-p34-Arc (1:100 upstate Biotechnology). Appropriate Cy3 or Alexa Fluor 633-labelled secondary antibodies were used. Alexa Fluor 488-labelled phalloidin was used to visualise filamentous actin (1:100 Molecular Probes). To investigate cell's ability to spread cells were imaged with a 20× objective under a Zeiss510meta confocal microscope. Spread and unspread cells were counted manually. In addition cell spreading areas of 50 cells per condition were measured using the volocity software. Cell spreading areas of IPA-3 and PIR-3.5 treated cells were normalised to the cell spreading areas of corresponding untreated schwannoma cells. Representative images of each condition were taken with a 63× objective and are shown in galleries of three

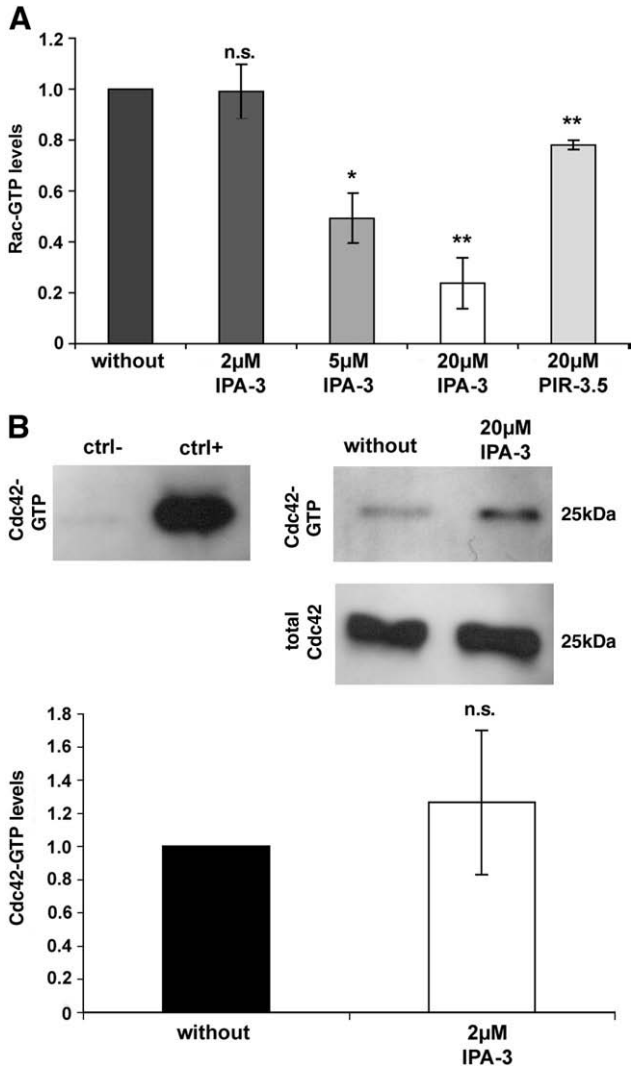

Fig. 2. IPA-3 effect on GTPase activation in human primary schwannoma cells. (A) Blocking of PAK activation with 5 μM and 20 μM IPA-3 reduced levels of Rac-GTP to about 50% (5 μM IPA-3) and 20% (20 μM IPA-3) of Rac-GTP levels of untreated cells (*: significantly for 5 μM IPA-3, $p<0.05$ and **: highly significantly for 20 μM IPA-3, $p<0.01$in student's t-test) in schwannoma cells. 2 μM IPA-3 and 20 μM of the control substance PIR-3.5 did not significantly alter Rac-GTP levels. Rac-GTP levels were determined using GLISA assays. Scale bar represent standard error of the mean (B) Western blot analysis for Cdc42 showed slightly increased Cdc42-GTP levels (after pull-down assay with the PAK-binding domain PBD) after 20 μM IPA-3 treatment (not significant in student's t-test, scale bars represent standard error of the mean). Total Cdc42 levels were measured to confirm equal Cdc42 expression. Positive control (ctrl+) and negative control (ctrl−): cell lysate from a mesothelioma cell line treated with GTPγS or GDP, respectively.

different cells. In addition, z-stacks from the confocal laser scanning microscope were exported to a workstation and used to create 3D animations of Schwann and schwannoma cells using the volocity software according to software manual. Schwann and schwannoma cells from 3 different patients/donors were analysed. Mean and standard error of the mean of cell spreading areas were calculated with Excel and the two-tailed student's *t*-test was performed to find out whether the detected differences are significant.

Adhesion assay

Schwann and schwannoma cells were serum starved overnight prior to trypsination. Trypsination was stopped as described above. Cells were centrifuged, the pellet resuspended in DMEM and left untreated or treated as above with IPA-3 or PIR-3.5 After stimulation as described, quintuples of equal cell numbers per condition were seeded into poly-L-lysine/laminin treated 24 well plates. After 3 h incubation at 37 °C, cells were rinsed twice with PBS to wash away loose cells. Adherent cells were fixed in 4% paraformaldehyde (Sigma-Aldrich) and subsequently counted under an Olympus phase contrast microscope. Number of adherent schwannoma cells under 2 μM, 5 μM or 20 μM IPA-3 or 20 μM PIR-3.5 were normalised to number of corresponding untreated schwannoma cells. Schwann and schwannoma cells from 3 different patients/donors were analysed. Mean and standard error of the mean were calculated with Excel and the two-tailed student's *t*-test was performed.

Results

IPA-3 reduces PAK2 phosphorylation at Ser192/197

To test if the novel Group I PAK inhibitor IPA-3 is effective in human primary schwannoma cells, we first analysed if it affected cell viability. Neither IPA-3 nor the control substance PIR-3.5 with concentrations up to 20 μM affected cell viability, as a cell viability assay (MTS test) revealed (Fig. 1A). IPA-3 has been shown to inhibit PAK autophosphorylation *in vitro* (Deacon et al., 2008) and Ser199/204 (PAK1)/Ser192/197 (PAK2) phosphorylation antagonises the Pix-PAK-interaction (Zhao and Manser 2005). The release of PAK from Pix is likely crucial for facilitating activation of Rac1 (ten Klooster et al., 2006). 20 μM of IPA-3 clearly reduced PAK2 phosphorylation (the major phosphorylated PAK isoform in human Schwann cells (Flaiz et al., 2007)) at Ser192/197 in human primary schwannoma cells, whereas 20 μM of the structurally related control compound PIR-3.5 (using the same highly diluted carrier) had only a mild effect on PAK phosphorylation (Fig. 1B, C). 2 μM and 5 μM IPA-3 only slightly decreased PAK2 phosphorylation. No band for phospho-PAK1 (Ser199/204) was detected. These findings show that IPA-3 efficiently

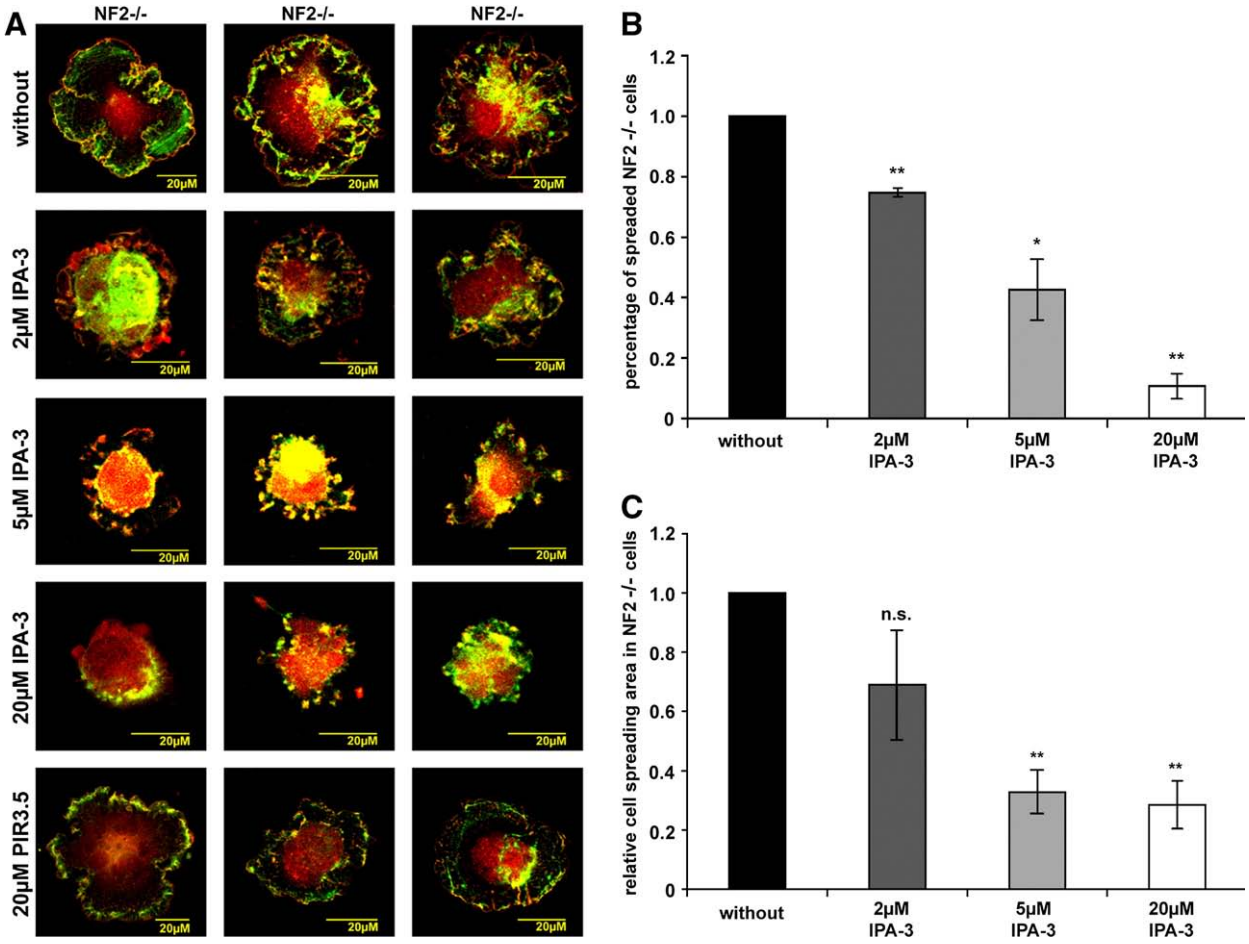

Fig. 3. IPA-3 effect on cell spreading in human primary schwannoma cells (NF2−/−). Schwannoma cells that were allowed to spread for 30 min in the absence or presence of the PAK inhibitor IPA-3 or the control substance PIR-3.5 on poly-L-lysine/laminin coated dishes were stained for the Arp2/3 complex (red) a marker for lamellipodia and ruffles and F-actin (green) to visualise cell morphology. The picture gallery shows three representative cells (A). The number of spreaded cells (B) and cell spreading area (C) were determined and normalised to values of untreated schwannoma cells. Cell spreading is reduced in the presence of IPA-3 in a dose-dependent manner. IPA-3 also reduced but not abolished cell ruffling in schwannoma cells. The control substance PIR-3.5 did not significantly alter cell spreading or ruffling (scale bars represent standard error of the mean; *: $p<0.05$ significant, **: $p<0.01$ highly significant, ***: $p<0.001$ very highly significant, n.s.: not significant in student's *t*-test).

blocks phosphorylation of PAK2 at Ser192/197 in human schwannoma cells.

IPA-3 reduces Rac1 but not Cdc42 activation

Previous results have already shown that at least part of the Rac activation in human schwannoma occurs through beta-Pix that localises to focal adhesions (Flaiz et al., 2009). PAK and Rac compete for binding to beta-Pix and PAK activation and subsequent dissociation from focal adhesions after phosphorylation could allow Rac to bind to beta-Pix (ten Klooster et al., 2006). Since IPA-3 reduced PAK2 autophosphorylation at Ser192/197, PAK should stay associated with beta-Pix and therefore prevent beta-Pix induced Rac activation. GLISA analysis showed clearly reduced Rac-GTP levels after incubation with 5 μM and 20 μM of the PAK inhibitor in a dose-dependent manner in human primary schwannoma cells supporting this hypothesis (Fig. 2A). 2 μM IPA-3 does not have a significant effect on Rac1 activation. The control compound PIR-3.5, used at a high concentration (20 μM), had only a mild effect on Rac activation. Whereas PAK activity clearly influences the activation of Rac, Cdc42 is reported to act upstream of PAK by promoting its autophosphorylation and activation (Manser et al., 1994). If this is true in human schwannoma cells, blocking of PAK activation by IPA-3 should not affect levels of Cdc42-GTP. Pull-down analysis showed that incubation with 20 μM IPA-3 that clearly reduced Rac-GTP levels, did not significantly alter Cdc42-GTP levels (Fig. 2B). Collectively these data suggest that PAK is downstream of Cdc42, but upstream of Rac in human schwannoma cells.

IPA-3 reduces cell spreading in human primary Schwann and schwannoma cells

Schwannoma cells characteristically display increased cell spreading and intense ruffling (Pelton et al., 1998; Rosenbaum et al., 1998; Utermark et al., 2005b), that have been linked to Rac1 activation. The commercially available Rac1 inhibitor NSC23766 that blocks Rac1 activation through its guanine exchange factors Tiam and Vav, efficiently blocked ruffling, but did not affect cell spreading in schwannoma cells (Nakai et al., 2006). We therefore determined if inhibiting the PAK-PIX-mediated Rac and PAK activation with IPA-3 would affect cell spreading and ruffling in human primary schwannoma cells. Schwannoma cells were left untreated or treated with 2 μM, 5 μM or 20 μM IPA-3 or with 20 μM PIR-3.5 for 10 min prior to seeding on poly-L-lysine/laminin coated dishes where they were allowed to spread for 30 min. In order to visualise cell borders, ruffles and the cell body, we stained the cells with p34-Arc, a subunit of the Arp2/3 complex that is enriched in lamellipodia and schwannoma cell periphery (Flaiz et al., 2007) and F-actin. Morphological analysis revealed that untreated schwannoma cells were well spread after 30 min (Fig. 3A). Increasing amounts of IPA-3 reduced numbers of spread cells in a dose-dependent manner (Figs. 3A, B). This was further verified when cell spreading areas were quantitatively measured using the volocity software (Fig. 3C). The control substance PIR-3.5 (20 μM) had no effect on cell spreading. If the inhibitor was removed through media changing after 30 min ("washout") and cells were allowed to spread for another 30 min, morphology of cells resembled untreated schwannoma cells (Fig. 4A). Washout of 5 μM IPA-3 restored cell spreading area completely and washout of 20 μM IPA-3 at least partly (Fig. 4B). These findings indicate that the effects of IPA-3 are reversible.

To visualise cell spreading and ruffling of the whole cell more clearly we created 3D animations of schwannoma cells in the presence or absence of 5 μM or 20 μM IPA-3. Untreated schwannoma cells show intense ruffling all around the cell periphery (Supplementary Fig. 1). As already analysed by other methods, the 3D animation of schwannoma cells treated with IPA-3 clearly showed disturbed cell spreading in a dose-dependent manner, with more rounded cells at higher inhibitor concentrations (Supplementary Figs. 2 and 3). Ruffling seems to be reduced but not abolished in inhibitor treated cells, compared to untreated cells. In summary we claim that PAK and/or the Pix-PAK-mediated Rac1 activation is involved in cell spreading, but seems not to abolish ruffling in human primary schwannoma cells.

To investigate if IPA-3 also affects normal cell spreading in healthy human primary Schwann cells we investigated this cellular process, using the same experiments as described above. Untreated Schwann cells that were allowed to spread for 30 min on poly-L-lysine/laminin already displayed the characteristic bipolarity, with protrusive areas at either end (Fig. 5A). Ruffling could not been observed in the untreated Schwann cells in accordance with previous data (Supplementary Fig. 4). Treatment with different concentrations of IPA-3 (2 μM, 5 μM and 20 μM) reduced the number of spreaded cells and cell spreading area (Figs. 5B, C). Schwann cells show ruffling around the cell periphery in the presence of 5 μM IPA-3 (Fig. 5A and Supplementary Figs. 5 and 6). This ruffling after the loss of spreading area is not as intense as in untreated schwannoma cells and could not be observed with higher concentrations of IPA-3 (20 μM). According to these results, PAK activity seems to play a role in Schwann cell spreading.

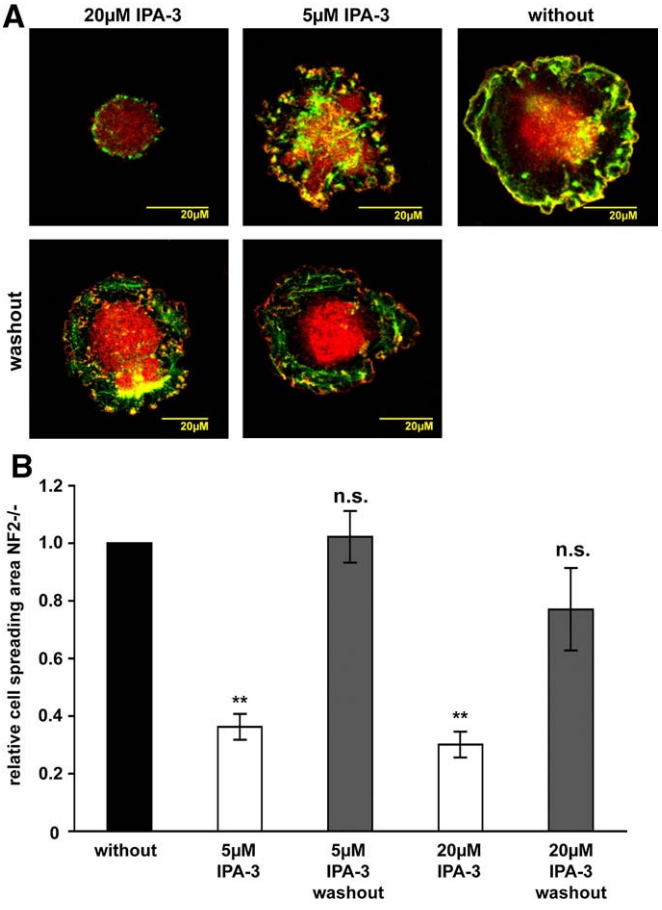

Fig. 4. Washout of IPA-3 in cell spreading experiments in human primary schwannoma cells (NF2−/−). Schwannoma cells that were allowed to spread for 30 min in the absence or presence of the PAK inhibitor IPA-3 or the control substance PIR-3.5 on poly-L-lysine/laminin coated dishes were stained for the Arp2/3 complex (red) a marker for lamellipodia and ruffles and F-actin (green) to visualise cell morphology. IPA-3 was washed out after 30 min by changing inhibitor-containing media to inhibitor-free media. Cells were allowed to spread for another 30 min. Washout restored normal schwannoma cell morphology (A). Washout of 5 μM IPA-3 leads to the same cell spreading area compared to untreated cells and washout of 20 μM IPA-3 to an only slightly reduced cell spreading area that was clearly higher than in cells where inhibitor was left on (B).

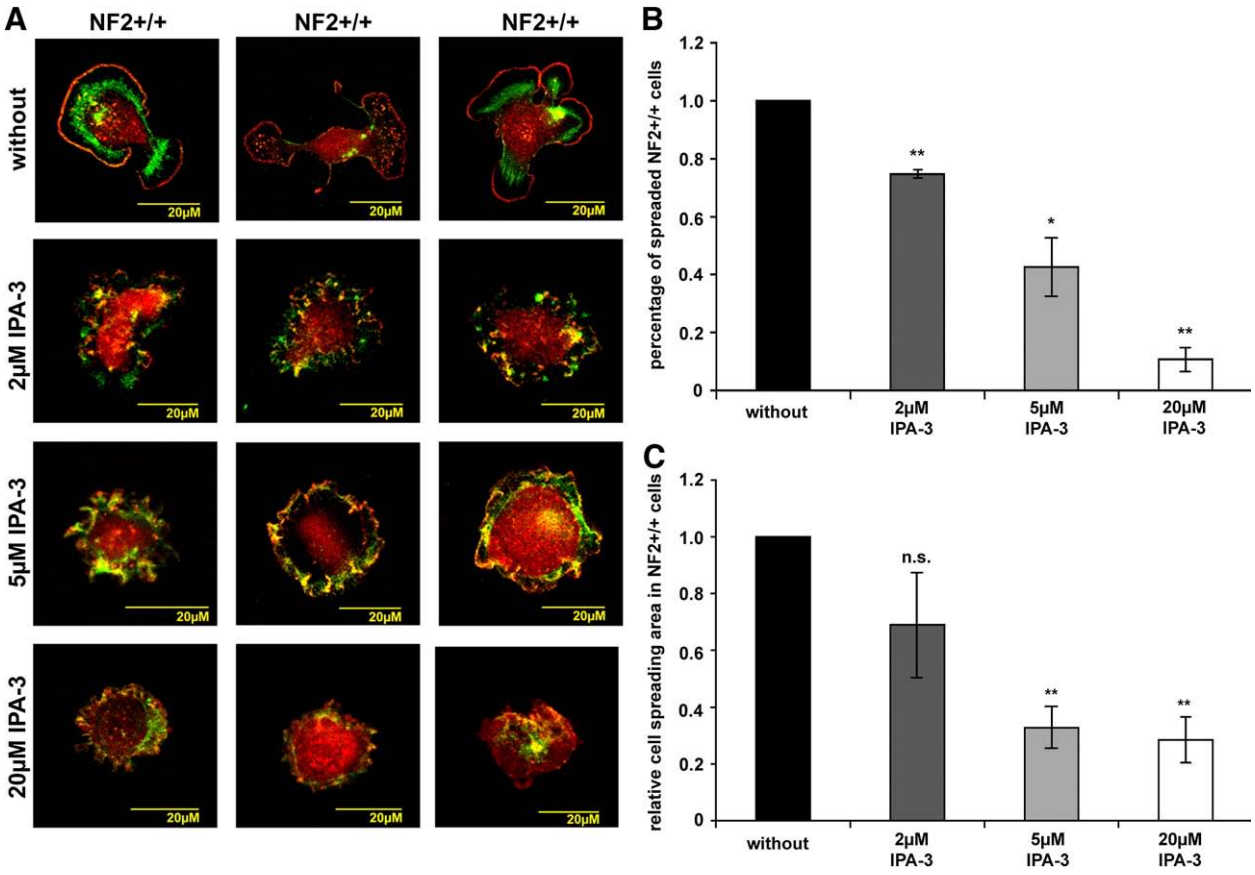

Fig. 5. IPA-3 effect on cell spreading in human primary Schwann cells (NF2+/+). Schwann cells that were allowed to spread for 30 min in the absence or presence of the PAK inhibitor IPA-3 on poly-L-lysine/laminin coated dishes were stained for the Arp2/3 complex (red) a marker for lamellipodia and ruffles and F-actin (green) to visualise cell morphology. The picture gallery shows three representative cells (A). Number of spreaded cells (B) and cell spreading area (C) were determined and normalised to values of untreated Schwann cells. Cell spreading is reduced in the presence of IPA-3 in a dose-dependent manner. Schwann cells treated with 2 μM and 5 μM IPA-3 showed mild ruffling (scale bars represent standard error of the mean; *: $p<0.05$ significant, **: $p<0.01$ highly significant, n.s.: not significant in student's *t*-test).

IPA-3 reduces cell adhesion in Schwann and schwannoma cells

The fact that IPA-3 clearly affects cell spreading suggests that PAK and/or Pix-PAK-mediated Rac activation are involved in the schwannoma cells' ability to adhere to the extracellular matrix. We therefore conducted an adhesion assay in which Schwann and schwannoma cells were left untreated or treated with 2 μM, 5 μM, 20 μM IPA-3 or 20 μM of the control substance PIR-3.5 prior to seeding to poly-L-lysine/laminin coated dishes for 3 h. Loose cells were washed away and adherent cells manually counted. IPA-3 treatment significantly reduced the number of adherent Schwann and schwannoma cells in a dose-dependent manner, whereas PIR-3.5 had no marked effect (Figs. 6A, B). We conclude that PAK activation has a clear effect on adhesion to the extracellular matrix in both human primary Schwann and schwannoma cells.

Discussion

In this study we investigated the role of PAK (p21-activated kinase) in human schwannoma cells to unravel its role on Rac activation and on cell spreading, ruffling and adhesion using the novel small-molecule Pak inhibitor IPA-3. Activation of the GTPase Rac at least partly occurs through beta-Pix at the levels of focal adhesions as our previous work showed (Flaiz et al., 2009). PAK (Bokoch 2003; Zhao and Manser 2005) localises to focal adhesions (Manser et al., 1998), where it competes with Rac for binding to beta-Pix (ten Klooster et al., 2006). According to this model (ten Klooster et al., 2006) phosphorylation of PAK induces a dissociation of PAK from beta-Pix which subsequently allows activation of Rac. To investigate the role of PAK in the Pix-mediated Rac1 activation (Flaiz et al., 2009) we used the inhibitor IPA-3 (Deacon et al., 2008) which blocks PAK autophosphorylation at Ser199/204(PAK1)/Ser192/197(PAK2). As IPA-3 is ineffective in inhibiting pre-activated PAK, we starved our cells and pre-incubated them with IPA-3 prior to stimulation, in all experiments.

We first investigated PAKs role in Rac activation. IPA-3 effectively inhibits phosphorylation of PAK2 at Ser192/197 that is known to induce a dissociation of PAK from beta-Pix (Zhao and Manser 2005; ten Klooster et al., 2006). Phospho-PAK1 Ser199/204 is at much lower amounts in schwannoma cells in accordance with previous studies (data not shown, Flaiz et al., 2007). Previous studies have shown that beta-Pix localises to focal adhesions, whereas phospho-PAK can be found all around the membrane in schwannoma cells (Flaiz et al., 2007; Flaiz et al., 2009). Inhibition of PAK2 by IPA-3 as shown here suggests that phospho-PAK stays associated with beta-Pix. Due to antibody incompatibility co-localisations are not possible and we were unable to get a quantitative immunoprecipitation. However we showed that phospho-PAK can no longer be found at the membrane. In addition, this stable interaction of beta-Pix with PAK would then block beta-Pix, thereby preventing an activation of Rac and accordingly, Rac-GTP levels would decrease after IPA-3 treatment. Indeed, IPA-3 treatment of human primary schwannoma cells reduced Rac-GTP levels in a dose-dependent manner. Rac inhibition was already significant at 5 μm where PAK inhibition was not yet significant. This could be explained by the sensitivity of the assays and the PAK antibodies known to be of low affinity. Another explanation could be

that PAK1 although expressed at very low levels in schwannomas is inhibited by IPA-3 efficiently and results in Rac inhibition as IPA-3 inhibits PAK1 even stronger than PAK2 (Deacon et al., 2008). However this is an important finding, since it puts PAK upstream of Rac in human schwannomas. Even when treated with higher amounts of IPA-3 (20 μM), a small amount of activated Rac-GTP (around 20% of the Rac-GTP levels in untreated schwannoma cells) remains. This could be because part of the Rac activation occurs through other guanine exchange factors like Tiam and Vav. The major part of the pathological Rac activation in schwannoma, however, occurs through Pix and seems to be regulated by PAK.

To test if PAK acts also upstream of Cdc42, which is pathologically activated in schwannoma cells as well (Flaiz et al., 2007), we investigated Cdc42-GTP levels in schwannoma after IPA-3 treatment. Even a high concentration (20 μM) of IPA-3 that significantly reduced Rac-GTP levels did not significantly inhibit Cdc42 activation. Rather a slight increase in Cdc42-GTP levels after IPA-3 treatment can be observed occasionally. One possible explanation for this slight increase which can also be seen in a different experiment in schwannoma cells (Ammoun et al., 2008) could be the phenomenon of hormesis (Calabrese 2008). Thus Cdc42 is unlikely to act downstream of PAK in schwannoma cells. This is supported by findings showing that merlin phosphorylation in Schwann cells is regulated by Cdc42 (but not Rac) that is induced by activation of PAK downstream

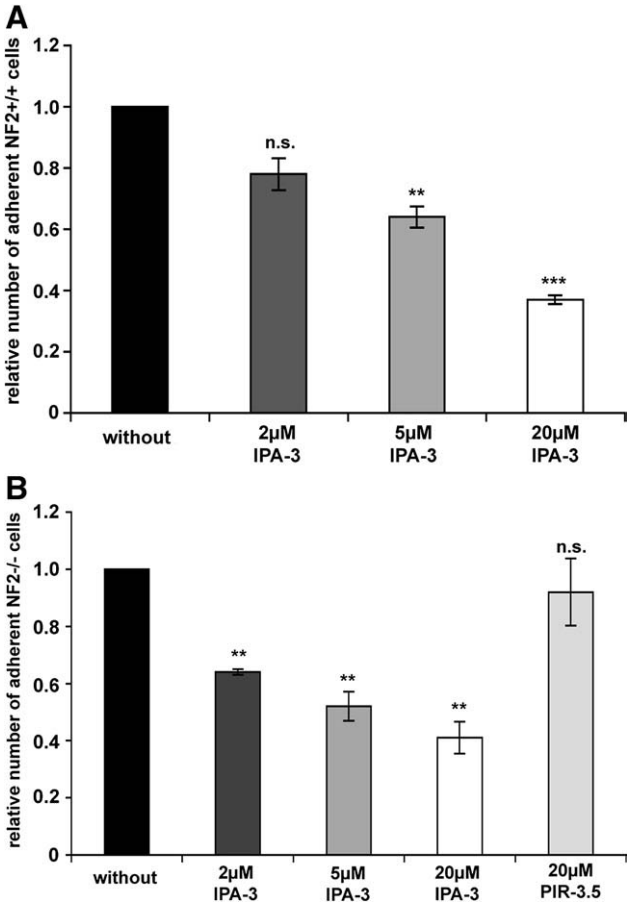

Fig. 6. IPA-3 effect on adhesion in human primary Schwann (NF2+/+) and schwannoma cells (NF2−/−). Human primary Schwann (NF2+/+) and schwannoma cells (NF2−/−) were allowed to adhere to poly-L-lysine/laminin coated dishes for 3 h in the absence or presence of the PAK inhibitor IPA-3 or the control substance PIR-3.5. IPA-3 reduced the number of adherent Schwann (A) and schwannoma cells (B) in a dose-dependent manner. PIR-3.5 did not affect adhesion to the extracellular matrix. (Scale bars represent standard error of the mean; *: $p<0.05$ significant, **: $p<0.01$ highly significant, ***: $p<0.001$ very highly significant, n.s.: not significant in student's *t*-test).

of integrins (Thaxton et al., 2007; Thaxton et al., 2008).Taken together we suggest that the model for Rac activation (ten Klooster et al., 2006) in fibroblasts could be true and relevant in human schwannoma cells. Integrin engagement would activate Cdc42 leading to PAK autophosphorylation in schwannoma. This is supported by previous findings (Flaiz et al., 2007; Kaempchen et al., 2003; Nakai et al., 2006). Phospho-PAK dissociates from beta-Pix at focal adhesions and localises to the membrane (Flaiz et al., 2007). Rac is subsequently activated by beta-Pix and also localises to the membrane (Kaempchen et al., 2003; Nakai et al., 2006). This study puts PAK upstream of Rac and reveals that Rac activation in schwannoma at least partially occurs through Pix and PAK. Recently our group has shown that PDGFRβ-mediated ERK1/2 activation is involved in schwannoma cell proliferation. We showed that PAK acts as a scaffold and is not an Erk1/2 activator in human schwannoma cells and IPA-3 does not inhibit ERK activation (Ammoun et al., 2008). As it is therefore unlikely that PAK is involved in schwannoma cell proliferation and as schwannomas are benign tumours with only slightly increased proliferation rates, we focused on PAK's role in schwannoma cell spreading and adhesion, which are major pathological characteristics of schwannoma.

To investigate cellular consequences of PAK activation and the Pix-PAK-mediated Rac activation in schwannoma we used cell spreading/ruffling and adhesion assays. Characteristically schwannoma cells show increased cell spreading (Pelton et al., 1998; Utermark et al., 2005b; Flaiz et al., 2007) a process that is controlled by Rac (Ridley and Hall 1992) and increased integrin-dependent adhesion to the extracellular matrix (Utermark et al., 2003). We therefore first conducted cell spreading/ruffling assays and adhesion assays that have been described before (Utermark et al., 2003; Nakai et al., 2006). IPA-3 efficiently blocks cell spreading and adhesion on poly-L-lysine/laminin. This implicates Pix-PAK-mediated Rac activation and therefore PAK activity in general to be involved in cell spreading and adhesion in schwannoma cells. Washout experiments restored the normal schwannoma phenotype and indicate that IPA-3 effects are reversible. As a control, cell spreading and adhesion assays were also conducted in healthy Schwann cells that display normal Rac activity (Kaempchen et al., 2003). Cell spreading and adhesion are also markedly reduced in Schwann cells when treated with IPA-3. This is not surprising as a certain amount of Rac activation can be detected in human Schwann cells (Kaempchen et al., 2003). This Rac activity is important for axonal myelination (Benninger et al., 2007) and occurs in an integrin-dependent fashion after adhesion to the extracellular matrix (Nodari et al., 2007). The Rac inhibitor NSC23766 did not inhibit cell spreading clearly (Nakai et al., 2006). This can be explained by the fact that NSC23766 binds Rac and inhibits its activation by a subset of guanine exchange factors (GEFs). In contrast, IPA-3 directly targets PAK, preventing its autophosphorylation and thereby sequestering the GEF Pix from Rac. Both, PAK and beta-Pix localise to focal adhesions (Manser et al., 1998; Rosenberger and Kutsche 2006) and are therefore involved in cell spreading and adhesion. NSC23766 effectively suppresses membrane ruffling, whereas IPA-3 reduces but not completely abolishes this process in schwannoma cells. In the presence of 5 μM IPA-3, detaching Schwann cells display ruffling. Ruffles can be seen as lamellipodia that lost the ability to adhere to the extracellular matrix (Small et al., 2002). As IPA-3 reduces the cell's adhesion potential, ruffles could evolve as a secondary effect. Interpreting IPA-3's influences on ruffling in Schwann and schwannoma cells is therefore difficult. Our results suggest that at least part of the Rac activation in Schwann cells occurs through beta-Pix and PAK at focal contacts. This findings fit nicely to previous reports in Schwann cells, showing that merlin phosphorylation and therefore inactivation occurs at paxillin-containing membrane domains (which we showed before to be the small and short-living focal complexes in Schwann cells) through PAK that has been activated by Cdc42 (Thaxton et al., 2007). This means that a locally restricted merlin inactivation and subsequent Rac activation occurs at the levels of focal

complexes in Schwann cells. Focal contacts are short-lived in Schwann cells, thereby guaranteeing that Rac activation stays within normal limits. In schwannoma cells, however, focal contacts are very stable and long-lived (Flaiz et al., 2009) leading to a constantly increased Pix-PAK-mediated Rac activation susceptible to inhibition with IPA-3. Thus PAK seems to be a reasonable target in schwannomas.

On a side line we showed that IPA-3 is an easy-to-use, efficient PAK inhibitor that can be used even in delicate primary cells to investigate cellular processes. Moreover, our human schwannoma *in vitro* model has been proven to be a good model system to investigate PAK effects.

Acknowledgments

Work was supported by Peninsula College of Medicine and Dentistry and Fritz Thyssen foundation (COH) and Department of Defence NF Research Program and a Career Development Award from the AACR (JP and JC).

Appendix A. Supplementary data

Supplementary data associated with this article can be found, in the online version, at doi:10.1016/j.expneurol.2009.04.019.

References

Ammoun, S., Flaiz, C., Ristic, N., Schuldt, J., Hanemann, C.O., 2008. Dissecting and targeting the growth factor-dependent and growth factor-independent extracellular signal-regulated kinase pathway in human schwannoma. Cancer Res. 68, 5236–5245.

Beeser, A., Jaffer, Z.M., Hofmann, C., Chernoff, J., 2005. Role of group A p21-activated kinases in activation of extracellular-regulated kinase by growth factors. J. Biol. Chem. 280, 36609–36615.

Benninger, Y., Thurnherr, T., Pereira, J.A., Krause, S., Wu, X., Chrostek-Grashoff, A., Herzog, D., Nave, K.A., Franklin, R.J., Meijer, D., Brakebusch, C., Suter, U., Relvas, J.B., 2007. Essential and distinct roles for cdc42 and rac1 in the regulation of Schwann cell biology during peripheral nervous system development. J. Cell Biol. 177, 1051–1061.

Bokoch, G.M., 2003. Biology of the p21-activated kinases. Annu. Rev. Biochem. 72, 743–781.

Calabrese, E.J., 2008. Hormesis: why it is important to toxicology and toxicologists. Environ. Toxicol. Chem. 27, 1451–1474.

Deacon, S.W., Beeser, A., Fukui, J.A., Rennefahrt, U.E., Myers, C., Chernoff, J., Peterson, J.R., 2008. An isoform-selective, small-molecule inhibitor targets the autoregulatory mechanism of p21-activated kinase. Chem. Biol. 15, 322–331.

Flaiz, C., Ammoun, S., Biebl, A., Hanemann, C.O., 2009. Altered adhesive structures and their relation to RhoGTPase activation in merlin-deficient Schwannoma. Brain Pathol. 19, 27–38.

Flaiz, C., Kaempchen, K., Matthies, C., Hanemann, C.O., 2007. Actin-rich protrusions and nonlocalized GTPase activation in Merlin-deficient Schwannomas. J. Neuropathol. Exp. Neurol. 66, 608–616.

Flaiz, C., Utermark, T., Parkinson, D.B., Poetsch, A., Hanemann, C.O., 2008. Impaired intercellular adhesion and immature adherens junctions in merlin-deficient human primary schwannoma cells. GLIA 56, 506–515.

Hanemann, C.O., Bartelt-Kirbach, B., Diebold, R., Kampchen, K., Langmesser, S., Utermark, T., 2006. Differential gene expression between human schwannoma and control Schwann cells. Neuropathol. Appl. Neurobiol. 32, 605–614.

Hirokawa, Y., Tikoo, A., Huynh, J., Utermark, T., Hanemann, C.O., Giovannini, M., Xiao, G.H., Testa, J.R., Wood, J., Maruta, H., 2004. A clue to the therapy of neurofibromatosis type 2: NF2/merlin is a PAK1 inhibitor. Cancer J. 10, 20–26.

Kaempchen, K., Mielke, K., Utermark, T., Langmesser, S., Hanemann, C.O., 2003. Upregulation of the Rac1/JNK signaling pathway in primary human schwannoma cells. Hum. Mol. Genet. 12, 1211–1221.

Kissil, J.L., Wilker, E.W., Johnson, K.C., Eckman, M.S., Yaffe, M.B., Jacks, T., 2003. Merlin, the product of the Nf2 tumor suppressor gene, is an inhibitor of the p21-activated kinase, Pak1. Mol. Cell 12, 841–849.

Lallemand, D., Curto, M., Saotome, I., Giovannini, M., McClatchey, A.I., 2003. NF2 deficiency promotes tumorigenesis and metastasis by destabilizing adherens junctions. Genes Dev. 1090–1100.

Manser, E., Leung, T., Salihuddin, H., Zhao, Z.S., Lim, L., 1994. A brain serine/threonine protein kinase activated by Cdc42 and Rac1. Nature 367, 40–46.

Manser, E., Loo, T.H., Koh, C.G., Zhao, Z.S., Chen, X.Q., Tan, L., Tan, I., Leung, T., Lim, L., 1998. PAK kinases are directly coupled to the PIX family of nucleotide exchange factors. Mol. Cell 1, 183–192.

Nakai, Y., Zheng, Y., MacCollin, M., Ratner, N., 2006. Temporal control of Rac in Schwann cell-axon interaction is disrupted in NF2-mutant schwannoma cells. J. Neurosci. 26, 3390–3395.

Nodari, A., Zambroni, D., Quattrini, A., Court, F.A., D'Urso, A., Recchia, A., Tybulewicz, V.L., Wrabetz, L., Feltri, M.L., 2007. Beta1 integrin activates Rac1 in Schwann cells to generate radial lamellae during axonal sorting and myelination. J. Cell Biol. 177, 1063–1075.

Obermeier, A., Ahmed, S., Manser, E., Yen, S.C., Hall, C., Lim, L., 1998. PAK promotes morphological changes by acting upstream of Rac. EMBO J. 17, 4328–4339.

Pelton, P.D., Sherman, L.S., Rizvi, T.A., Marchionni, M.A., Wood, P., Friedman, R.A., Ratner, N., 1998. Ruffling membrane, stress fiber, cell spreading and proliferation abnormalities in human Schwannoma cells. Oncogene 17, 2195–2209.

Ridley, A.J., Hall, A., 1992. The small GTP-binding protein Rho regulates the assembly of focal adhesions and actin stress fibers in response to growth factors. Cell 70, 389–399.

Rosenbaum, C., Kluwe, L., Mautner, V.F., Friedrich, R.E., Mueller, H.W., Hanemann, C.O., 1998. Isolation and characterization of Schwann cells from neurofibromatosis type 2 patients. Neurobiol. Dis. 5, 55–64.

Rosenberger, G., Kutsche, K., 2006. AlphaPIX and betaPIX and their role in focal adhesion formation. Eur. J. Cell Biol. 85, 265–274.

Shaw, R.J., Paez, J.G., Curto, M., Yaktine, A., Pruitt, W.M., Saotome, I., O'Bryan, J.P., Gupta, V., Ratner, N., Der, C.J., Jacks, T., McClatchey, A.I., 2001. The Nf2 tumor suppressor, merlin, functions in Rac-dependent signaling. Dev. Cell 1, 63–72.

Small, J.V., Stradal, T., Vignal, E., Rottner, K., 2002. The lamellipodium: where motility begins. Trends Cell Biol. 12, 112–120.

ten Klooster, J.P., Jaffer, Z.M., Chernoff, J., Hordijk, P.L., 2006. Targeting and activation of Rac1 are mediated by the exchange factor beta-Pix. J. Cell Biol. 172, 759–769.

Thaxton, C., Lopera, J., Bott, M., Baldwin, M.E., Kalidas, P., Fernandez-Valle, C., 2007. Phosphorylation of the NF2 tumor suppressor in Schwann cells is mediated by Cdc42-Pak and requires paxillin binding. Mol. Cell Neurosci. 34, 231–242.

Thaxton, C., Lopera, J., Bott, M., Fernandez-Valle, C., 2008. Neuregulin and laminin stimulate phosphorylation of the NF2 tumor suppressor in Schwann cells by distinct protein kinase A and p21-activated kinase-dependent pathways. Oncogene 27, 2705–2715.

Utermark, T., Kaempchen, K., Hanemann, C.O., 2003. Pathological adhesion of primary human schwannoma cells is dependent on altered expression of integrins. Brain Pathol. 13, 352–363.

Utermark, T., Kaempchen, K., Antoniadis, G., Hanemann, C.O., 2005a. Reduced apoptosis rates in human schwannomas. Brain Pathol. 15, 17–22.

Utermark, T., Schubert, S.J., Hanemann, C.O., 2005b. Rearrangements of the intermediate filament GFAP in primary human schwannoma cells. Neurobiol. Dis. 19, 1–9.

Xiao, G.H., Beeser, A., Chernoff, J., Testa, J.R., 2002. p21-activated kinase links Rac/Cdc42 signaling to Merlin. J. Biol. Chem. 277, 883–886.

Zhao, Z.S., Manser, E., 2005. PAK and other Rho-associated kinases—effectors with surprisingly diverse mechanisms of regulation. Biochem. J. 386, 201–214.

p21-activated kinases are required for transformation in neurofibromatosis type 2

Hoi Yee Chow and Jonathan Chernoff[1]

Fox Chase Cancer Center,
333 Cottman Avenue,
Philadelphia, PA 19111.

[1]corresponding author

email: J_Chernoff@fccc.edu
tel: 215 728 5319
fax: 215 28 3616

characters = 19,366

Running Title: Role of Pak in NF2.

Key Words: transformation, protein kinase, Merlin, signal transduction, schwannoma, tumor suppressor.

Abstract

NF2 is an autosomal dominant disease characterized by development of bilateral vestibular schwannomas and other benign tumors in central nervous system. Loss of the NF2 gene product, Merlin, leads to aberrant Schwann cell proliferation, motility, and survival, but the mechanisms by which this tumor suppressor functions remain unclear. One well-defined target of Merlin is the group I family of p21-activated kinases, which are allosterically inhibited by Merlin and which, when activated, stimulate cell cycle progression, motility, and increased survival. Here, we examine the effect of Pak inhibition on NF2 function. Using a specific peptide inhibitor of group I Paks, we show that loss of Pak activity restores normal cell movement and reduces cell proliferation to cells lacking Merlin function. In addition, xenografts of such cells form fewer and smaller tumors than do cells without Pak inhibition. However, in cells or tumors, loss of Pak activity does not reduce Erk or Akt activity, two signaling proteins that are thought to mediate Pak function in growth factor pathways. These results suggest that Pak functions in novel signaling pathways in NF2, and may serve as a useful therapeutic target in this disease.

Abbreviations

Blue Box, BB; extracellular-signal regulated kinase, Erk; Ezrin-Radixin-Moesin, ERM; Four-point one, Ezrin, Radixin, and Moesin, FERM; glutathione-S-transferase, green fluorescent protein, GFP; GST; L107F, LF; mitogen activated protein kinases, MAPKs; 3-[4,5-dimethylthiazol-2-yl]-2,5-diphenyl tetrazolium bromide, MTT; Neurofibromatosis type 2, NF2; p21-activated kinase, Pak; phosphate-buffered saline, PBS; Pak inhibitor domain, PID.

Introduction

Neurofibromatosis type 2 (NF2) is an autosomal dominant disorder characterized by the development of bilateral vestibular schwannomas and other benign tumors in central nervous system (1, 2). While several mitogenic pathways are known to be upregulated in *NF2*-mutant cells, despite considerable effort, there is as yet no consensus as to how loss of the *NF2* tumor suppressor gene leads to schwannoma growth, nor are there effective medical therapies for this disorder.

The protein encoded by the *NF2* gene, Merlin, exhibits significant homology to Ezrin-Radixin-Moesin (ERM) proteins, sharing a FERM (Four-point one, Ezrin, Radixin, and Moesin) domain at the N-terminus followed by an alpha-helical segment. Merlin has a unique C-terminal domain lacking a binding region for F-actin that exists in all other ERM proteins (3). Within the FERM domain, a seven amino-acid conserved sequence (termed the “Blue Box”), is important for Merlin functions. Deletion of the Blue Box (ΔBB) or substitution of polyalanine within this region results in a dominant-negative form of the protein (4), most likely by disrupting intramolecular association between the N- and C-termini of Merlin (5). This self-interaction can also be disrupted by phosphorylation of Merlin at residue serine 518, leading to a functionally inactive “open state” (6). Merlin phosphorylation at this site is stimulated by Rac1 and Cdc42 GTPases via activation of their downstream effectors, p21-activated kinases (Paks) (7, 8).

Merlin is known to play an inhibitory role in Rac-mediated signaling (6). NF2-deficient Schwannoma cells display aberrant membrane ruffling and concomitant hyperactivation of Rac and Pak1 (9-11). Fibroblasts and keratinocytes lacking Merlin lose contact inhibition and *Nf2*-null neuroendocrine cells are defective in assembly of tight junctions and adherens junctions (12), a process disrupted by activated Rac and Pak (13-15) require. Merlin affects Rac trafficking to the plasma membrane and is a direct inhibitor of Pak1, suggesting a negative feed-forward loop between Rac/Pak and Merlin (16). For these reasons, The Rac/Pak signaling axis has garnered increasing attention as a possible therapeutic target in NF2.

As downstream mediators of Rac function, Paks have been implicated in regulating cell morphology, motility proliferation, and survival (17-19). Group I Paks (Pak1, -2, and -3) affect a wide variety of central signaling pathways, including positively regulating mitogen activated kinases (MAPKs), Akt, and NFκB (20, 21). In addition, group I Paks influence the G2/M transition by activating Aurora-A and Polo-like kinase 1 (Plk-1) (22, 23). In Ras-transformed cells, expression of dominant- negative Pak1 blocks transformation and prevents full activation of Erk and Jnk, and it is thought such MAPKs represent important signaling targets for Pak in cancer (24, 25). In the Erk pathway, Pak has been shown to phosphorylate c-Raf at S338 and Mek1 at S298 (26-29). These phosphorylations are thought to be necessary, but not sufficient, for full activation of c-Raf and Mek by Ras.

In this study, we show that inhibition of group I Paks in *Nf2*-mutant fibroblasts and Schwann cells reduces proliferation, restores normal morphology, and reduces invasiveness of cells lacking Merlin function, as well as the tumorigenicity of such cells in nude mice. However, these changes are not associated with reductions in Erk or Akt activity, suggesting that the beneficial effects of inhibiting Pak in these cells involves novel signal transduction pathways.

Materials and Methods

Cell culture conditions and retroviral transductions*.* NIH-3T3 cells and human HEI-193 schwannoma cells (a gift from Marco Giovannini) (30), were cultured in high-glucose DMEM supplemented with 10% fetal calf serum, 2 mM L-glutamine and 100 U/ml penicillin/streptomycin at 37°C in a humidified 5% CO_2 incubator. The ϕNX packaging cell line (Orbigen) was transfected using Lipofectamine 2000 (Invitrogen). Viral supernatants were harvested 48 hr post-transfection and filtered. Cells were incubated with retroviral supernatant supplemented with 4 μg/ml polybrene for 4 hr at 37°C, and then were cultured in growth media for 48 hr for viral integration. Infected cells were selected with 2 μg/ml of puromycin or by flow cytometry for cells with green fluorescent protein (GFP).

Expression Plasmids*.* A GST-PID (Pak1 amino acids 83-149) or Gst-PID L107F cDNA (27) was subcloned as a *Bgl*II/*Xho*I fragment into the retroviral expression

vector pBMN-I-GFP (http://stanford.edu/group/nolan/plasmid_maps/pmaps.html), restricted with *Bam*HI/*Xho*I.

Cell proliferation assay. 10^4 cells were plated in 96-well plates and 10 µl 3-[4,5-dimethylthiazol-2-yl]-2,5-diphenyl tetrazolium bromide (MTT) solution was added to each well to a final concentration of 0.5 mg/ml. The reaction was stopped after 4 hr at 37°C by adding 100 µl of solubilization solution (10% SDS in 0.01 M HCl) and the samples were analyzed at 595 nm on Perkin Elmer Envision plate reader. Triplicates were performed for each sample and medium alone was used as a blank, and experiments were performed on three occasions.

Cell invasion assay. Matrigel invasion chamber (BD Biosciences) were rehydrated in serum-free DMEM medium for 2 hr and then placed in 0.75 ml of DMEM medium supplemented with 5% fetal calf serum. Cells at a density of 1.5 X 10^4 suspended in 0.5ml of DMEM, and seeded onto Matrigel chambers. Cells were allowed to invade for 24 hr and cells on the upper surface were gently removed with a cotton bud, and cells that had migrated through the 8 µm pores were fixed with 4% paraformaldehyde for 15 min and stained with 0.1% crystal violet for 15 min. Membranes were washed, removed and mounted on a glass slide, and the level of invasion was quantified by visual counting using a microscope with a 20X objective.

Cell cycle analysis. Cell cycle profiles were analyzed using flow cytometry with propidium iodide staining. Cells were trypsinized and washed with PBS and fixed in 70% ethanol at -20°C. After fixation, cells were washed once with PBS and resuspended in 0.5ml of a solution containing 1M Tris-HCl pH 8.0, 0.1% Nonidet P-40, 10 mM NaCl, 50 µg/ml propidium iodide and 70 Kunitz units/ml RNase A. FACS analysis was performed using CELLQuest™ software (Becton Dickinson). A minimum of 10,000 events was collected per sample.

Immunoblot analysis. Whole cell extracts were prepared by washing the cells in cold PBS and lysed in a buffer containing 50 mM Tris-HCl pH 7.5, 150 mM NaCl, 1% Nonidet P-40, and 0.25% sodium deoxycholate, 1 mM Na_3VO_4, and 1 mM NaF, plus complete protease inhibitor cocktail tablets (Roche). Protein concentrations were determined using bicinchoninic protein assay reagent according to manufacture's

instructions (Pierce). Pak activation was stimulated by adding PDGF-BB (Sigma) at 5 ng/ml for 5 min to serum-starved cells. The antibodies used in this study include Pak1; Pak2; Mek1/2; phospho-MEK1 (Ser298); Erk1/2; phospho-Erk1/2 (Thr202/Tyr204); p90 RSK; phospho-RSK (Thr359/Ser363); mTOR; phospho-mTOR (Ser2448); p70 S6 kinase; phospho-p70 S6 kinase (Thr389); S6 ribosomal protein; phospho-S6 ribosomal protein (Ser240/244); Akt; phospho-Akt (Thr308); PDK1; phospho-PDK1 (Ser241); Merlin (Cell Signaling Technology); phospho-Pak1-3 (Ser141; Invitrogen); GST (Santa Cruz Biotechnology); and β-actin (Sigma). All antibodies were used at a dilution of 1:1,000, except for β-actin, which were diluted in 1:20,000.

Immunofluorescence. Cells were plated on glass coverslips in 6-well culture plates and fixed in 4% paraformaldehyde for 10 min, permeabilized with 0.2% Triton X-100 for 5 min and blocked with 1% BSA in PBS for 30 min. Filamentous actin and nuclei were visualized by staining with Rhodamine-phalloidin (Molecular Probe) and DAPI (Sigma), respectively. Images were observed and captured on an inverted phase/fluorescence microscope (Nikon TE300).

Tumorigenicity assays. Cells were trypsinized, washed with PBS and resuspended at 10^7 cells per ml in PBS. 2×10^6 cells were injected subcutaneously into flanks of 5-week old nude mice (BALB/c *nu/nu*). Mice were monitored and tumor diameters were measured every 3 days using caliper for 6 weeks following injection. Tumor volume was calculated by the following formula: volume = 0.5 x (length) x $(\text{width})^2$. The mice were sacrificed and the tumors were resected for histological examination and immunoblot analysis.

Data analysis. All experiments were performed at least three times. Results are reported as means ± SD. The significance of the data was determined by two-tailed, unpaired Student's *t*-test, and differences were considered statistically significant at $P < 0.05$.

Results

Establishing Merlin-deficient cells that express a Pak inhibitor. To study the influence of Pak inhibition in cells lacking Merlin function, we used two Merlin-deficient cells lines. First, we established a stable NIH-3T3 fibroblast cell line overexpressing Merlin ΔBB, a mutant form of the tumor suppressor that lacks the "Blue Box" motif and acts in a dominant negative fashion, in effect mimicking loss of the NF2 gene (Fig. 1A) (31). The expression level of Merlin ΔBB in such infected cells was about 5-fold higher than endogenous Merlin (Fig. 1B). Note that, despite deletion of the Blue Box motif, exogenous Merlin ΔBB migrates at the same position as endogenous Merlin in SDS/PAGE. The second NF2 cell model was HEI-193 cells, which are derived from a human schwannoma and which do not express Merlin isoforms 1 and 2 (Fig. 1B) (32). NIH-3T3 cells expressing dominant negative Merlin (ΔBB cells) and HEI-193 cells were then infected with recombinant retrovirus encoding GST-tagged Pak inhibitor domain (PID) or a nonfunctional inhibitor control, PID L107F (PID LF) (Fig. 1A) (27). Both ΔBB and HEI-193 cells infected with the PID or PID LF retrovirus displayed readily detected signals in anti-GST immunoblots (Fig. 1B).

Effects of Pak inhibition on invasiveness in cells lacking functional Merlin. We first examined the effect of Merlin on cell invasiveness and asked if such effects could be reversed by PID expression. Cells were plated in a chamber above a layer of Matrigel and assessed for their ability to penetrate through this layer, indicating invasiveness. As shown in Fig. 2A, the invasiveness of ΔBB cells was almost twice that of control NIH-3T3 cells. Expression of PID, but not inactive PID LF, significantly inhibited the invasive capacity of Merlin ΔBB cells. As in ΔBB cells, PID expression also decreased the invasiveness of HEI-193 cells, whereas PID LF expression did not (Fig. 2B). Thus, in both cell lines, a Pak inhibitor substantially reduced invasiveness in the absence of Merlin function.

Pak inhibition suppresses cell growth via a G2/M blockade. Wild-type Merlin is known to inhibit cell proliferation, in part by to limiting cyclin D expression and perhaps also by effects on the mTOR pathway (33-35). We therefore assessed the effect of PID expression on cell proliferation in cells lacking functional Merlin. As expected, ΔBB cells showed an increased growth rate compare to vector control cells (Fig. 3A). Co-expression of PID in these cells inhibited proliferation. Conversely, cells expressing PID

LF resulted in slight stimulation on cell proliferation. Even more pronounced effects were found in HEI-193 Schwanomma cells expressing PID, which showed substantially slowing of proliferation relative to controls (Fig. 3B). Expression of PID LF had no effect in these cells.

To better understand the effects of Pak blockade on cell proliferation, we analyzed the effect of PID expression on the cell cycle (Fig. 3C). In ΔBB cells, PID expression led to a significant accumulation of cells in G2/M, an effect not seen in ΔBB/PID LF cells. Similar effects were noted in HEI-193 cells, in which PID expression substantially increased the percentage of cells in G2/M (Fig. 3D).

Effects of PID on Erk cascade. To determine the molecular basis of the effects of PID expression on Merlin signaling, we examined a number of signal transduction pathways. In many cell types, group A Pak function is required for activation of Erk, most likely by phosphorylation of c-Raf at S338 and Mek1 at S298 (24, 26, 27, 36, 37). As expected, PID effectively blocked Pak, Mek, and Erk activation in NIH-3T3 fibroblast cells after PDGF stimulation, whereas inactive inhibitor did not (Supplemental Fig. 1). These results are consistent with our previous studies that Paks are required for PDGF-mediated activation of Mek and Erk in fibroblasts (27). In ΔBB cells, basal levels of Pak, Mek, and Erk activity were elevated but could be further stimulated by PDGF (Fig. 4). PID expression suppressed Pak activation, as assessed by two distinct anti-phospho Pak antibodies. Surprisingly, despite the suppressive effects of PID on Merlin ΔBB invasion, and proliferation, expression of this inhibitor did not have a significant effect on the activity of Mek and Erk, even though it did reduce Pak activity significantly.

We also assessed the effects of Pak inhibition in HEI-193 Schwannoma cells. As in ΔBB cells, PID expression substantially reduced Pak activity in Schwannoma cells, with little effect on Mek or Erk activities. However, unlike the results in ΔBB cells, PID expression extinguished phosphorylation of Mek at S298, the putative site of Pak phosphorylation. Thus, in these cells, despite effective suppression of Pak, with consequent reduction of phosphorylation of one of its major targets in the Erk pathway, Mek activity (as assessed by phospho Ser 217/221 antibodies) and downstream Erk activity were unaffected.

Two groups have recently shown a connection between Merlin deficiency and the mTOR signaling pathway (35, 39). Loss of Merlin in HUVEC cells and in malignant mesothelioma cells leads to activation of mTORC1, and these cells are sensitive to inhibitors of mTOR (35). Given these results, we examined mTOR activity in NIH-3T3 cells expressing Merlin ΔBB plus or minus PID. In this cell type, we found that loss of Merlin function was not associated with elevated mTOR and S6 phosphorylation under basal conditions or in response to PDGF stimulation. Pak inhibition by PID did not notably alter the phosphorylation status of these signaling events (Supplemental Fig. 2).

Inhibition of tumor formation by Pak inhibition. HEI-193 cells do not grow as xenografts (40); therefore, to assess the effects of Pak inhibition on NF2-related tumorigenicity, we injected nude mice only with ΔBB, ΔBB/PID, or ΔBB/PID LF cells. In agreement with previous studies, ΔBB cells developed substantial tumors by 6 weeks post-injection (average volume >200 mm^3) (31, 41). Tumors derived from ΔBB/PID cells were much smaller in size, with an average volume of 38 mm^3 (Fig. 5). Interestingly, mice injected with ΔBB/PID LF cells developed tumors even larger (average volume ~450 mm^3) than those injected with ΔBB cells.

Lastly, we examined signaling activity in tumor lysates from these xenografts. Pak activity was inhibited in ΔBB/PID cells, indicating that this suppressor remained effective *in vivo*. Surprisingly, while Akt and Erk were not active in tumors derived from animals injected with ΔBB or ΔBB/PID LF cells, both Akt and Erk were activated in lysates from the small tumors that developed in mice injected with ΔBB/PID (Fig. 6). It is also of interest that, in the tumors from ΔBB/PID mice, Merlin expression (presumably exogenous Merlin ΔBB) was substantially elevated. These data show that PID expression strongly inhibited tumor formation in the NF2 xenograft model, suggesting that Group I Paks are required for transformation in cells that have lost Merlin function. Despite this requirement, loss of Pak function did not reduce Akt or Erk activity; on the contrary, it activated them.

Discussion

In this report, we have shown that the effects of a dominant acting Merlin protein can be largely reversed by inhibition of group I Paks. As has been noted previously, expression of the dominant mutant Merlin ΔBB alters the actin cytoskeleton, promotes invasiveness, increases cell proliferation rate, and confers the ability to form tumors in nude mice (31). Given that Pak is activated in cells lacking functional Merlin (41) and that some of these aberrant phenotypes resemble those shown in cells with hyperactivation of Pak1 (42-44), blockade of Pak might represent a reasonable therapeutic strategy in NF2.

The data reported here are in general agreement with a previous study conducted by Yi *et al.*, in which Pak inhibition by shRNAs reduced tumor volume (41), but also have some intriguing differences. Interestingly, in the study by Yi *et al.*, escape from Pak knock-down occurred when expression of the Pak1 shRNA hairpin was silenced by methylation of the H1 promoter in the NF2 tumor cells. In our studies, which employed a peptide inhibitor of Pak rather than shRNA, we noted that the few, small tumors that arose in animals injected with ΔBB/PID cells did not shut off the PID transgene but did show significant increases in Merlin ΔBB expression (Fig. 6). The most likely explanation for these findings is that increased Merlin ΔBB expression was required for the tumor cells to escape inhibition consequent to diminished Pak function. Thus, both the results of our study and that of Yi *et al*. suggest that Pak activity is required for efficient tumorigenesis in cells that have lost Merlin function. In addition, our study shows that down-regulating Pak expression *per se* is not required for inhibiting tumor formation; inhibiting the catalytic activity of endogenous Pak is sufficient for these beneficial effects.

The involvement of Akt and Erk in NF2 pathobiology is controversial. Some studies report elevated Akt and Erk in NF2-deficient cells (45-51), whereas others report no correlation (35, 39). Our results are consistent with these latter studies, in that cells lacking Merlin, whether grown *in vitro* or when recovered from xenograft tumors, displayed low basal Akt and Erk activity. Curiously, in the few small tumors that developed from ΔBB/PID xenografts, Akt and Erk activities were elevated. The same was true for ΔBB/PID cells grown *in vitro*. These activations may reflect an altered signaling strategy in the tumor cells, necessary to overcome loss of Pak activity due to PID expression. Curiously, increased Erk activity was observed in Schwannoma cells,

even though Mek S298 phosphorylation was suppressed by PID (Fig. 4). These unexpected results indicate that Mek S298 phosphorylation, though a faithful reporter of Pak activity in these Schwannoma cells, does not always correlate with Mek activity. It is possible that altered signaling in Merlin-deficient Schwann cells abrogates the requirement for S298 phosphorylation, perhaps by phosphorylation of Mek at another site by another kinase.

While loss of Pak function reduced invasiveness, proliferation, and tumorigenesis of Merlin-deficient cells, it did not affect Erk, Akt, or mTOR signaling. Thus, the molecular basis for Pak's effects in these cells is uncertain. Interestingly, we found that Merlin ΔBB cells expressing the Pak inhibitor accumulate in the G2/M phase of the cell cycle. This finding is consistent with the observation that Pak1 localizes to centrosomes at late stages of the cell cycle and this localization is blocked by Pak inhibitors, leading to abnormal spindle formation and G2/M phase arrest (22). The mechanisms underlying these effects are not entirely clear, but could be related to the role of group I Paks in activating Aurora A and Polo-like kinases, which are important for mitotic progression and other mitotic-associated events (23). Thus, the basis for Pak's effects in NF2 likely involves novel signaling pathways that have not been previously considered or targeted.

A number of peptide based reagents, such as PID and cell-penetrating peptides based on the Nck or PIX binding regions of Pak, have been used to effectively block Pak function in cells and *in vivo* (52-54). Recently, a few specific small molecule inhibitors of group I Paks have also been described, including OSU03012, λ-FL172 (55), and IPA-3 (38). The latter of these three compounds has been shown to inhibit membrane ruffling and cell spreading in $NF2^{-/-}$ schwannoma cells (56). Interestingly, in these experiments, blockade of Pak with IPA-3 reduced Rac activity, suggesting that Pak acts upstream of Rac in these cells. Though Rac also activates Pak, such an idea is consistent with models which link Pak to further Rac activation via the Pak-bound guanine-nucleotide exchange factor, PIX (35, 57). These results, like ours, support the notion that the Rac/Pak signaling axis is activated as a consequence of Merlin loss, and that these enzymes might provide useful targets for therapy in NF2.

Acknowledgements

We thank Marco Giovannini for HEI-193 cells and Gary Nolan for the retroviral vector

pBMN-I-GFP. This work was supported by grants from the Department of Defense to JC (W81XWH-06-1-0213) and from the NIH to JC (CA117884) and to the Fox Chase Cancer Center (P30 CA006927), as well as by an appropriation from the state of Pennsylvania.

References

1. Reed N, Gutmann DH. Tumorigenesis in neurofibromatosis: new insights and potential therapies. Trends Mol Med 2001;7(4):157-62.
2. Evans DG, Sainio M, Baser ME. Neurofibromatosis type 2. J Med Genet 2000;37(12):897-904.
3. Shimizu T, Seto A, Maita N*, et al.* Structural basis for neurofibromatosis type 2. Crystal structure of the merlin FERM domain. J Biol Chem 2002;277(12):10332-6.
4. LaJeunesse DR, McCartney BM, Fehon RG. Structural analysis of Drosophila merlin reveals functional domains important for growth control and subcellular localization. J Cell Biol 1998;141(7):1589-99.
5. Sherman L, Xu HM, Geist RT*, et al.* Interdomain binding mediates tumor growth suppression by the NF2 gene product. Oncogene 1997;15:2505-9.
6. Shaw RJ, Paez JG, Curto M*, et al.* The Nf2 tumor suppressor, merlin, functions in Rac-dependent signaling. Dev Cell 2001;1(1):63-72.
7. Xiao GH, Beeser A, Chernoff J, Testa JR. p21-activated kinase links Rac/Cdc42 signaling to merlin. J Biol Chem 2002;277(2):883-6.
8. Kissil JL, Johnson KC, Eckman MS, Jacks T. Merlin phosphorylation by p21-activated kinase 2 and effects of phosphorylation on merlin localization. J Biol Chem 2002;277(12):10394-9.
9. Bashour AM, Meng JJ, Ip W, MacCollin M, Ratner N. The neurofibromatosis type 2 gene product, merlin, reverses the F-actin cytoskeletal defects in primary human Schwannoma cells. Mol Cell Biol 2002;22(4):1150-7.
10. Pelton PD, Sherman LS, Rizvi TA*, et al.* Ruffling membrane, stress fiber, cell spreading and proliferation abnormalities in human Schwannoma cells. Oncogene 1998;17(17):2195-209.
11. Kissil JL, Wilker EW, Johnson KC, Eckman MS, Yaffe MB, Jacks T. Merlin, the product of the Nf2 tumor suppressor gene, is an inhibitor of the p21-activated kinase, Pak1. Mol Cell 2003;12(4):841-9.
12. McLaughlin ME, Kruger GM, Slocum KL*, et al.* The Nf2 tumor suppressor regulates cell-cell adhesion during tissue fusion. Proc Natl Acad Sci U S A 2007;104(9):3261-6.
13. Lozano E, Frasa MA, Smolarczyk K, Knaus UG, Braga VM. PAK is required for the disruption of E-cadherin adhesion by the small GTPase Rac. J Cell Sci 2008;121(Pt 7):933-8.
14. Hage B, Meinel K, Baum I, Giehl K, Menke A. Rac1 activation inhibits E-cadherin-mediated adherens junctions via binding to IQGAP1 in pancreatic carcinoma cells. Cell Commun Signal 2009;7:23.
15. Ray RM, Vaidya RJ, Johnson LR. MEK/ERK regulates adherens junctions and migration through Rac1. Cell Motil Cytoskeleton 2007;64(3):143-56.

16. Okada T, Lopez-Lago M, Giancotti FG. Merlin/NF-2 mediates contact inhibition of growth by suppressing recruitment of Rac to the plasma membrane. J Cell Biol 2005;171(2):361-71.
17. Bokoch GM. Biology of the p21-Activated Kinases. Annu Rev Biochem 2003;72:743-81.
18. Arias-Romero LE, Chernoff J. A tale of two Paks. Biol Cell 2008;100(2):97-108.
19. Kumar A, Molli PR, Pakala SB, Nguyen TM, Rayala SK, Kumar R. PAK thread from amoeba to mammals. J Cell Biochem 2009.
20. Hofmann C, Shepelev M, Chernoff J. The genetics of Pak. J Cell Sci 2004;117(Pt 19):4343-54.
21. Dummler B, Ohshiro K, Kumar R, Field J. Pak protein kinases and their role in cancer. Cancer Metastasis Rev 2009;28(1-2):51-63.
22. Zhao ZS, Lim JP, Ng YW, Lim L, Manser E. The GIT-Associated Kinase PAK Targets to the Centrosome and Regulates Aurora-A. Mol Cell 2005;20(2):237-49.
23. Maroto B, Ye MB, von Lohneysen K, Schnelzer A, Knaus UG. P21-activated kinase is required for mitotic progression and regulates Plk1. Oncogene 2008;27(36):4900-8.
24. Tang Y, Chen Z, Ambrose D*, et al.* Kinase deficient Pak1 mutants inhibit Ras transformation of Rat-1 fibroblasts. Mol Cell Biol 1997;17:4454-64.
25. Tang Y, Marwaha S, Rutkowski JL, Tennekoon GI, Phillips PC, Field J. A role for Pak protein kinases in Schwann cell transformation. Proc Natl Acad Sci U S A 1998;95(9):5139-44.
26. King AJ, Sun H, Diaz B*, et al.* The protein kinase Pak3 positively regulates Raf-1 activity through phosphorylation of serine 338. Nature 1998;396(6707):180-3.
27. Beeser A, Jaffer ZM, Hofmann C, Chernoff J. Role of group A p21-activated kinases in activation of extracellular-regulated kinase by growth factors. J Biol Chem 2005;280(44):36609-15.
28. Slack-Davis JK, Eblen ST, Zecevic M*, et al.* PAK1 phosphorylation of MEK1 regulates fibronectin-stimulated MAPK activation. J Cell Biol 2003;162:281-91.
29. Eblen S, Slack JK, Weber MJ, Catling AD. Rac-PAK signaling stimulates extracellular signal-regulated kinase (ERK) activation by regulating formation of MEK1-ERK complexes. Mol Cell Biol 2002;22:6023-33.
30. Fraenzer JT, Pan H, Minimo L, Jr., Smith GM, Knauer D, Hung G. Overexpression of the NF2 gene inhibits schwannoma cell proliferation through promoting PDGFR degradation. Int J Oncol 2003;23(6):1493-500.
31. Johnson KC, Kissil JL, Fry JL, Jacks T. Cellular transformation by a FERM domain mutant of the Nf2 tumor suppressor gene. Oncogene 2002;21(39):5990-7.
32. Lepont P, Stickney JT, Foster LA, Meng JJ, Hennigan RF, Ip W. Point mutation in the NF2 gene of HEI-193 human schwannoma cells results in the expression of a merlin isoform with attenuated growth suppressive activity. Mutat Res 2008;637(1-2):142-51.
33. Lutchman M, Rouleau GA. The neurofibromatosis type 2 gene product, schwannomin, suppresses growth of NIH 3T3 cells. Cancer Res 1995;55(11):2270-4.
34. Xiao GH, Gallagher R, Shetler J*, et al.* The NF2 tumor suppressor gene product, merlin, inhibits cell proliferation and cell cycle progression by repressing cyclin D1 expression. Mol Cell Biol 2005;25(6):2384-94.
35. Lopez-Lago MA, Okada T, Murillo MM, Socci N, Giancotti FG. Loss of the tumor suppressor gene NF2, encoding merlin, constitutively activates integrin-dependent mTORC1 signaling. Mol Cell Biol 2009;29(15):4235-49.

36. Sun H, King AJ, Diaz HB, Marshall MS. Regulation of the protein kinase Raf-1 by oncogenic Ras through phosphatidylinositol 3-kinase, Cdc42/Rac and Pak. Curr Biol 2000;10(5):281-4.
37. Li W, Chong H, Guan KL. Function of the Rho family GTPases in Ras-stimulated Raf activation. J Biol Chem 2001;276(37):34728-37.
38. Deacon SW, Beeser A, Fukui JA*, et al.* An isoform-selective, small-molecule inhibitor targets the autoregulatory mechanism of p21-activated kinase. Chem Biol 2008;15(4):322-31.
39. James MF, Han S, Polizzano C*, et al.* NF2/merlin is a novel negative regulator of mTOR complex 1, and activation of mTORC1 is associated with meningioma and schwannoma growth. Mol Cell Biol 2009;29(15):4250-61.
40. Mukherjee J, Kamnasaran D, Balasubramaniam A*, et al.* Human Schwannomas Express Activated Platelet-Derived Growth Factor Receptors and c-kit and Are Growth Inhibited by Gleevec (Imatinib Mesylate). Cancer Res 2009;69:5099-.
41. Yi C, Wilker EW, Yaffe MB, Stemmer-Rachamimov A, Kissil JL. Validation of the p21-activated kinases as targets for inhibition in neurofibromatosis type 2. Cancer Res 2008;68(19):7932-7.
42. Sells MA, Boyd JT, Chernoff J. p21-activated kinase 1 (Pak1) regulates cell motility in mammalian fibroblasts. J Cell Biol 1999;145(4):837-49.
43. Sells MA, Knaus UG, Bagrodia S, Ambrose DM, Bokoch GM, Chernoff J. Human p21-activated kinase (Pak1) regulates actin organization in mammalian cells. Curr Biol 1997;7(3):202-10.
44. Li F, Adam L, Vadlamudi RK*, et al.* p21-activated kinase 1 interacts with and phosphorylates histone H3 in breast cancer cells. EMBO Rep 2002;3(8):767-73.
45. Lim JY, Kim H, Jeun SS, Kang SG, Lee KJ. Merlin inhibits growth hormone-regulated Raf-ERKs pathways by binding to Grb2 protein. Biochem Biophys Res Commun 2006;340(4):1151-7.
46. Lim JY, Kim H, Kim YH*, et al.* Merlin suppresses the SRE-dependent transcription by inhibiting the activation of Ras-ERK pathway. Biochem Biophys Res Commun 2003;302(2):238-45.
47. Jin H, Sperka T, Herrlich P, Morrison H. Tumorigenic transformation by CPI-17 through inhibition of a merlin phosphatase. Nature 2006;442(7102):576-9.
48. Morrison H, Sperka T, Manent J, Giovannini M, Ponta H, Herrlich P. Merlin/neurofibromatosis type 2 suppresses growth by inhibiting the activation of Ras and Rac. Cancer Res 2007;67(2):520-7.
49. Rong R, Tang X, Gutmann DH, Ye K. Neurofibromatosis 2 (NF2) tumor suppressor merlin inhibits phosphatidylinositol 3-kinase through binding to PIKE-L. Proc Natl Acad Sci U S A 2004;101(52):18200-5.
50. Chadee DN, Xu D, Hung G*, et al.* Mixed-lineage kinase 3 regulates B-Raf through maintenance of the B-Raf/Raf-1 complex and inhibition by the NF2 tumor suppressor protein. Proc Natl Acad Sci U S A 2006;103(12):4463-8.
51. Ammoun S, Flaiz C, Ristic N, Schuldt J, Hanemann CO. Dissecting and targeting the growth factor-dependent and growth factor-independent extracellular signal-regulated kinase pathway in human schwannoma. Cancer Res 2008;68(13):5236-45.
52. Zhao L, Ma QL, Calon F*, et al.* Role of p21-activated kinase pathway defects in the cognitive deficits of Alzheimer disease. Nat Neurosci 2006;9(2):234-42.
53. Reutershan J, Stockton R, Zarbock A*, et al.* Blocking p21-activated kinase reduces lipopolysaccharide-induced acute lung injury by preventing polymorphonuclear leukocyte infiltration. Am J Respir Crit Care Med 2007;175(10):1027-35.
54. Kiosses WB, Hood J, Yang S*, et al.* A dominant-negative p65 PAK peptide inhibits angiogenesis. Circ Res 2002;90(6):697-702.

55. Maksimoska J, Feng L, Harms K*, et al.* Targeting large kinase active site with rigid, bulky octahedral ruthenium complexes. J Am Chem Soc 2008;130:15764-675.
56. Flaiz C, Chernoff J, Ammoun S, Peterson JR, Hanemann CO. PAK kinase regulates Rac GTPase and is a potential target in human schwannomas. Exp Neurol 2009;218:137-44.
57. Obermeier A, Ahmed S, Manser E, Yen SC, Hall C, Lim L. PAK promotes morphological changes by acting upstream of Rac. EMBO J 1998;17:4328-39.

Figure Legends

Figure 1. Establishment of cells with loss of Merlin and/or Pak function. (**A**) Schematic of experimental design. NIH-3T3 cells were infected with a control retrovirus or a retrovirus encoding dominant negative Merlin (Merlin ΔBB). These cells were then infected with a retrovirus encoding the Pak inhibitor (PID) or an inactive control (PID LF). (**B**) Cells were starved overnight and then stimulated with PDGF for 5 min. Immunoblots for Merlin, (GST)-PID, actin, and phospho-Pak expression are shown.

Figure 2. Effects of PID on invasion. (**A**) The invasiveness of control cells or cells expressing Merlin ΔBB, Merlin ΔBB/ PID, or Merlin ΔBB/PID LF was determined by Matrigel invasion chamber assay as compared against uninfected control cells. The experiments were performed three times with similar results. The data are presented as the means ± S.D. of duplicate well measurements from one representative experiment. (**B**) Staining pattern of cells that have migrated and adhered to the bottom surfaces of filters in cell invasion assay. The small circles are cross-sections of 8 μm pores. Scale bar = 50 μm.

Figure 3. Inhibition of cell proliferation and induction of G2/M arrest by expression of PID. (**A**) Equal numbers of the indicated cells were seeded in 96-well plate and monitored by MTT assay for 7 days. The experiments were conducted three times with similar results. (**B**) Cells were stained with propidium iodide and subjected to cell cycle analysis by FACS. Results are representative of three independent experiments.

Figure 4. Lack of effect of Pak inhibition on Erk pathway in Merlin ΔBB transformed cells. Cells were cultured in serum-free medium for 24 hr and then stimulated with 5 ng/ml of PDGF for 5 min, as described in Material and Methods. Lysed cells were separated by SDS-PAGE and incubated with the indicated antibodies. Data shown represent the means ± SD of data from three experiments.

Figure 5. Effects of PID on tumor formation. Tumor formation was assessed by subcutaneously inoculating 1 X 10^6 NIH-3T3 cells infected with empty vector (Vector) into left flanks and equal number of Merlin-expressing cells (ΔBB, ΔBB/PID and ΔBB/PID

LF, respectively) into right flank of the same mice. Five mice were used for each cell line. Tumor diameters were measured every 3 days using caliper for 6 weeks following injection. (**A**) Representative photographs of nude mice with solid tumors (left panel). Enlarged images of boxed area in the left panel (right panel). (**B, C**) Tumor volume was calculated by the formula described in Material and Methods. Horizontal lines represent the average tumor diameter.

Figure 6. Activity of signaling pathways in tumor samples from xenografts. Tumor were resected and immediately lysed in a buffer containing 10 mM PBS pH 7.2, 1% Triton X-100, 0.1% SDS, 20% glycerol, plus complete protease and phosphatase inhibitor tablets (Roche). Lysates were separated by SDS-PAGE and incubated with the indicated antibodies.

Supplemental Figure 1. Effect of Pak inhibiton on signaling in NIH-3T3 cells. Control NIH-3T3 cells and NIH-3T3 cells stably expressing PID or PID LF were starved for 24 hrs in serum-free medium, then stimulated for 5 min with 5 ng/ml; PDGF. Protein lysates were separated by SDS-PAGE, blotted, and probed with the indicated antibodies.

Supplemental Figure 2. Effect of Pak inhibition on mTOR pathway in NF2 cells. The indicated cells were starved for 24 hrs in serum-free medium, then left untreated or stimulated for 5 min with 5 ng/ml PDGF. Protein lysates were separated by SDS-PAGE, blotted, and probed with the indicated antibodies.

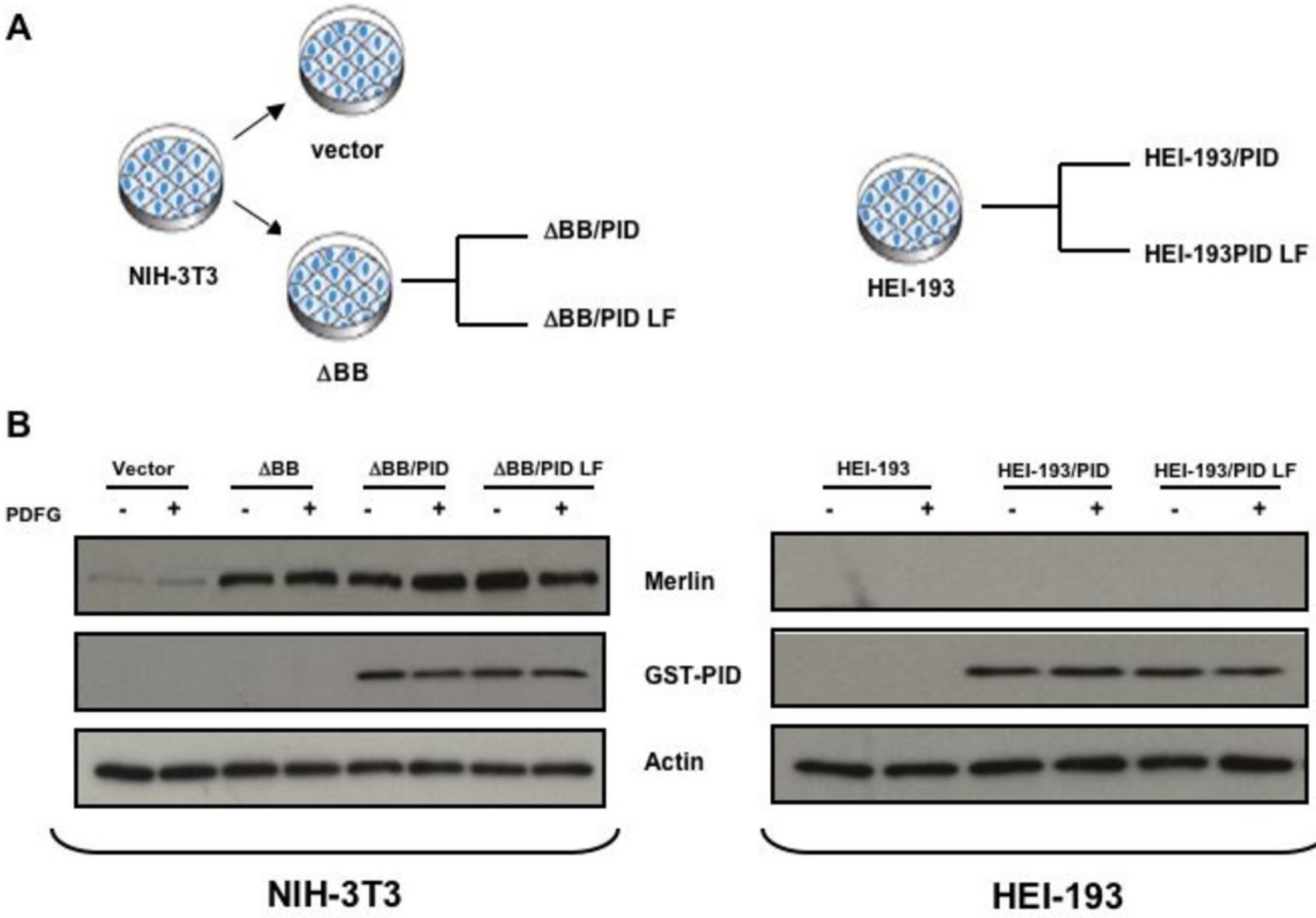
A
vector
NIH-3T3
ΔBB/PID
ΔBB/PID LF
ΔBB
HEI-193/PID
HEI-193PID LF
HEI-193
B
Vector
ΔBB
ΔBB/PID
ΔBB/PID LF
PDFG
- + - + - + - +
Merlin
GST-PID
Actin
NIH-3T3
HEI-193
HEI-193
HEI-193/PID
HEI-193/PID LF
- + - + - +

Fig. 1

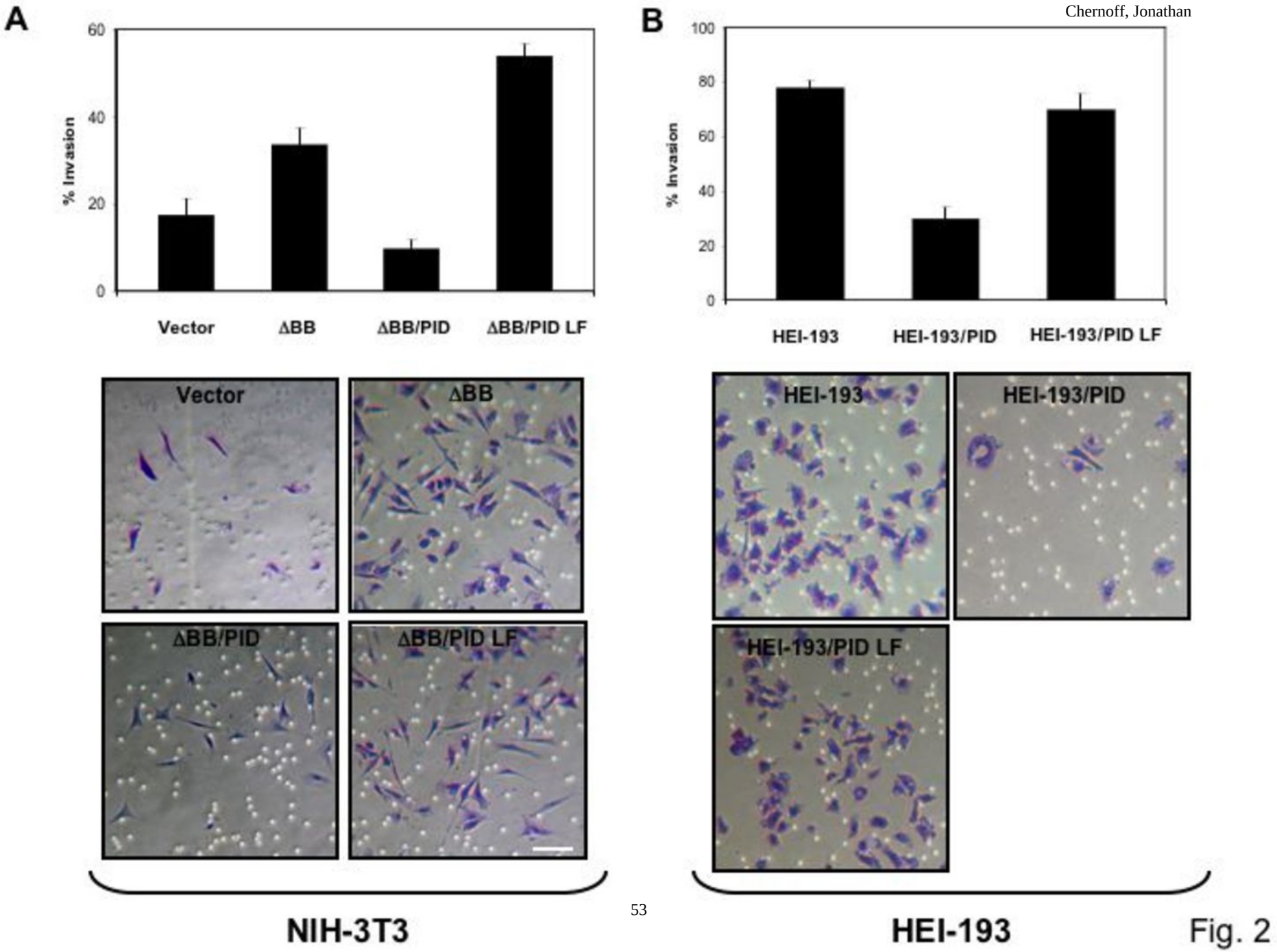
A
% Invasion
60
40
20
0
Vector
ΔBB
ΔBB/PID
ΔBB/PID LF
B
% Invasion
100
80
60
40
20
0
HEI-193
HEI-193/PID
HEI-193/PID LF
Vector
ΔBB
ΔBB/PID
ΔBB/PID LF
HEI-193
HEI-193/PID
HEI-193/PID LF
NIH-3T3
HEI-193

Fig. 2

A

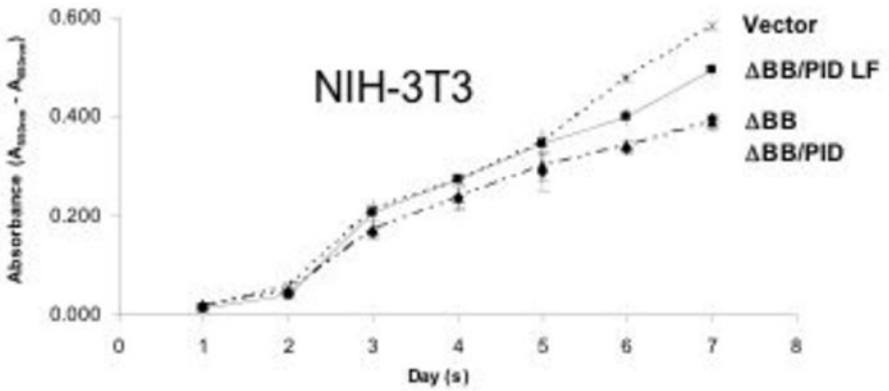

C

	% G0/G1	% S	%G2/M
Vector	57	26	14
ΔBB	55	30	12
ΔBB/PID	43	26	28
ΔBB/PID LF	53	27	16

B

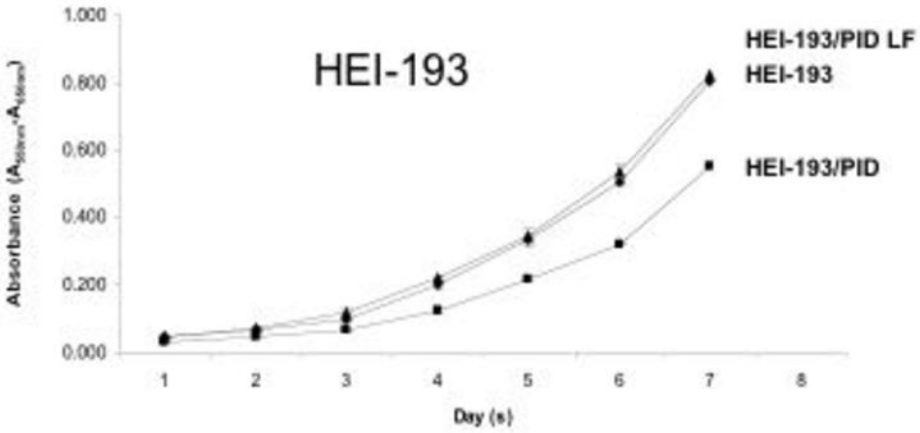

D

	% G0/G1	% S	%G2/M
HEI-193	31	39	20
HEI-193 /PID	37	31	31
HEI-193 /PID LF	32	36	23

Fig. 3

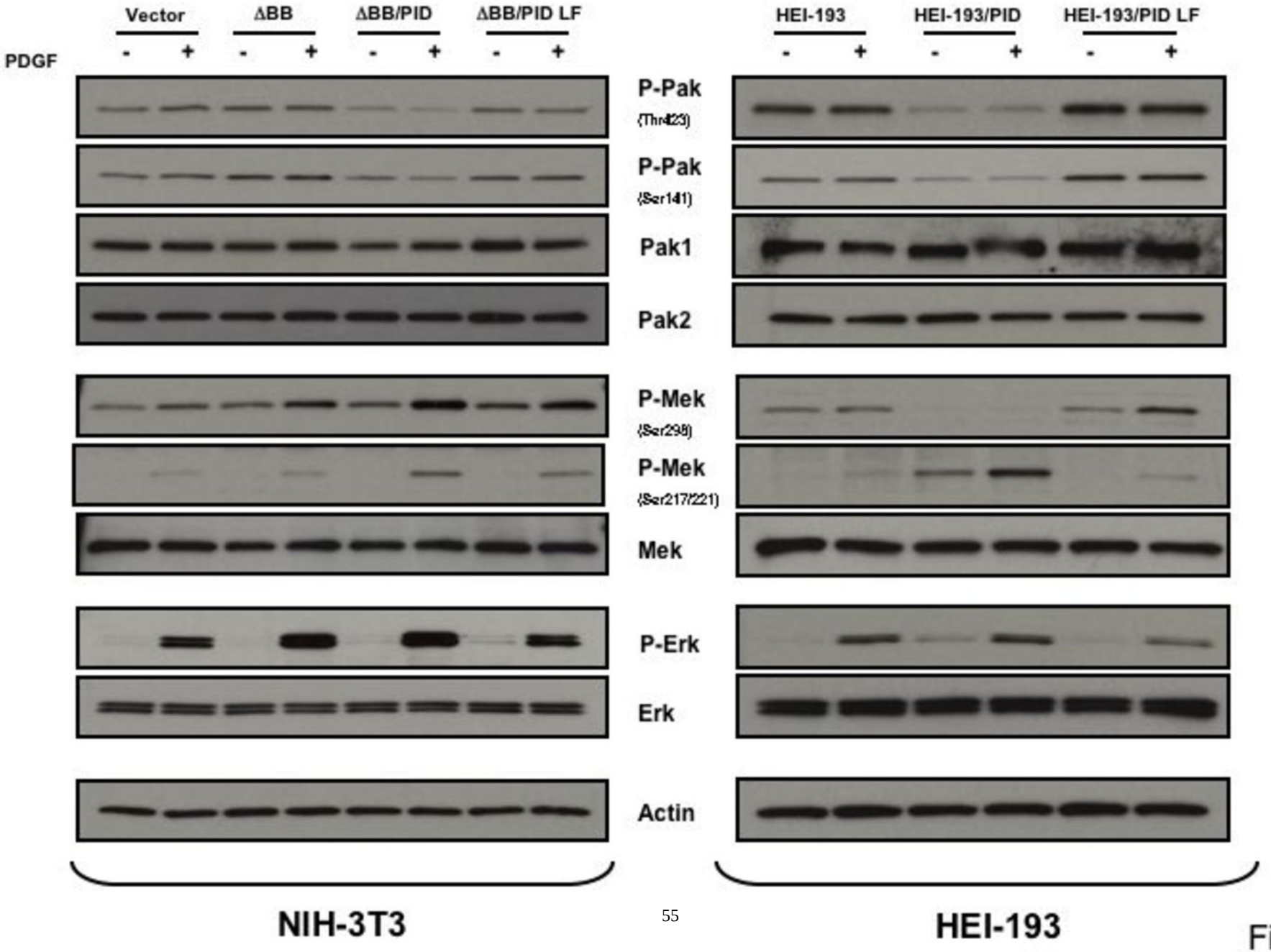
Vector
ΔBB
ΔBB/PID
ΔBB/PID LF
HEI-193
HEI-193/PID
HEI-193/PID LF
PDGF
- + - + - + - + - + - + - +
P-Pak (Thr423)
P-Pak (Ser141)
Pak1
Pak2
P-Mek (Ser298)
P-Mek (Ser217/221)
Mek
P-Erk
Erk
Actin
NIH-3T3
HEI-193

Fig. 4

A

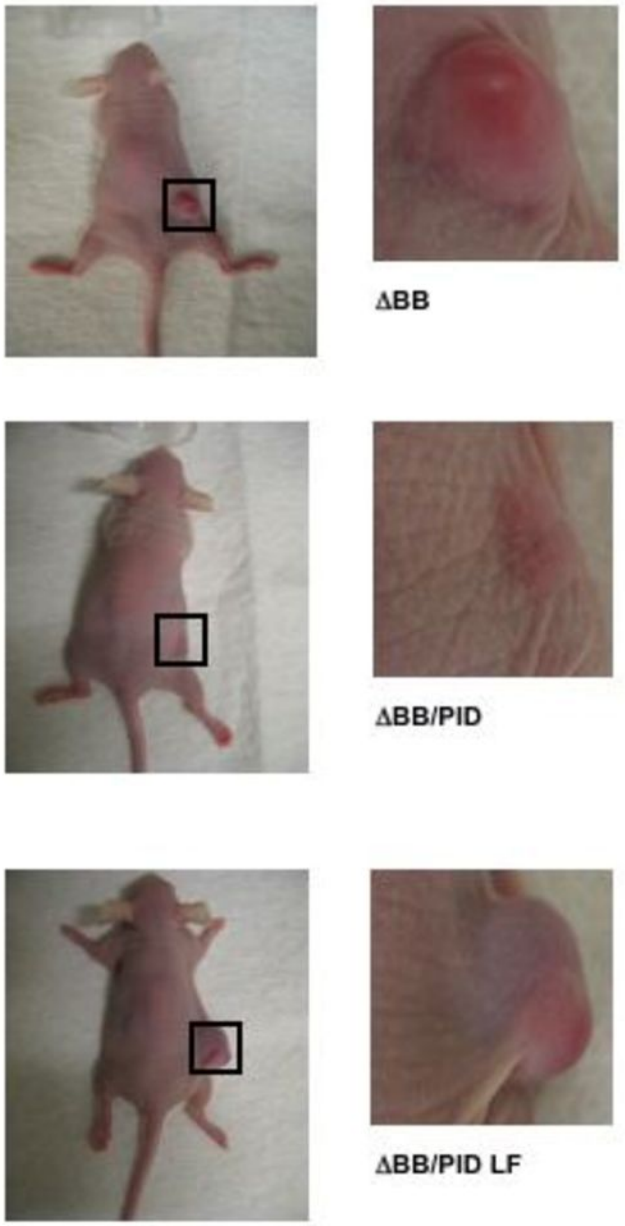

B

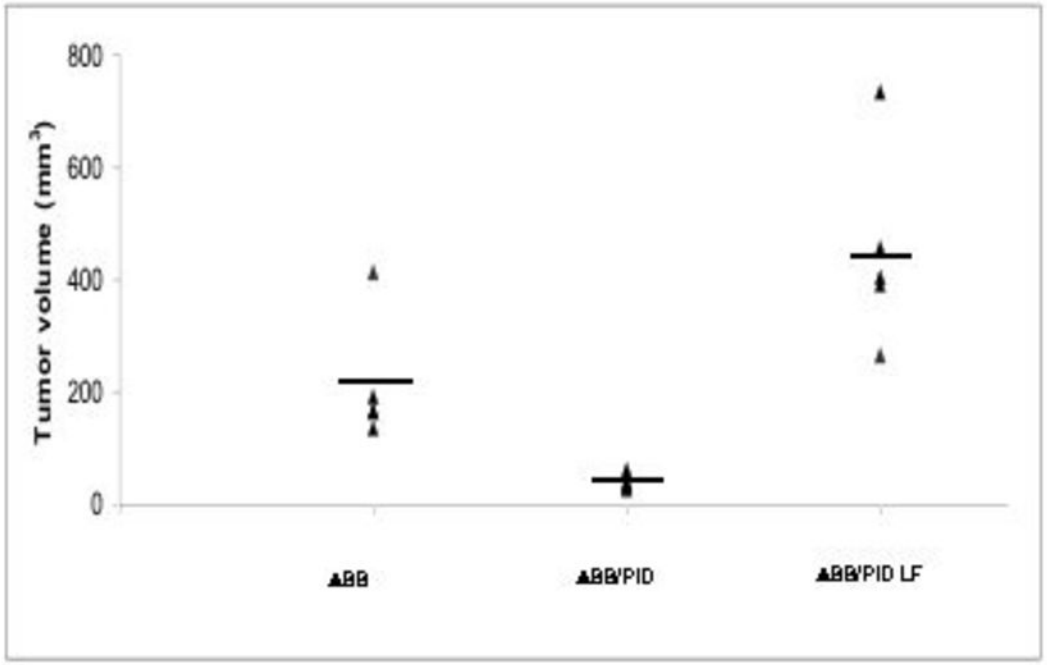

C

Injected cell types	ΔBB	ΔBB/PID	ΔBB/PID LF
Average tumor volume (mm^3)	213.56	38.37	450.61

Fig. 5

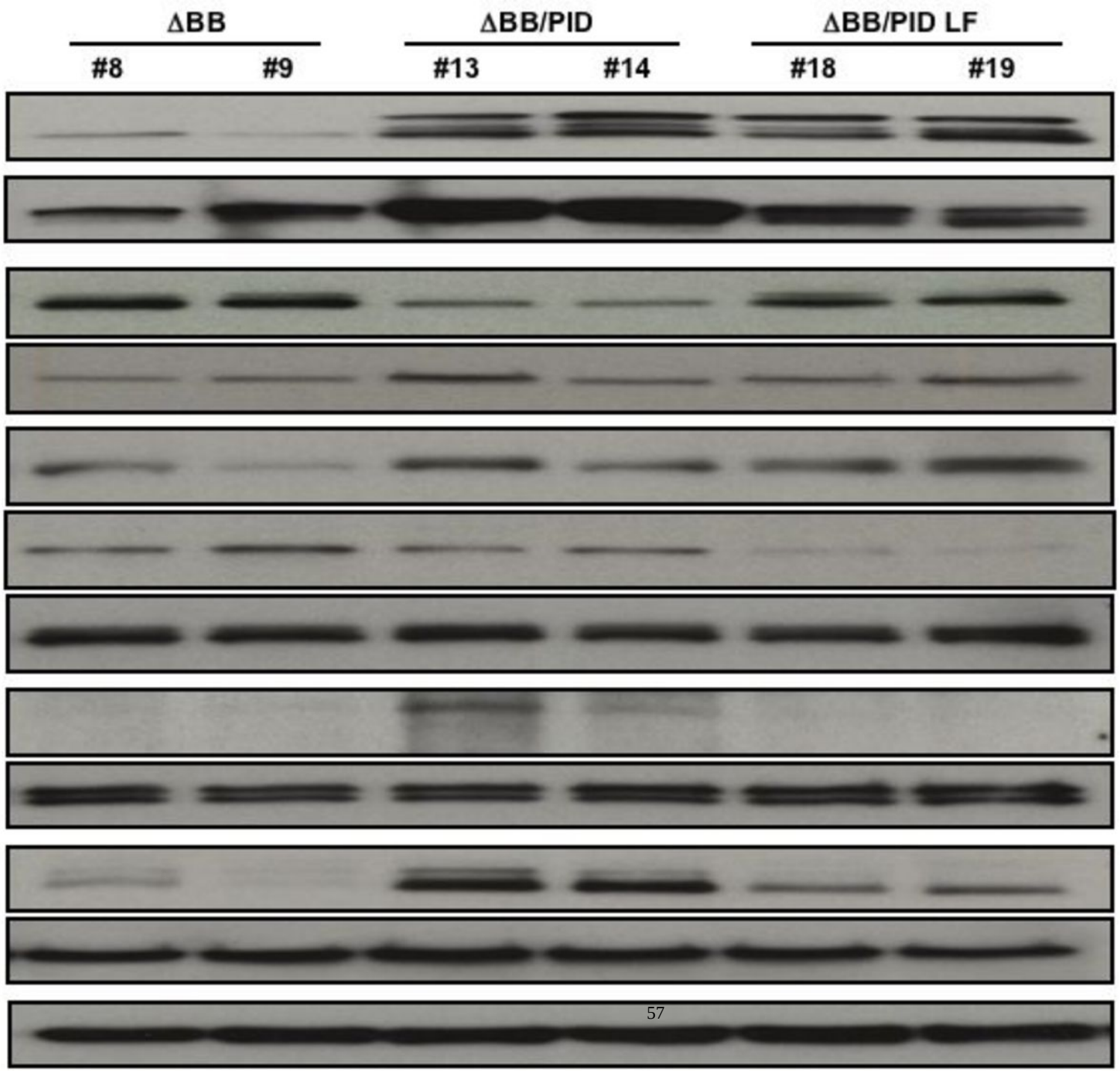
ΔBB
ΔBB/PID
ΔBB/PID LF
#8
#9
#13
#14
#18
#19
GST-PID
Merlin
P-Pak1-3 (Ser141)
Pak1
P-Mek1 (Ser298)
P-Mek1
(Ser217/221)
Mek
P-Erk1/2
(Thr202/Tyr204)
Erk1/2
P-Akt (Ser473)
Akt
Actin

Fig. 6